Topics in BSM Physics: Supersymmetry, Dark Matter and Baryogenesis

Matthew McCullough

New College

University of Oxford

A thesis submitted for the degree of

Doctor of Philosophy

Trinity 2011

Abstract

Under the umbrella of Theoretical Physics, progress in 'Beyond the Standard Model' (BSM) physics proceeds broadly along two main avenues of investigation. The first is concerned with constructing theories that attempt to explain observations, or address theoretical problems, which cannot be explained within the tremendously successful Standard Model (SM) of particle physics. The second involves looking for new ways to observe or test BSM physics, and such tests are usually developed with current experimental hints, or attractive theoretical models, in mind. This thesis contains material which falls under both approaches.

Part I is concerned with Supersymmetry (SUSY). We review the basics of SUSY, and the current state of this field, and then present a novel model for SUSY at the TeV scale. This model has a Higgs sector similar to the SM and possesses a continuous $U(1)_R$ symmetry, dramatically suppressing contributions to flavour-changing neutral currents, which can be problematic in SUSY models. After this we demonstrate that if more than one SUSY-breaking sector is present then this could lead to a rich spectrum of states with mass roughly twice the gravitino mass. In particular, if SUSY-breaking in a hidden sector arises dynamically then multiple 'Goldstini' and 'Modulini' states can arise, which couple to visible sector fields via the 'Goldstino Portal'. We also demonstrate a new phenomenon which can occur in the context of multiple hidden sectors. If one sector breaks SUSY then this can 'stimulate' other sectors into also breaking SUSY, even if they are incapable of doing so on their own.

Part II focusses on the matter in our Universe. We review our current understanding of how the visible matter in our Universe came into existence, and our current understanding of the nature of dark matter (DM). Following this we describe how DM could potentially be indirectly observed through its effects on cold white dwarf stars. Alternatively, if DM were detected by independent means, then observed cold white dwarfs could be used to place limits on the DM density in globular clusters, giving clues as to how these clusters of stars formed. We then present a new model for the co-generation of both the visible and dark matter in our Universe. This proceeds by generating a particle anti-particle asymmetry in the dark sector, which is then shared with the visible sector. This model predicts the existence of a light, $m \lesssim 5$ eV, scalar particle which derivatively couples to DM, and provides a final state for the symmetric DM component to annihilate away into.

Work completed during the period of this D.Phil is contained in [1–8], however only material in [3–6, 8] is presented in this thesis.

Acknowledgments

I acknowledge generous financial support from an STFC Postgraduate Studentship, and a Stipendiary Lectureship at University College, Oxford.

First of all, I would like to thank my A-level maths teacher, Geoff Brown, for showing me the fun in doing maths and physics and sowing the seeds which grew into my passion for these subjects.

In the Oxford Theoretical Physics department I would like to thank Joe Conlon, Graham Ross and Subir Sarkar for answering numerous questions and broadening my knowledge greatly. I would also like to thank my contemporaries and collaborators, Nathaniel Craig, Rhys Davies, Malcolm Fairbairn, Mads Frandsen, Felix Kahlhoefer, Christopher McCabe, Philipp Mertsch, Seshadri Nadathur, Thomas Pickup, James Unwin and Kai Schmidt-Hoberg for numerous beneficial conversations.

I am extremely indebted for the great deal I have learned from my supervisor, John March-Russell. His relentless enthusiasm, attention to detail, and keen eye for finding and comprehending the really interesting physics has formed a lasting influence.

Outside of physics, but within Oxford, I would like to thank my friends Richard Bowman, Rhys and Emma Davies, Jonathan and Rita Floyd, and Guy Kingham for keeping me sane.

I would like to thank my parents, Alison and Trevor, and my brother and sister, Adam and Holly, for their continual love and encouragement, and particularly my parents for supporting the decisions I made for my future, whether in music or physics from a young age. I am also grateful to the Andrews and Carmichael families, and to my grandparents, Hedgley and McCullough, for their support and understanding.

Above all others, my deepest gratitude is to my wife Kate, my greatest collaborator, for her guidance, inspiration, and love.

Contents

Chapter 1

Introduction

1.1 The Standard Model of Particle Physics

The Standard Model (SM) of particle physics took more than a century to construct, and this culminated in the early 1970's in a model containing the fundamental particles detailed in table 1.1, with the parameters in table 1.2 and the particle interactions detailed in table 1.3. With the exception of the Higgs, all of the particles predicted by this model have been observed. Their masses and charges have been determined to good accuracy, and these are detailed in table 1.4. With the exception of the last two parameters of table 1.2, which are again related to the Higgs sector, experimental observations have either determined, or set bounds on, the remainder of the free parameters. This leaves only 2 of the initial 19 free parameters undetermined. The SM, with the addition of with General Relativity, provides a good description of fundamental physics from scales larger than the size of the solar system down to distances as small as one hundredth the size of a proton, and from times as early as when nuclei began to form, when the Universe was less than 1 second old, to the present day. It is remarkable that, when combined with the framework of quantum field theory, such a successful model can be detailed in tables 1.1, 1.2, 1.3, and 1.4.

The SM is based on three theories, QCD, the electroweak theory, and QED, which are examples of gauge theories. A gauge theory is a theory where global symmetries under which the matter fields transform are promoted to local symmetries, i.e. symmetry transformations become dependent on space-time co-ordinates. When this is done then new gauge fields are required which also transform under the gauge symmetry. In the case of the SM the gauge symmetries are $G_{SM} \equiv SU(3)_c \times SU(2)_W \times U(1)_Y$, and the gauge fields are the gluons, W and Z bosons, and the photon. QED is an abelian gauge theory, based on Maxwell's formulation of electrodynamics combined with quantum field theory [9–14], whereas the electroweak theory and QCD are non-abelian, or Yang-Mills [15], theories. If the gauge symmetry is unbroken then the gauge field must be massless to maintain the gauge symmetry, explaining why the photon is massless. Massive gauge bosons can arise if the gauge symmetry is spontaneously broken, and this is well described by the Higgs mechanism [16–18]. In section 1.1.1 we will consider the successes of QCD, the electroweak theory, and QED, and we will see that the overarching structure of gauge theories has been extremely effective in explaining the structure of interactions in the SM. This general structure of particle interactions, dictated by gauge theory, is detailed in table 1.3.

Following this, in sections 1.1.2 and 1.1.3, we will discuss the failures and puzzles facing the SM. These problems, some of which are purely theoretical, justify the motivation to look beyond the SM, particularly above the electroweak scale, and provide hints towards what physics might lie above this scale.

Field	$SU(3)_c \times SU(2)_W \times U(1)_Y$	Spin
Q_i	$(\mathbf{3}, \mathbf{2}, \frac{1}{6})$	$\frac{1}{2}$
U_i^c	$(\overline{\mathbf{3}}, \mathbf{1}, -\frac{2}{3})$	$\frac{1}{2}$
D_i^c	$(\overline{\mathbf{3}}, \mathbf{1}, \frac{1}{3})$	$\frac{1}{2}$
L_i	$(\mathbf{1}, \mathbf{2}, -\frac{1}{2})$	$\frac{1}{2}$
E_i^c	$(\mathbf{1}, \mathbf{1}, 1)$	$\frac{1}{2}$
B_μ	$(\mathbf{1}, \mathbf{1}, 0)$	1
W_μ	$(\mathbf{1}, \mathbf{3}, 0)$	1
G_μ	$(\mathbf{8}, \mathbf{1}, 0)$	1
H	$(\mathbf{1}, \mathbf{2}, \frac{1}{2})$	0

Table 1.1: The particle content of the Standard Model, before electroweak symmetry breaking. The subscript 'i' denotes the generation of the particle, of which there are three.

1.1.1 Successes

Undoubtedly one of the great successes of the SM is that it describes the interactions of the known particles detailed in table 1.4. The existence of many of these particles, including the charm [19, 20], bottom and top quarks[21] , and the $W^\pm$ and Z^0 bosons [22–24], was predicted well in advance of their discovery. By way of indirect measurements the masses of the weak gauge bosons were predicted to good accuracy before

Parameter	Role
g_1	$U(1)_Y$ coupling constant
g_2	$SU(2)_W$ coupling constant
g_3	$SU(3)_C$ coupling constant
$\lambda_{u,c,t}$	Up-type quark Yukawa coupling to Higgs
$\lambda_{d,s,b}$	Down-type quark Yukawa coupling to Higgs
$\lambda_{e,\mu,\tau}$	Charged lepton Yukawa coupling to Higgs
$\theta_{12,13,23}$	Angles in quark mixing matrix
δ	Phase in quark mixing matrix
θ_{QCD}	QCD vacuum angle
m_h	Higgs mass
λ_h	Higgs quartic coupling

Table 1.2: The free parameters of the Standard Model.

their discovery. Although the SM does not explain the magnitude and structure of fermion masses, it does allow for an adequate description of their mass as a result of electroweak symmetry breaking through their Yukawa couplings with the Higgs field, shown in table 1.3. With an exception for the neutrinos, which according to the SM should have zero mass.

Both QCD and the role of quarks as fundamental constituents of composite nucleons have been experimentally verified in a number of ways. The first hint that QCD and the quark model are correct is that they lead to the prediction of the observed baryons and mesons, and simplified models give good estimates for decay widths and masses [26–28]. Deep inelastic scattering experiments in the 1960's demonstrated that the cross-section for electron scattering on protons, as a function of Q^2, displays a scaling behaviour consistent with what one expects if the proton is made up of less massive constituent particles [29, 30], known as partons [31, 32], which are now known to include quarks and gluons. These experiments also showed that quarks carry fractional electric charges. However, quarks were found to carry roughly less than half of the momentum of the proton, hinting at the presence of additional neutral particles. These particles, now known as gluons, the force carriers of QCD, were observed as final-state radiation from quarks in the 1970's at the PETRA collider at DESY [33], an effect which was predicted earlier [34]. The SM also predicts that the QCD coupling constant should become weaker at higher energies [35, 36]. This

Interaction	Lagrangian term
Fermion gauge	$\overline{\psi}\gamma^\mu i(\partial_\mu - i\sum_{G_{SM}} gA^a_\mu t^a)\psi$
Higgs gauge	$\frac{1}{2}\lvert(\partial_\mu - i\sum_{G_{SM}} gA^a_\mu t^a)H\rvert^2$
Gauge boson	$-\frac{1}{4}\sum_{G_{SM}} F^a_{\mu\nu}F^{a\mu\nu}$, $F^a_{\mu\nu} = \partial_\mu A^a_\nu - \partial_\nu A^a_\mu + gf^{abc}A^b_\mu A^c_\nu$
Higgs Yukawa	$-\lambda_\psi H\overline{\psi}\psi + \text{h.c.}$
Higgs potential	$-\lambda_H(\lvert H\rvert^2 - \frac{v^2}{2})^2$

Table 1.3: The SM gauge and Yukawa interactions and the mass and self-coupling of the Higgs doublet before electroweak symmetry breaking. The SM gauge group is denoted by G_{SM}, and the coupling constant is g for a given gauge group. Fermions of the SM are represented by ψ. The generators of the gauge group are denoted by t^a, and they satisfy the commutation relations $[t^a, t^b] = if^{abc}t^c$. If we denote by v the vacuum expectation value of the Higgs field, then we have the relation $m_\psi = \lambda_\psi v$.

'running' of the coupling constant has been observed and verified over two orders of magnitude. Many additional experimental tests involving the high energy scattering and production of coloured particles verify the correctness of QCD. Non-perturbative studies, such as those that can be performed on the lattice [37], have also shown good agreement with observations [38].

The electroweak theory has also been unequivocally verified. This theory predicts the charged current processes leading to nuclear β-decay and additional neutral current processes. These neutral current Z-exchange processes are the only way in which a neutrino can scatter elastically from a quark or an electron, and were observed at CERN in 1973 [39]. Since then the W and Z bosons were both discovered at CERN, and their masses have been measured [25]. These masses have been measured down to a fractional precision of about 10^{-3}, and agree well with the predictions of electroweak theory [25]. Additional observables, such as decay widths and branching ratios, have been measured to a high degree of precision and agree well with theory. Trilinear couplings between the electroweak gauge bosons and photons are predicted by the SM gauge symmetry and experiments have shown that the full set of these couplings is required in order to describe diboson production. The mixing between quark mass eigenstates participating in the weak interactions describes the decays of the strange and bottom quarks well.

QED also stands up extremely well to experiment, and precision tests now verify QED predictions down to less than a part in a billion. An example of such a precision test is the measurement of the anomalous magnetic dipole moment of the electron,

Field	$SU(3)_c$	$U(1)_{EM}$	Mass [GeV]	Spin
u	$\mathbf{3}$	$\frac{2}{3}$	$1.7 - 3.1 \times 10^{-3}$	$\frac{1}{2}$
c	$\mathbf{3}$	$\frac{2}{3}$	$1.29^{+0.05}_{-0.11}$	$\frac{1}{2}$
t	$\mathbf{3}$	$\frac{2}{3}$	$172.9 \pm 0.6 \pm 0.9$	$\frac{1}{2}$
d	$\mathbf{3}$	$-\frac{1}{3}$	$4.1 - 5.7 \times 10^{-3}$	$\frac{1}{2}$
s	$\mathbf{3}$	$-\frac{1}{3}$	$100^{+30}_{-20} \times 10^{-3}$	$\frac{1}{2}$
b	$\mathbf{3}$	$-\frac{1}{3}$	$4.67^{+0.18}_{-0.06}$	$\frac{1}{2}$
e	$\mathbf{1}$	-1	511×10^{-6}	$\frac{1}{2}$
μ	$\mathbf{1}$	-1	105.7×10^{-3}	$\frac{1}{2}$
τ	$\mathbf{1}$	-1	1.78	$\frac{1}{2}$
ν_1	$\mathbf{1}$	0	$m_{\nu_1} \lesssim 2 \times 10^{-9}$	$\frac{1}{2}$
ν_2	$\mathbf{1}$	0	$m_{\nu_2} \lesssim 2 \times 10^{-9}$	$\frac{1}{2}$
ν_3	$\mathbf{1}$	0	$m_{\nu_3} \lesssim 2 \times 10^{-9}$	$\frac{1}{2}$
γ_μ	$\mathbf{1}$	0	0	1
Z_μ	$\mathbf{1}$	0	91.2	1
W^+_μ	$\mathbf{1}$	1	80.4	1
G_μ	$\mathbf{8}$	0	0	1

Table 1.4: The observed particles. Charges under the unbroken symmetries of the Standard Model are given. Charged particles have an antiparticle with gauge charges equal in magnitude and opposite in sign. Masses are taken from the Particle Data Group [25].

which is predicted to be non-zero in QCD, and this prediction has been confirmed in experiment [25].

1.1.2 Failures

Despite the manifold successes of the SM, some observations exist for which the SM cannot offer an explanation. The first of these, which is also the closest to home, is that the Universe contains unequal abundances of baryons and anti-baryons. Such a baryon asymmetry can develop in the early Universe, in a CPT-invariant theory, however this requires baryon-number violation occurring at a rate greater than the expansion rate of the Universe, sufficient CP-violation, and out-of-thermal equilibrium conditions. These are the famous 'Sakharov' conditions [40]. Although all three conditions can be realised within the SM, unfortunately they are not satisfied to a great enough extent to explain the observed asymmetry. The greatest problem lying in the fact that the overall effective CP-violation in the SM is too small in magnitude. Thus, if we wish to explain the observed baryon asymmetry, we are forced to look beyond the SM for new sources of CP-violation, baryon number violation, or out-of-thermal equilibrium dynamics. We will consider baryogenesis in more detail in Chapter 6, and give a new model for baryogenesis in Chapter 8.

Another problem with the SM is that the lack of neutral right-handed neutrinos, with no gauge charges whatsoever, leads to the prediction that neutrinos are massless in the renormalizable model, however neutrino-oscillation observations imply that at least two neutrino species have mass, and this mass is small $m_\nu \lesssim 2$ eV [25]. This can be remedied with relative ease by going beyond the SM. Although many solutions exist, the simplest, and arguably most compelling, solution is to simply add right-handed neutrinos. However this still leaves some open questions. If, once these extra neutrinos are added, neutrino masses are purely Dirac in nature then one is left with the question of why neutrino Yukawa couplings to the Higgs are so much smaller than for other charged fermions. In fact, neutrino Yukawa couplings would need to be of $\mathcal{O}(10^{-11})$ for this scenario to work. Alternatively, one can allow Majorana masses for the right handed neutrinos and then make use of the 'seesaw' mechanism which leads to Majorana masses for the lightest neutrinos of $m_\nu \sim \lambda_\nu^2 \langle H \rangle^2 / M_{\nu_R}$, where M_{ν_R} is the Majorana mass of the right-handed neutrinos.[1] Thus if $\lambda_\nu \sim 1$ we find the correct neutrino masses for $M_{\nu_R} \sim 10^{10}$ GeV. This scale is very large, and hence requires some form of explanation. Thus we see that, if we wish to explain the small neutrino masses by taking the conservative step beyond the SM of adding in right-handed neutrinos, we face more questions that lead even further beyond the SM.

Another observation that hints at more particle physics beyond the SM is the observed abundance of dark matter (DM) in the Universe. The case for the existence of non-baryonic DM is strong, and the evidence now comes from a variety of independent observations (see e.g. [42] for a review). There is evidence resulting from velocity-dependent observations such as galactic rotation curves and the velocity dispersions of galaxies and galaxy clusters [43–49]. There also exist observations of gravitational lensing of light passing by galaxies and galaxy clusters [50], the most compelling of which is the Bullet Cluster, which shows a distribution of matter extending beyond the observed hot gas, consistent with the expected behaviour of DM [51]. There are also cosmological observations, such as the cosmic microwave background radiation [52], baryon acoustic oscillations (see e.g. [53]), supernovae redshift-distance relations

[1] See e.g. [41] and references therein.

and even the formation of large-scale structure [54, 55]. Thus particle physicists are obliged to try to explain these observations from a particle physics perspective. Intriguingly the SM does offer a DM candidate in the form of cosmic neutrinos. However, as the neutrino masses are constrained to be less than ~ 2 eV, [25], the energy density due to their relic abundance cannot constitute all of the DM [42]. In addition, as these neutrinos are light they stay relativistic until late times and hence their motion also suppresses the formation of structure until late times [56], however, contrary to this prediction, galaxies have been observed at high red-shift [57], adding to the arguments against neutrino DM. As a result the predictions for DM are in conflict with observations, and neutrinos are unsuccessful as a candidate for the majority of the DM. As neutrinos are the only neutral matter in the SM, this forces us to consider neutral, massive, particles which may exist beyond the SM. Building new theories of DM is not a trivial task, as one must evade constraints arising from the lack of observations of direct and indirect DM interactions with matter, and also explain the observed abundance in a cosmologically consistent manner, without spoiling any of the successes of SM cosmology. Thus usually additional structure beyond the simple addition of a neutral, massive particle is typically assumed, taking us further beyond the SM. However it should be noted that simple models involving just the addition of a single particle to the SM are still viable, for example in the 'Minimal DM' scenarios [58].

We discuss DM in greater detail in Chapter 6. In Chapter 7 we describe a new way in which the indirect effects of a particular class of DM, known as inelastic DM, could potentially be observed. In Chapter 8 we present a new model that simultaneously generates DM and baryon abundances in the early Universe, linking the two.

Finally, the SM has nothing to say about the quantum nature of gravity and simply coupling classical gravity to the SM leads to a non-renormalizable theory, and thus the loss of predictive power. The scale at which effects arising due to quantum gravity should become important lies close to the Planck scale, $M_P = 1.22 \times 10^{19}$ GeV, which is well beyond the energies at which we probe SM processes. However, we will see in section 1.1.3 that such effects may well be important for physics at the weak scale, and thus although the SM is a good effective theory below the weak scale, steps towards a more complete theory, beyond the SM, should in some way allow for the potential effects of quantum gravity.

1.1.3 Puzzles

In the previous section we discussed some observations which cannot be explained without adding greater particle content to the SM. However there also exist an additional set of puzzles which hint at new physics beyond the SM, even though the SM does not fail as an effective theory if these puzzles remain unaddressed.

The first of these puzzles has its origin in recent cosmological observations, which suggest the presence of a cosmological constant, Λ, in Einstein's field equations. This constant cannot be forbidden by any symmetries and is thus perfectly acceptable from a theoretical point of view. However, as this constant cannot be forbidden by any symmetries, then from an effective theory perspective one would expect it to take values close to the fundamental scale of the theory. For a gravitational theory we would expect the relevant scale to be the Planck scale. However, if we write $\Lambda = M^2$, then observations suggest that $M/M_P \sim 2 \times 10^{-61}$. This is a very small number. Further, even if we wished to set the bare value of Λ to this value by hand then, by the lack of a protecting symmetry, quantum corrections should drive it back up to the Planck scale. Thus, even if one could find a consistent cosmology in which $\Lambda = 0$, the problem persists - why not $\Lambda \sim M_P^4$, or even $\Lambda \sim \Lambda_{QCD}^4$? With the SM alone one is then forced to choose an extreme fine tuning of parameters, such that the bare value, plus quantum corrections, leads to the small value of Λ observed today. This fine tuning might be indicative of some extra dynamics beyond the SM, which could perhaps explain this mystery.

Another apparent fine tuning in the SM appears in a dimensionless quantity, namely the QCD vacuum parameter: θ_{QCD}. This, physical, CP-violating parameter is allowed in the QCD Lagrangian, and enters as

$$\mathcal{L} \supset -\frac{n_f g^2 \theta_{QCD}}{32\pi^2} F_{\mu\nu}\tilde{F}^{\mu\nu} \quad . \tag{1.1}$$

If we define $\overline{\theta} = \theta_{QCD} - \arg\det(M_q)$, where M_q is the quark mass matrix, then if $\overline{\theta} \sim 1$ this would lead to an electric dipole moment of the neutron comparable to 10^{-18} e.m. However, experimental limits on this quantity set an upper bound on $\overline{\theta}$ of $\overline{\theta} < 10^{-9}$ [59–63]. Again, this is an unexpected fine-tuning of a free parameter in the SM. It is possible to explain this small value if one is willing to go beyond the SM, and the QCD axion is perhaps currently the most compelling dynamical solution to this problem [63–67].

An additional puzzle arises when we consider the masses, and mixing structure of the massive fermions of the SM. All charged SM fermions obtain mass after electroweak symmetry breaking, however these masses span five orders of magnitude (not including neutrino masses). Although the SM accommodates this possibility in a technically natural way, it offers no explanation for why the SM fermions have such a range of couplings to the Higgs. Further puzzles arise in the form of the mixing parameters in the quark and lepton sector. The quark mixing parameters seem to obey a rough hierarchy with $\theta_{12} \sim \epsilon$, $\theta_{13} \sim \epsilon^2$, $\theta_{23} \sim \epsilon^3$, whereas the neutrinos have similar, large θ_{23} and θ_{12}, and small θ_{13}. It behoves the theorist to explain the observed structure in these parameters, however limits on flavour-violating rare decays, and on hadron oscillations, are strong and suggest that any physics associated with the generation of flavour structure should lie well above the weak scale.

The final puzzle concerns the sensitivity of the SM to physics at much higher energies, in the UV. The SM fermions are protected from gaining mass until electroweak symmetry is broken, due to the chiral nature of their gauge charges. The vector bosons in the SM are protected from gaining mass by gauge symmetry, and thus the electroweak bosons can only gain mass at the scale of electroweak symmetry breaking. However the remaining, as yet undiscovered, particle, the Higgs boson, is special.

Whenever we consider the new physics that we expect to exist at higher scales, such as the Planck or GUT scales, then any corrections to the SM that might arise due to these new fundamental degrees of freedom should come associated with these mass-scales.[2] From an effective field theory perspective, then at low scales there should be corrections to already existing operators, or even the generation of new operators, in the SM involving powers of the Planck mass or the GUT scale. We would then also expect the Higgs mass to be subject to these corrections, and expect it to be dragged up to these high scales by integrating out the new physics, even if the 'bare' mass is at the weak scale. The scale of electroweak symmetry breaking is determined from the Higgs mass, and thus we are left with a well-defined puzzle: why is $M_{EW} \sim 10^{-16} M_P$, or $M_{EW} \ll M_{GUT}$? Thus if we are to embed the SM into a larger theory containing higher mass-scales, in the absence of any symmetry or principle protecting the Higgs from these corrections, we have to accept unnatural fine-tunings at all loop orders. This is the hierarchy problem, and has been a central consideration to many ideas concerning physics beyond the SM. This puzzle hints at

[2] A clear analogy arises when we consider nuclear beta-decay. Nuclear beta-decay occurs at energies many orders of magnitude below the weak-scale, however it can be well described by a non-renormalisable four-fermion operator suppressed by a weak-scale mass-squared. Thus the presence of new physics at energies of ~ 80 GeV could be inferred well before the W-boson was produced in colliders.

some extra physics, or symmetry, which protects the Higgs mass down to much lower energies, making it insensitive to physics at the Planck-scale, or any other high scale.

1.2 Beyond the Standard Model

Any theory of physics beyond the SM should attempt to address the failures of the SM discussed before. However, as the number of possibilities in any such attempt is very large, it is appealing to use the puzzles of the SM as a guide towards general structures. Developing theories with DM candidates, small neutrino masses, or successful baryogenesis, typically requires the addition of some new particles. However the nature of the hierarchy problem is such that radical changes to the theory are required if the Higgs sector is to be protected from physics at energy scales 16 orders of magnitude above the weak scale. For example, these radical changes can include additional strongly-coupled sectors, of which the Higgs boson is a composite of strongly coupled fermions. Or they can come in the form of small, warped, extra spatial dimensions in addition to the three we are familiar with from everyday experience. Or, perhaps most radical, is to introduce additional, fermionic, space-time symmetries under which the Higgs boson transforms. This last option is called Supersymmetry.

Part I

Supersymmetry

Chapter 2

Supersymmetry

2.1 Supersymmetric theories

We saw in section 1.1.3 that in order to address the hierarchy problem it is necessary to protect the Higgs from receiving large corrections to its mass from physics at high scales. It is difficult to do this by charging the Higgs under a bosonic symmetry, such as a $U(1)$ symmetry, as the mass-term is already invariant under such a symmetry. However, this is not necessarily true if we allow the Higgs be charged under a symmetry which has non-trivial space-time structure. In 1967 Coleman and Mandula proved that it is impossible to combine the Poincaré and internal symmetries in any but a trivial way. Intriguingly, this proof only applied to Lorentz scalar, i.e. bosonic, internal symmetries, and in 1975 Haag, Lopuszanski, and Sohnius showed that, in addition to internal and Poincaré symmetries, it is possible to extend the Poincaré symmetry to include spin-1/2 generators in a consistent quantum field theory. This extension is known as supersymmetry. The supersymmetry generators must commute with the Hamiltonian, and convert fermionic states to bosonic states, and vice-versa. We call the SUSY generators Q_α ($\alpha = 1, 2$) and their complex conjugate $\overline{Q}_{\dot{\alpha}}$ ($\dot{\alpha} = \dot{1}, \dot{2}$). These are spinor quantities, and obey the commutation and anti-commutation relations

$$[P^\mu, Q_\alpha] = [P^\mu, \overline{Q}_{\dot{\alpha}}] = 0 \tag{2.1}$$

$$\{Q_\alpha, Q_\beta\} = \{\overline{Q}_{\dot{\alpha}}, \overline{Q}_{\dot{\beta}}\} = 0 \tag{2.2}$$

$$\{Q_\alpha, \overline{Q}_{\dot{\beta}}\} = 2\sigma^\mu_{\alpha\dot{\beta}} P_\mu \tag{2.3}$$

where P^μ is the generator of translations. I have shown only the commutation and anti-commutation relations for one set of supercharges, e.g. $\mathcal{N} = 1$ SUSY, however it is straightforward to generalise these relations to more supercharges. I will continue to focus on the case of $\mathcal{N}=1$ SUSY throughout this thesis. As these generators change the spin of a state by a unit of 1/2, one would expect that in a supersymmetric theory states come with some sort of 'multiplet' structure, in which there is a state of spin S and a state of spin $S+1/2$, where $S=0,1/2$ for a renormalizable theory. These multiplets are called 'supermultiplets', and we will now consider how they are constructed.

In order to begin constructing such multiplets it is instructive to begin by considering the supersymmetry algebra as a graded Lie algebra. By extending the analogy with space-time translations, we define the group element

$$G(x,\theta,\overline{\theta}) = e^{-i(x_\mu P^\mu - \theta Q - \overline{\theta Q})} \quad , \tag{2.4}$$

where θ and $\overline{\theta}$ are anti-commuting parameters. Now, using Hausdorff's formula one can show that under a transformation with parameters $\{x,\theta,\overline{\theta}\}$ followed by a SUSY transformation with parameters $\{\zeta,\overline{\zeta}\}$ we have the set of transformations

$$x^\mu \;\rightarrow\; x^\mu + i\theta\sigma^\mu\overline{\zeta} - i\zeta\sigma^\mu\overline{\theta} \tag{2.5}$$

$$\theta \;\rightarrow\; \theta+\zeta \tag{2.6}$$

$$\overline{\theta} \;\rightarrow\; \overline{\theta}+\overline{\zeta} \quad . \tag{2.7}$$

This transformation in parameter space can be generated by the differential operators Q and $\overline{Q}$

$$\zeta Q + \overline{\zeta Q} = \zeta^\alpha \left(\frac{\partial}{\partial\theta^\alpha} - i\sigma^\mu_{\alpha\dot{\alpha}}\overline{\theta}^{\dot{\alpha}}\partial_\mu\right) + \overline{\zeta}_{\dot{\alpha}}\left(\frac{\partial}{\partial\overline{\theta}_{\dot{\alpha}}} - i\theta^\alpha\sigma^\mu_{\alpha\dot{\beta}}\epsilon^{\dot{\beta}\dot{\alpha}}\partial_\mu\right) \quad . \tag{2.8}$$

Again, by analogy with fields which are functions of space-time co-ordinates, we can define a superfield as a field which is a function of the co-ordinates $\{x,\theta,\overline{\theta}\}$. Henceforth we will write superfields in bold font, and their component fields in plain font. As θ and $\overline{\theta}$ are Grassmann parameters, the Taylor expansion of a superfield in these co-ordinates terminates as, e.g. $\theta_1\theta_1=0$. Thus, calling our superfield $\boldsymbol{F}(x,\theta,\overline{\theta})$, and expanding in the Grassmann parameters, we have

$$\begin{aligned}\boldsymbol{F}(x,\theta,\overline{\theta}) \;=\;& f(x) + \theta\phi(x) + \overline{\theta}\overline{\chi}(x) + \theta\theta m(x) + \overline{\theta\theta}n(x) + \theta\sigma^\mu\overline{\theta}v_\mu(x)\\ &+\theta\theta\overline{\theta\lambda}(x) + \overline{\theta\theta}\theta\psi(x) + \theta\theta\overline{\theta\theta}d(x)\end{aligned} \tag{2.9}$$

which transforms under a SUSY transformation as

$$\delta_\zeta \boldsymbol{F}(x,\theta,\overline{\theta}) \equiv (\zeta Q + \overline{\zeta Q})\boldsymbol{F} \quad . \tag{2.10}$$

By comparing individual powers of θ after applying the SUSY transformation of eq.(2.10) we can determine how the individual fields transform. Also, as the Taylor expansion in θ terminates, we can see that the product of two, or more, superfields must itself be a superfield, where the individual component fields are products of component fields of the original 'fundamental' superfields.

Now we have a linear representation of the SUSY algebra, however, this representation can be reduced. We define a chiral superfield, $\mathbf{\Phi}$, by the constraint $\overline{D}_{\dot{\alpha}}\mathbf{\Phi} = 0$, where $\overline{D}_{\dot{\alpha}} = -\partial/\partial\overline{\theta}^{\dot{\alpha}} - i\theta^{\alpha}\sigma^{\mu}_{\alpha\dot{\alpha}}\partial_{\mu}$. Thus our chiral superfield takes the form

$$\begin{aligned}\mathbf{\Phi}(x,\theta) &= A(x) + i\theta\sigma^{\mu}\overline{\theta}\partial_{\mu}(x)A(x) + \frac{1}{4}\theta\theta\overline{\theta\theta}\partial_{\mu}\partial^{\mu}A(x) \\ &\quad +\sqrt{2}\theta\psi(x) + \frac{i}{\sqrt{2}}\theta\theta\partial_{\mu}\psi\sigma^{\mu}\overline{\theta} + \theta\theta F(x) \qquad (2.11)\end{aligned}$$

and an anti-chiral superfield takes a similar form, following from $D_{\alpha}\mathbf{\Phi}^{\dagger} = 0$.

The components of the superfield in eq.(2.11) transform under SUSY transformations as

$$\delta_{\zeta}A = \sqrt{2}\zeta\psi \qquad (2.12)$$

$$\delta_{\zeta}\psi = i\sqrt{2}\sigma^{\mu}\overline{\zeta}\partial_{\mu}A + \sqrt{2}\zeta F \qquad (2.13)$$

$$\delta_{\zeta}F = i\sqrt{2}\overline{\zeta}\overline{\sigma}^{\mu}\partial_{\mu}\psi \quad . \qquad (2.14)$$

From these transformations we see that the F-term transforms into a total derivative. If all fields vanish at infinity then the F-term of a chiral superfield forms a SUSY-invariant Lagrangian term. It follows that the F-term of any product of chiral superfields is a SUSY-invariant Lagrangian term. In addition, the $\theta^2\overline{\theta}^2$ term in $\Phi^{\dagger}\Phi$ also transforms into a total derivative. This term is then also a candidate for a SUSY-invariant term in the Lagrangian, and is given in component form as

$$\begin{aligned}\mathbf{\Phi}^{\dagger}\mathbf{\Phi}|_{\overline{\theta}^2\theta^2} &= F^*F + \frac{1}{4}A^*\partial^2 A + \frac{1}{4}\partial^2 A^* A - \frac{1}{2}\partial_{\mu}A^*\partial^{\mu}A \\ &\quad +\frac{i}{2}\partial_{\mu}\overline{\psi}\overline{\sigma}^{\mu}\psi - \frac{i}{2}\overline{\psi}\overline{\sigma}^{\mu}\partial_{\mu}\psi \qquad (2.15)\end{aligned}$$

clearly giving the kinetic terms for the individual component fields.

Thus we are in a position to construct a SUSY-invariant theory with chiral superfields. We can introduce one further ingredient which simplifies notation. If we define $\int d\theta = 0$ and $\int \theta d\theta = 1$, then we can write our supersymmetric Lagrangian as

$$\mathcal{L} = \int d^2\overline{\theta}d^2\theta\mathbf{\Phi}_i^{\dagger}\mathbf{\Phi}_i + [\int d^2\theta(f_i\mathbf{\Phi}_i + m_{ij}\mathbf{\Phi}_i\mathbf{\Phi}_j + \lambda_{ijk}\mathbf{\Phi}_i\mathbf{\Phi}_j\mathbf{\Phi}_k) + \text{h.c}] \quad , \qquad (2.16)$$

where the first term is usually referred to as the Kähler potential, K, and the second term is the Superpotential, W, so we can re-write this Lagrangian as

$$\mathcal{L} = \int d^2\overline{\theta}d^2\theta K(\mathbf{\Phi}_i^\dagger, \mathbf{\Phi}_i) + \int d^2\theta W(\mathbf{\Phi}_i) + \int d^2\overline{\theta} W^*(\mathbf{\Phi}_i^*) \quad , \tag{2.17}$$

where W is a function of chiral superfields only, and not their conjugates. Because of this we say that the superpotential is a 'holomorphic' function of the chiral superfields. By defining $W^i = \frac{\partial W}{\partial A_i}|_{\theta=0}$, and W^{ij} by analogy, then we find

$$\int d^2\theta W(\mathbf{\Phi}_i) = W^i F_i - \frac{1}{2} W^{ij}\psi_i\psi_j - \text{(total derivative)} \quad . \tag{2.18}$$

By inspecting the kinetic terms for the component fields in eq.(2.15) we can see that there are no derivative terms for the field F, and thus it does not propagate. We can then simplify the supersymmetric Lagrangian by solving the Euler-Lagrange equation for F, i.e. solving $\partial\mathcal{L}/\partial F = 0$. After performing this final step we find that $F_i = -W^{*i}$. Using this, rearranging total derivative terms, and employing the equations of motion, our final supersymmetric Lagrangian, in component form, is

$$\mathcal{L} = \partial_\mu A^{*i}\partial^\mu A_i + i\overline{\psi}^i\overline{\sigma}^\mu\partial_\mu\psi_i - \frac{1}{2}\left(W^{ij}\psi_i\psi_j + W^*_{ij}\overline{\psi}^i\overline{\psi}^j\right) - W^{*i}W_i \quad . \tag{2.19}$$

This completes the construction of theories with $\mathcal{N} = 1$ supersymmetry containing scalars and fermions.

In order to include gauge interactions we must also construct theories with vector fields, which are contained in real vector superfields. These arise by considering a superfield, $\boldsymbol{V}$, which is constrained to satisfy $\boldsymbol{V}^* = \boldsymbol{V}$. Such a superfield can be constructed from the general superfield in eq.(2.9). The general form for $\boldsymbol{V}$ contains numerous component fields, however it is possible to remove some of these fields by performing a suitable gauge transformation. The supersymmetric generalisation of an Abelian gauge transformation acts on $\boldsymbol{V}$ as $\boldsymbol{V} \to \boldsymbol{V} + \mathbf{\Lambda} + \mathbf{\Lambda}^*$, where $\mathbf{\Lambda}$ is a chiral superfield. It can be seen by comparing eq.(2.9) and eq.(2.11) that this will correspond to a gauge transformation of $v_\mu(x) \to v_\mu(x) + \partial_\mu(A(x) - A^*(x))$, as expected.

By choosing the 'Wess-Zumino' gauge, in which the extra unwanted component fields are gauged away, we have

$$\boldsymbol{V} = -\theta\sigma^\mu\overline{\theta}v_\mu(x) + i\theta\theta\overline{\theta}\overline{\lambda}(x) - i\overline{\theta}\overline{\theta}\theta\lambda(x) + \frac{1}{2}\theta\theta\overline{\theta}\overline{\theta}D(x) \quad , \tag{2.20}$$

where $v_\mu(x)$ is a vector field, $\lambda(x)$ is its fermionic partner, the 'gaugino', and $D(x)$ is a scalar field. We see that $\boldsymbol{V}$ is the supersymmetric generalisation of the Yang-Mills potential A^μ. The transformation of the component fields under supersymmetry can again be calculated, and it is found that the field $D(x)$ transforms into a total derivative. We will also need to construct a gauge-invariant field strength. From eq.(2.20) we see that the lowest gauge-invariant components are λ and $\overline{\lambda}$. Hence we can construct a gauge invariant chiral superfield $\boldsymbol{W}_\alpha = -\frac{1}{4}\overline{DD}D_\alpha \boldsymbol{V}$, where chirality follows from $\overline{D}_{\dot{\beta}}\boldsymbol{W}_\alpha = 0$.

Now we can construct supersymmetric kinetic terms for the gauge fields as

$$\int d^2\theta \frac{1}{4}\boldsymbol{W}^\alpha \boldsymbol{W}^\alpha + \int d^2\overline{\theta}\frac{1}{4}\overline{\boldsymbol{W}}^{\dot{\alpha}}\overline{\boldsymbol{W}}_{\dot{\alpha}} = \frac{1}{2}D^2 - \frac{1}{4}F^{\mu\nu}F_{\mu\nu} - i\lambda\sigma^\mu\partial_\mu\overline{\lambda} \quad . \tag{2.21}$$

This completes the construction of an Abelian SUSY gauge sector, however it now remains to include gauge interactions with matter fields.

The lowest component of a chiral superfield is a complex scalar field, which will transform under Abelian gauge transformations by multiplication of a space-time dependent phase. It is clear, then, that in the language of superfields, a gauge transformation of a chiral superfield will proceed as $\boldsymbol{\Phi} \to e^{-ig\boldsymbol{\Lambda}}\boldsymbol{\Phi}$. By considering the gauge transformation of a vector superfield we then see that the combination $\boldsymbol{\Phi}^* e^{g\boldsymbol{V}}\boldsymbol{\Phi}$ is gauge invariant, however $\boldsymbol{\Phi}^*\boldsymbol{\Phi}$ is not. Therefore, to construct a supersymmetric theory with gauge interactions we use the gauge kinetic terms of eq.(2.21), we impose that the superpotential W is gauge invariant, and we adapt the Kähler potential terms to the form $\boldsymbol{\Phi}^*\boldsymbol{\Phi} \to \boldsymbol{\Phi}^* e^{g\boldsymbol{V}}\boldsymbol{\Phi}$

Finally, from eq.(2.21) we see that we have a new non-propagating auxiliary field, D. Once again we can solve for $\partial\mathcal{L}/\partial D = 0$ and find that $D = g\sum_i q_i A^{*i}A_i$. After performing this final simplification, rearranging total derivative terms, and extending to the case where the chiral superfields transform under a non-abelian gauge symmetry, we have a supersymmetric gauge theory, with Lagrangian

$$\begin{aligned}
\mathcal{L} \quad = \quad & -\frac{1}{4}F^{a\mu\nu}F^a_{\mu\nu} + i\overline{\lambda}^a\sigma^\mu D_\mu\lambda^a + D_\mu A^{*i}D^\mu A_i + i\overline{\psi}^i\overline{\sigma}^\mu D_\mu\psi_i \\
& + i\sqrt{2}g\sum_a (A^{*i}T^a\psi_i\lambda^a - \overline{\lambda}^a T^a A_i\overline{\psi}^i) - \frac{g^2}{2}\sum_a(\sum_i A^{*i}T^aA_i)^2 \\
& -\frac{1}{2}\left(W^{ij}\psi_i\psi_j + W^*_{ij}\overline{\psi}^i\overline{\psi}^j\right) - W^{*i}W_i \quad ,
\end{aligned} \tag{2.22}$$

where D_μ is the gauge-covariant derivative, and T^a is a generator of the non-abelian gauge group. This completes the construction of supersymmetric gauge theories.

It is possible, but not required, that a supersymmetric theory can possess a global $U(1)$ symmetry under which θ transforms. This symmetry is usually referred to as an

R-symmetry, and it is special as it distinguishes between components of a supermultiplet. If this symmetry is present, and θ has charge q_R then the superpotential has charge $2q_R$ and individual physical components of a chiral or vector superfield differ in charge by a unit of q_R. Any other global symmetries act on individual components of a chiral multiplet in the same way, and do not act on vector multiplets.

2.1.1 Quadratic divergences

One of the most attractive features of SUSY is the absence of quadratic divergences. This can be explained quite simply, although this section does not constitute a rigourous proof. As shown before, the superpotential is a holomorphic function of the chiral superfields. In addition, any relevant operators must arise from the superpotential in a renormalizable SUSY theory. We can consider any parameters as SUSY-preserving vacuum expectation values (vevs) of some background chiral superfield, and can then write our superpotential with the understanding that all parameters are actually vevs of fields, and assign global symmetry charges to these vevs to find the selection rules. For example, we can consider a toy model with superpotential

$$W = \frac{m}{2}\boldsymbol{\phi}^2 + \frac{\lambda}{3}\boldsymbol{\phi}^3 \quad . \tag{2.23}$$

This theory has a global $U(1)_R$ symmetry and a global $U(1)$ symmetry, which are both broken by non-zero values for m and λ, i.e. VEVs. However we can still use the selection rules that arise as a result of these symmetries. We can then write down all renormalizable, holomorphic, terms which behave well in the limits $m \to 0$ and $\lambda \to 0$. Doing this we find that the only superpotential terms that are allowed are those already in eq.(2.23). Thus if we consider renormalizing this theory down to some scale then no new terms can arise in the superpotential involving the cut-off. This has been proven at a greater level of rigour for SUSY theories using supergraph techniques [68–71], and using the holomorphicity of the superpotential [72, 73], and is general referred to as the 'Non-renormalization' theorem.

The Kähler potential gives the standard kinetic terms, which are still renormalized, giving rise to wavefunction renormalization. Therefore terms in the superpotential are only renormalized through wavefunction renormalization. Wavefunction renormalization is only logarithmic in the cut-off, hence no quadratic divergences occur in this theory. Again, it can be shown, along these lines, that this is true in general for SUSY theories.

2.1.2 Supersymmetry breaking

As we have not observed any scalar particles with electric charge -1 and a mass of 511 keV we must conclude that the Universe is not supersymmetric, i.e. supersymmetry is broken. However, this does not mean that supersymmetric theories don't offer a resolution to the hierarchy problem: If supersymmetry is restored at high energies then the hierarchy problem is relieved to the point that the only troublesome hierarchy is between the electroweak scale and the scale at which the theory becomes supersymmetric.

If we want a theory in which a symmetry is present at high energies, but apparently absent at low energies, we require that the symmetry is spontaneously broken somewhere along the way. As supersymmetry is inherently tied to space-time symmetries we must be careful if we want to break supersymmetry spontaneously but not Lorentz symmetry. From the last of the anti-commutation relations in eq.(2.3) we see that the vacuum energy, P_0, is given by

$$H = P_0 = \frac{1}{4}(\{Q_1, \overline{Q}_{\dot{1}}\} + \{Q_2, \overline{Q}_{\dot{2}}\}) \quad . \tag{2.24}$$

As a result, in a globally supersymmetric theory, $\langle 0|H|0\rangle \neq 0$ implies that $Q_\alpha|0\rangle \neq 0$ or $\overline{Q}_{\dot{\alpha}}|0\rangle \neq 0$, and supersymmetry is broken. If we want to find a vacuum in which supersymmetry is spontaneously broken we must then find one with non-vanishing energy density. If we want to maintain Lorentz symmetry then the only fields which obtain vacuum expectation values (VEVs) must be Lorentz scalars, hence the only candidate terms are from the scalar potential. However the scalar potential comes from $V_{\text{scalar}} = \frac{1}{2}F^{*i}F_i + \frac{g^2}{2}D^aD^a$. Thus we know that for a supersymmetric theory to spontaneously break supersymmetry requires a cosmologically stable vacuum in which $F_i \neq 0$ or $D^a \neq 0$.

By analogy with spontaneously broken global symmetries, which give rise to a massless Nambu-Goldstone boson, when global SUSY is spontaneously broken this leads to a massless Nambu-Goldstone fermion, named the 'Goldstino'. Why this is so can be seen quite simply for F-term breaking of SUSY. At the minimum of the scalar potential we require that $dV/dA_i = 0$ and this implies that $W_i^* W^{ij} = 0$. If there is F-term SUSY breaking then $\text{Abs}[W_i^*] \neq 0$, and hence W_{ij} has a zero eigenvalue, with eigenvector W_i^*. But the fermion mass matrix is given by W_{ij}, and, as a result, there must exist a massless fermion, which lives in the chiral multiplet that breaks SUSY. A similar argument applies for D-term breaking, however in this case the goldstino is a gaugino of a vector multiplet. In Chapter 4 we investigate the possibility of multiple

'Goldstini' which might arise if SUSY is broken dynamically by a SUSY QCD-like theory.

The spontaneous breaking of supersymmetry leads to mass-splittings between component fields of a superfield. It can be shown that in a theory with spontaneous SUSY breaking a mass-sum rule, $\mathrm{Tr}[M^2_{\mathrm{scalars}}] = 2\mathrm{Tr}[M^2_{\mathrm{fermions}}]$, where the scalars are real, is obeyed. This rule implies that if SUSY is broken spontaneously in the visible sector we should have observed scalars with SM charges as light as the lightest fermions. As these scalars have not been observed then SUSY must be broken in another sector, and then this SUSY-breaking must be communicated to the visible sector, raising the masses of the unobserved superpartners.

This pattern of SUSY-breaking can be accounted for if we allow for some 'spurion' superfield, $\boldsymbol{X}$, with non-zero F-term in the vacuum, i.e. $\langle \boldsymbol{X} \rangle = \theta^2 F_X$. Alternatively one can consider a vector superfield with a non-zero D-term. If some 'messengers' which communicate with the SUSY-breaking sector and the visible sector have mass $M_M \gg M_{\mathrm{weak}}$ we can integrate them out, and include their effects by considering the effective field theory, with higher dimension operators involving the field $\boldsymbol{X}$ and the visible sector fields. Operators such as

$$K \supset \frac{\boldsymbol{X}^\dagger \boldsymbol{X}}{M_M^2} \boldsymbol{\Phi}_i^* \boldsymbol{\Phi}_i \quad , \quad W \supset \frac{\boldsymbol{X}}{M_M} \boldsymbol{\Phi}_i \boldsymbol{\Phi}_j \boldsymbol{\Phi}_k \quad , \quad W \supset \frac{\boldsymbol{X}}{M_M} \boldsymbol{W}^\alpha \boldsymbol{W}_\alpha \quad , \tag{2.25}$$

lead to SUSY-breaking mass-terms for the scalars of a chiral superfield, $\tilde{m} = F_X/M_M$, trilinear scalar interactions, $|A_{ijk}| = F_X/M_M$, or mass terms for the gauginos in a vector superfield, $M_\lambda = F_X/M_M$. All such terms break supersymmetry 'softly', as they do not introduce new quadratic UV-divergences into the theory, and only lead to quadratic divergences up to the scale of the soft-terms.

The messenger superfields could be associated with some UV-completion, and would thus typically have $M_M \simeq M_P$, where M_P is the Planck mass. This scenario is usually referred to as 'Gravity Mediation'. Alternatively they could potentially have much lower mass, and communicate with the visible sector through gauge interactions. In this case M_M is not set, but the soft terms come dressed with a loop-factor involving gauge charges.

As SUSY must be broken in a 'hidden sector' this raises the possibility that there may be multiple sectors which break SUSY. In Chapter 5 we show that even if only one fundamental spontaneous SUSY-breaking sector exists this SUSY breaking can lead to other sectors being 'stimulated' into spontaneously breaking SUSY at much higher scales than the breaking experienced due to the fundamental SUSY breaking.

In Chapter 4 we also study the implications that multiple SUSY-breaking sectors would have for physics at the weak scale.

2.1.3 Supergravity

General relativity (GR) is a successful theory of gravity on macroscopic scales, and is hence desirable in any physical theory. We can think of GR as a theory of gauged local Lorentz transformations, however, by going to a SUSY theory we have extended the Lorentz group to include fermionic generators. Thus, if we gauge the Lorentz transformations we must also gauge local SUSY transformations in order to maintain SUSY. In doing so we find a theory of *local* supersymmetry. This theory is called 'Supergravity' (SUGRA). It is sometimes touted as a surprising, and/or compelling, feature that gauging SUSY leads to GR, however this should really come as no surprise as we still have the Lorentz group as a subgroup of the general SUSY transformations, and one should then expect that gauging these transformations would lead to GR.

There are many interesting features of SUGRA, which is a subject of much study in its own right, however, for brevity, we will only comment on the features relevant to this thesis. Perhaps the most interesting relevant feature of SUGRA is the requirement of a new spin-3/2 field, called the gravitino, which is partnered with the graviton. This field has its own set of Planck-suppressed interactions with other SUSY fields. An interesting analogy with local gauge theories arises when SUSY is spontaneously broken. When a global symmetry is spontaneously broken we expect a massless Nambu-Goldstone boson, and if this symmetry is gauged we expect this boson to be 'eaten' by the massless gauge boson, leading to a massive gauge boson. Interestingly, when SUSY is spontaneously broken we have a massless fermion, the goldstino, however in a SUGRA theory this goldstino is 'eaten' by the gravitino, leading to a massive gravitino.

If multiple SUSY-breaking sectors are imbedded in SUGRA then only one combination of the multiple goldstini is eaten by the gravitino. However, somewhat surprisingly, the other 'left-over' goldstini acquire a tree-level mass of $2m_{3/2}$ [74, 75]. In Chapter 4 we demonstrate this explicitly, along with alterations and additions to this scenario that can arise.

2.1.4 The MSSM

Now we are equipped to construct a supersymmetric theory of the known particles and interactions. We will consider first the minimal model, a.k.a. the 'Minimal Supersymmetric Standard Model' (MSSM). In a supersymmetric version of the SM we will have to introduce superpartners for all of the known fields of the standard model. It is conventional notation to denote a superpartner of a SM field with a tilde, i.e. a $\tilde{e}_L$ is the superpartner of the left-handed electron. The fermions of the standard model are contained in chiral superfields, and thus we introduce 'squarks' in addition to the quarks, and 'sleptons' in addition to leptons. Scalar partners of SM fermions are individually named with an 's' in front of the name of their fermion partner, i.e. sneutrino, selectron, sbottom, etc. The gauge fields will have to live in a vector superfield and will thus have fermionic superpartners. The partners of the gauge fields are termed 'gauginos' and, in specific cases, are differentiated from their bosonic partners by the suffix 'ino'. Thus along with gluons we now have gluinos, with W-bosons winos, and with the hypercharge boson the bino. After electroweak symmetry breaking we have charginos and two neutralinos from the electroweak gauge sector.

The simple extension of the SM to a SUSY theory enters difficulties when we consider the SM Higgs boson. Because the Higgs is a scalar, in a SUSY theory it will have a fermionic partner, the higgsino. This higgsino will have SM gauge charges and is a new fermion contributing to anomalies in the previously anomaly-free SM. Thus in order to cancel this new contribution we must add an additional chiral superfield with the opposite gauge charges of the Higgs. Hence a supersymmetric theory has two Higgs doublets, as opposed to one in the SM, and these doublets are 'vector-like', as they have equal and opposite gauge charges. It is often stated that, as the superpotential is holomorphic and terms such as $H_U^\dagger Q D^c$ are not allowed, then an extra Higgs doublet must be introduced in order to give down-type fermions mass. However this is not strictly true, as we know that SUSY must be broken, and once SUSY is broken such arguments do not apply. In Chapter 3 we construct an explicit SUSY model which makes use of this fact. This model has only one Higgs doublet, and thus the Higgs sector is very close to that of the SM, unlike in the MSSM.

The superfields of the MSSM are summarised in table 2.1.4. The kinetic terms and gauge interactions for all fields are as in eq.(2.22), and the superpotential for the MSSM is

$$W_{\text{MSSM}} = \mu \boldsymbol{H_u H_d} + \lambda_u \boldsymbol{H_u Q U^c} + \lambda_d \boldsymbol{H_d Q D^c} + \lambda_e \boldsymbol{H_d L E^c} \tag{2.26}$$

where the λ are 3×3 Yukawa couplings and summation over flavour indices is implied. Additional gauge-invariant, renormalizable, terms which violate baryon or lepton number are also allowed. These are $\boldsymbol{LLE^c}$, $\boldsymbol{U^c D^c D^c}$, $\boldsymbol{LQD^c}$ and $\mu_L \boldsymbol{LH_u}$. These terms can lead to rapid proton decay, amongst other forbidden processes, and

Field	Gauge rep.	R-parity	Supermultiplet
$\boldsymbol{Q}$	$(\mathbf{3}, \mathbf{2}, \frac{1}{6})$	-1	Chiral
$\boldsymbol{U^c}$	$(\overline{\mathbf{3}}, \mathbf{1}, -\frac{2}{3})$	-1	Chiral
$\boldsymbol{D^c}$	$(\overline{\mathbf{3}}, \mathbf{1}, \frac{1}{3})$	-1	Chiral
$\boldsymbol{L}$	$(\mathbf{1}, \mathbf{2}, -\frac{1}{2})$	-1	Chiral
$\boldsymbol{E^c}$	$(\mathbf{1}, \mathbf{1}, 1)$	-1	Chiral
$\boldsymbol{H_u}$	$(\mathbf{1}, \mathbf{2}, \frac{1}{2})$	1	Chiral
$\boldsymbol{H_d}$	$(\mathbf{1}, \mathbf{2}, -\frac{1}{2})$	1	Chiral
$\boldsymbol{G}$	$(\mathbf{8}, \mathbf{1}, 0)$	1	Vector
$\boldsymbol{W}$	$(\mathbf{1}, \mathbf{3}, 0)$	1	Vector
$\boldsymbol{B}$	$(\mathbf{1}, \mathbf{1}, 0)$	1	Vector

Table 2.1: The superfield content of the MSSM.

thus should be suppressed. To do this we impose an additional global symmetry by hand. This symmetry is a discrete $\mathbb{Z}_2$ symmetry known as R-parity. The R-parity charges of the MSSM superfields are shown in table 2.1.4, and the Grassmann parameter θ is also odd under this parity, hence the name 'R'-parity. As θ is charged under this parity superpartners within a supermultiplet have different charges. Thus all SM fermions, gauge bosons, and both scalar Higgs doublets are even under this parity, whereas all superpartners such as gauginos, squarks, sleptons and higgsinos, are odd. Hence R-parity distinguishes between the SM particles and those which we have added, with the exception of the extra Higgs doublet. The model in Chapter 3 extends this R-parity to a full, anomaly-free, $U(1)_R$ symmetry.

The model as described so far is completely supersymmetric, however we have not observed any R-parity odd particles, and thus we must softly break the supersymmetry. This is achieved at a phenomenological level by adding soft masses for all scalar fields and all gauginos. We must also add to the scalar potential trilinear scalar interactions with the same structure as the trilinear terms in the superpotential in eq.(2.26), as well as a 'B_μ' term $\mathcal{L} \supset B\mu H_u H_d$ which mixes the two Higgs fields. All such soft-parameters are, in general, complex, and need not have the same flavour structure as the SM Yukawa couplings. This completes the construction of the MSSM as a phenomenological model.

2.1.5 Successes and motivation

The greatest success of the MSSM is that it addresses the hierarchy problem by removing quadratic divergences, thus stabilising the electroweak scale against corrections from unknown physics in the far UV. There are however, additional hints that add to the appeal of the MSSM. We briefly discuss these in no particular order.

It has long been hoped that all of the observed forces could be unified into one unique structure. Including gravity in this unification would likely require drastic measures, and one good candidate for such unification is string theory. However, a more modest goal is to unify the three non-gravitational forces, strong, weak and electromagnetic, into a grand unified theory (GUT). The weak and electromagnetic forces are successfully described by the electroweak theory, however it still remains to unify the strong with the electroweak. Evidence for such unification would arise if all three coupling constants unify at a given energy, at which point additional new physics enters the game and all three forces unite into one gauge theory. One hint that the MSSM may underpin the structure of the SM comes from how the three gauge couplings run. With the particle content of the SM, when you run the gauge couplings for $SU(3)_C$, $SU(2)_W$ and $U(1)_Y$ up to arbitrarily high energies they almost converge, but eventually miss each other. When one includes the additional particles of the MSSM and calculate the running of the gauge couplings at one-loop they meet very accurately [76], however at two-loops the gauge-couplings have to be taken away from their central values at the electroweak scale in order to maintain the unification (see e.g. [77]). This happens at an energy scale of $\sim 10^{16}$ GeV, however the precise value depends on the masses of the superpartners. This could just be a coincidence, but can also be interpreted as a hint that the MSSM may fit into a GUT, and is in fact a hint of such structures at high energies.

An additional, unexpected feature of the MSSM is that, for a large range of parameters, the mass of the up-type Higgs boson is driven negative by radiative corrections. The result being that even if the electroweak gauge symmetry is unbroken in the theory at high energies, when one runs all of the parameters down to the weak scale the Higgs mass-squared becomes negative, and the electroweak gauge symmetry is spontaneously broken. This is due to the large Yukawa coupling of the Higgs multiplet to the top multiplet. Electroweak symmetry breaking in this manner is not always guaranteed, however it does seem to be a fairly generic feature of the MSSM, and similar extensions. Additionally, the Higgs seems to be special in this respect as for most parameter regions no other scalars are driven to develop a vev.

Another hint lies in the problem of baryogenesis. It is known that in order to generate an asymmetry between baryons and antibaryons in the early Universe the three conditions of baryon-number violation, CP-violation, and out of thermal equilibrium dynamics must be satisfied. It was once hoped that such conditions could be present during the electroweak phase transition, as there is CP-violation in the quark sector, baryon-number violation due to electroweak non-perturbative effects (sphalerons) and if the electroweak phase transition is strongly first-order enough then in the bubble walls, which separate the symmetric phase from the broken phase, there should exist out of thermal equilibrium conditions. Unfortunately, in the SM these conditions are not met to the extent that the observed asymmetry can be achieved. However, going beyond the SM it is possible to meet these conditions, with the introduction of new sources for all three necessary conditions. A plethora of models for baryogenesis exist, but even within the MSSM such a scenario is now possible.

A further attractive feature of the MSSM arises as a result of protecting protons from decaying. In section 2.1.4 we showed that an extra global symmetry, R-parity, must be imposed in order to conserve baryon number and lepton number at the renormalizable level. This extra symmetry largely distinguishes between SM particles and their partners, and has the consequence that the lightest of the superpartners cannot decay, and is thus cosmologically stable. If this stable particle is charged, or coloured then this stability is disastrous, however if it is neutral then it may be a candidate for DM. It turns out that there are ten neutral particles, four 'neutralinos' which are each a mixture of the bino, zino, and two higgsinos, and there are also three neutral sneutrinos. The correct abundance of all of these particles can remain as a result of the thermal freeze-out mechanism, suggesting that they could be the DM. DM direct detection experiments place stringent bounds on how strongly the DM can couple to nucleons, and this rules out the left-handed sneutrinos as DM candidates, however if the lightest neutralino is dominantly made up of higgsino, or bino, components then it can still make a good candidate for DM. Thus, as a result of protecting the proton from decay, the MSSM contains a good candidate for DM.

The MSSM as described so far does not offer a mechanism to generate neutrino masses, however simple alterations or additions can allow for the generation of non-zero neutrino masses.

Thus we see that even the simplest supersymmetric extension of the SM comes with appealing features, and may lead to remedies for the failures of the SM, while offering a solution to the hierarchy problem.

2.1.6 Experiment

As yet there exists no experimental evidence for the existence of SUSY. However, a dearth of experimental evidence is at the moment no cause for concern, however it does imply that supersymmetric models are pushed into parameter regions where they become less natural as a solution to the hierarchy problem. This is because experiments have only, within the last year, begun to probe the energies at which we expect SUSY to become manifest. The limits on the Higgs mass from LEP, $m_h \gtrsim 114$ GeV indirectly suggest that, in a SUSY theory, the stop squarks should have a mass at the TeV scale. This is because large radiative corrections are required to push the Higgs mass up this high, and this requires a small hierarchy between the top and stop to give large enough quadratic corrections. At the time of writing current limits from the LHC running at 7 TeV, with 165pb^{-1} of integrated luminosity, require that squark and gluino masses should be roughly greater than a TeV, [78]. This is a model-dependent bound, and relies on the assumption that all squarks of the first two generations are degenerate in mass. If one relaxes this assumption then the bounds on squark masses are substantially weakened. It is not always clear how such limits will translate to models other than the MSUGRA/CMSSM model that has been studied, however, one would expect that the limits on coloured particles such as gluinos are relatively robust against changes to the model, as the QCD processes contributing to sparticle production are set by SUSY and gauge invariance, and cannot be altered.

The allowed parameter range for R-parity conserving SUSY theories is also limited by DM considerations. One requires that the LSP must be neutral, and must also not contribute more DM than is observed. In addition, bounds from both direct and indirect detection experiments limit the dark-matter nucleon scattering cross-section and the DM annihilation cross-section and products. These properties are set by the parameters in a SUSY theory, and are thus indirectly restricted.

A quantitative approach aimed at understanding the experimental situation is to consider how 'fine-tuned' a SUSY model which evades all constraints is [79]. If the sparticle masses, and other parameters, need to be pushed too far then the fine-tuning increases and SUSY becomes a less appealing solution to the hierarchy problem. It should be noted that most models with low fine-tuning are already in conflict with experimental limits, although some models with low fine-tuning have squark and gluino masses in excess of 1 TeV, and are yet to be probed [79].

The LHC experiments have already collected 1fb^{-1} of data, and results from analysis of this data are expected to be made public soon. With this amount of data the LHC will be probing much, but not all, of the favoured parameter space for

SUSY models, and will have the potential to discover, or cast serious doubt, on SUSY. Within the next few years the LHC should discover any new physics at the TeV scale, and will thus give the final word on whether or not our Universe is supersymmetric at the TeV scale.

2.1.7 Remaining, and new, puzzles

Although the MSSM has many attractive features, it does not explain why the cosmological constant is positive, and so small, although it does relieve the hierarchy a little. This is because unbroken global supersymmetry implies zero vacuum energy, and unbroken SUGRA implies negative semi-definite vacuum energy. Thus, when SUSY is spontaneously broken, the vacuum energy is tied to the SUSY-breaking scale, which is necessarily below the Planck scale. The magnitude of the SUSY-breaking scale is not known, however it must be greater than a TeV, which is still many orders of magnitude greater than the observed scale of the cosmological constant. In addition, although it is straightforward to implement solutions to the strong-CP problem within SUSY, SUSY does not itself offer an explanation for this puzzle.

SUSY also comes with some new puzzles and problems. Possibly the greatest problem once SUSY is broken lies in the flavour structure of squark and slepton masses and trilinear couplings. There is no reason, a priori, for the flavour structure of the soft terms to match that of the SM. However, unless there are hierarchies in the squark and slepton masses, a high degree of degeneracy, or an identical flavour structure to the fermion masses, then these particles lead to unacceptably high rates of flavour violating processes. Thus particular structures must be imposed at the TeV scale, or particular forms of SUSY-breaking assumed at higher scales. This puzzle is taken seriously when considering how SUSY is broken, and how this breaking is communicated to the MSSM. In Chapter 3 we present a model in which these problems are ameliorated due to an R-symmetry which suppresses the processes which lead to high rates of flavour-violating processes.

There is also the problem of the μ-parameter in the Higgs sector. Although this parameter is safe from quadratic corrections, it is supersymmetric and could thus, in principle, take on any value, unlike the SUSY-breaking parameters which should all be determined by the scale of SUSY-breaking. If we wish for electroweak symmetry breaking to occur we then require that μ is similar to the scale of soft SUSY-breaking terms in the MSSM. Why this is so, and why μ does not take on Planckian values, is know as the μ-problem.

Another puzzle takes the guise of R-parity. As discussed, R-parity, or some suitable global symmetry, must be imposed in order to protect the proton from decaying. However in the SM the proton is automatically stable as baryon-number conservation is an automatic consequence of the gauge charges of the SM fields (at low temperatures). In effect proton stability comes for free in the SM, but not in the MSSM. Why the Universe should choose to exhibit such a discrete symmetry is a puzzle.

These problems are not fatal, and are puzzles rather than failures. Simple solutions or explanations exist for all of the new puzzles which have arisen as a consequence of SUSY, and the puzzles themselves are useful in guiding us towards the possible structure of physics well above the TeV scale.

2.1.8 Alternatives to SUSY

It should be noted that alternative solutions to the hierarchy problem do exist. One very plausible solution is known as 'Technicolor' and protects the electroweak scale from quadratic divergences by requiring that all fundamental particles are fermions, making scales only logarithmically sensitive to the UV. In this way electroweak symmetry breaking occurs whenever some fermions, charged under a strongly-coupled gauge group, condense. If this condensate transforms under the electroweak gauge symmetry then its condensation will break this symmetry down to electromagnetism. Such theories are, however, difficult to construct and study due to the strongly-coupled nature of the problem. However Technicolor does still constitute a viable alternative to SUSY.

Perhaps less plausible, but still worth considering, are extra-dimensional scenarios. In this scenario the SM lives on a 4D 'brane' in a higher dimensional background. If gravity propagates in the extra dimensions, (which could even be warped), but the SM forces are constrained to the brane, then the extra dilution of gravity leads to a natural hierarchy between the scale of gravity and the weak scale. This class of theories has received a great deal of attention and are also interesting alternatives to the SUSY paradigm.

2.1.9 Summary

We have seen that SUSY is a very rich framework in which to address the failures and puzzles of the SM. While the ATLAS and CMS experiments at the LHC continue to probe the energy scales at which we expect SUSY to become manifest, there is much work still to be done from a theoretical perspective. Much focus, at the TeV scale, for the last thirty or so years has been concentrated on the MSSM, however it is interesting to explore avenues along which the MSSM is modified. In Chapter 3 we present a new SUSY model for the TeV scale, which has a number of appealing features over the MSSM.

It also remains to understand SUSY-breaking fully, and how such SUSY-breaking fits in with our current ideas about physics in the far UV, up to the Planck scale. In Chapter 4 we consider the low energy phenomenology of multiple SUSY breaking sectors, and how this depends on the details of how SUSY is broken in each sector. In particular, we show that if a hidden SUSY QCD-like sector lies in a metastable SUSY-breaking vacuum then a rich spectrum of multiple 'Goldstini' and 'Modulini' can arise within this one sector, all with mass $\sim 2m_{3/2}$, leading to novel possibilities for probing the dynamics of hidden SUSY-breaking sectors.

One might also wish to understand how multiple sectors may influence each other. In Chapter 5 we describe a novel phenomenon which can arise in the context of multiple sectors. If one, primary, sector breaks SUSY spontaneously then this can trigger other, secondary, sectors into breaking SUSY spontaneously, even if they are incapable of doing so without the influence of the initial SUSY-breaking sector. This process is, in some senses, catalytic as the resultant SUSY breaking in the secondary sector can be much greater than the SUSY breaking it experiences due to the primary sector.

Chapter 3

A Supersymmetric One Higgs Doublet Model

In this chapter we present a supersymmetric extension of the Standard Model in which only one electroweak doublet acquires a vacuum expectation value and gives mass to Standard Model fermions. As well as the novel accommodation of a Standard Model Higgs within a supersymmetric framework, this leads to a very predictive model, with some advantages over the MSSM. In particular, problems with proton decay, flavour changing neutral currents and large CP violation are ameliorated, primarily due to the presence of an anomaly-free R-symmetry. Since supersymmetry must be broken at a low scale, gravity-mediated effects which break the R-symmetry are naturally small. The R-symmetry requires the presence of adjoint chiral superfields, to give Dirac masses to the gauginos; these adjoints are the only non-MSSM fields in the visible sector. The LSP is a very light neutralino, which is mostly bino. Such a light neutralino is not in conflict with experiment, and is a striking prediction of the minimal model. Additional scenarios to raise the mass of this neutralino to the weak scale are also outlined. Prospects for discovery at the LHC are briefly discussed, along with viable scenarios for achieving gauge-coupling unification.

3.1 Introduction

It is common lore that a supersymmetric extension of the Standard Model (SM) requires the existence of two Higgs doublets, H_u and H_d, in order to give masses to both up-type and down-type quarks (as well as charged leptons). This is because holomorphy forbids the usual SM down-type Yukawa couplings $H_u^\dagger Q D^c$. Furthermore, the fermionic partners of H_u also contribute to gauge anomalies, which are cancelled by the partners of H_d. Here we pursue the goal of simplifying the Higgs structure of supersymmetric extensions of the SM, as opposed to commonly studied variants of the MSSM which often involve a more complex Higgs sector.

It has been noticed by many authors that after supersymmetry (SUSY) breaking there is typically a contribution to down-quark masses from induced couplings to H_u (e.g. [80–86]). Recently, it was suggested that down-type masses might arise solely from such supersymmetry-breaking couplings, so that either H_d acquires a vacuum expectation value (VEV) but does not couple to SM fermions, or can be left out of the spectrum entirely [85–87]. The latter necessitates the introduction of a number of new fields in the electroweak sector, in order to cancel gauge anomalies.

In this chapter, we advocate a different scenario. As the most economical way to cancel the gauge anomalies of H_u, the doublet H_d is retained, but forbidden from acquiring a VEV, or coupling directly to SM fermions. As such, it is not really a 'Higgs' field at all; to reflect this we re-label it as η, and the usual H_u field simply as H. In fact, as the usual B_μ-induced mixing with η is forbidden, the bosonic components of H become indistinguishable from a SM Higgs. We will refer to this set-up as the 'Supersymmetric One Higgs Doublet Model' (SOHDM).

A very natural way to implement the above scenario is to impose an anomaly-free R-symmetry,[1] which we describe in Section 3.2. We stress that this is a different R-symmetry to those commonly studied in the literature, and has a number of comparative advantages. In particular, the field content of the model is smaller than that of the 'Minimal R-symmetric Supersymmetric Standard Model' (MRSSM) of [109]. The R-symmetry forbids Majorana gaugino masses, so we are required to add chiral superfields in the adjoint of $SU(3)\times SU(2)$, in order to give the gauginos Dirac masses. These are the only fields in our model which do not appear in the MSSM. The R-symmetry allows a μ-term, so there is no need to introduce the extra doublets of the MRSSM to generate acceptable chargino masses.

We expect effects from Planck-scale physics to violate any global symmetry, (see e.g. [110–119]). Henceforth when referring to the R-symmetry we do so in the understanding that it is broken either by Planck-suppressed, or non-perturbatively small operators. As such our continuous R-symmetry is to be viewed as an emergent 'accidental' symmetry of the low-energy theory.

The following sections will describe the model in detail, but it may be useful to list its main features here:

[1] Although we assume a $U(1)$ R-symmetry throughout, the $\mathbb{Z}_p$ subgroup for sufficiently large p does the same job and is well motivated from a theoretical perspective [88]. Previously discussed models which consider some semblance of an R-symmetry, whether in the full model or solely in the gauge sector include [89–108].

- Couplings between the Higgs and SM fermions are the same as for the SM Higgs.
- One-loop corrections to the Higgs mass from stop/top loops automatically saturate the MSSM correction, reducing fine-tuning.
- Supersymmetry must be broken at a low scale, in order to generate acceptable down-type quark masses. This suggests a gauge-mediated scenario, but the usual $\mu/B\mu$ problem of such models is avoided, since the $B\mu$ term is neither present nor required.
- R-symmetry should be preserved at the TeV scale, allowing simple models of SUSY-breaking to be employed, as comparable SUSY and R-symmetry breaking are not required. R-symmetry breaking effects arising from the expectation value of the superpotential, which is required in order to set the vacuum energy density to a small value, are negligible.
- The anomaly-free R-symmetry forbids all dimension four and five baryon number violation, implying a proton lifetime well above the experimental lower bound. This is in contradistinction to the MSSM, where dangerous dimension five operators are allowed by R-parity and must be suppressed by some other means.
- Flavour physics is necessarily connected to supersymmetry breaking, in contrast to standard assumptions.
- The R-symmetry has profound implications for flavour physics and CP-violation. All A-terms are forbidden, as are Majorana masses for the gauginos, and these two facts significantly reduce the contributions to flavour-changing neutral currents (FCNCs) and CP-violation relative to the MSSM [109].
- The symmetries of the model allow small neutrino masses to be generated via a standard high-scale seesaw mechanism.
- The field content differs from that of the MSSM only in the addition of chiral superfields in the adjoint of $SU(3)\times SU(2)$, required to give gauginos mass in the presence of unbroken R-symmetry.
- The minimal version of the model predicts a very light neutralino, which is nevertheless consistent with all experimental constraints.

The layout of the rest of the chapter is as follows. In Section 3.2 we describe the field content and symmetries of the model and in Section 3.3 we describe the mass spectrum, including the generation of small neutrino masses. Between them, Section 3.2 and Section 3.3 contain all of the original details of the SOHDM, and are thus a self-contained reference for a reader interested purely in the structural features of the model. Following these sections we discuss constraints and phenomenological aspects, and review work by previous authors. Constraints from flavour physics, CP-violation and precision electroweak physics are discussed in Section 3.4. A brief discussion of gauge coupling unification is included in Section 3.5. Potential collider signals and ways to unambiguously distinguish this model from other supersymmetric models are discussed in Section 3.6. We conclude in Section 3.7.

Finally a word on notation. We will write superfields in bold, and use the same symbol for their individual components. Component fields with R-charge ± 1 (squarks, sleptons, '–inos') will carry tildes. So the left-handed electron superfield, for instance, is

$$\boldsymbol{e_L} = \tilde{e}_L + \sqrt{2}\,\theta\, e_L + \dots \ . \tag{3.1}$$

As already mentioned, since there is only one Higgs doublet, we refer to the superfield with the quantum numbers of the up-type Higgs as $\boldsymbol{H}$, and the superfield with the quantum numbers of the usual down-type Higgs as $\boldsymbol{\eta}$.

3.2 The model

The field content of the model is that of the MSSM, along with chiral superfields in the adjoint of $SU(3)\times SU(2)$, needed to give Dirac masses to the gauginos.[2] We will denote by $\boldsymbol{O}$ the $SU(3)$ octet, and by $\boldsymbol{T}$ the $SU(2)$ triplet. We summarise the spectrum, including gauge and global-symmetry charges, in Table 3.1.

Throughout, SUSY breaking will be parametrised by two spurion chiral superfields. The first source is the F-term of a chiral superfield $\boldsymbol{X}$, to which we assign R-charge 2 so that R-symmetry remains unbroken, and the second is the D-term of an additional $U(1)'$ gauge superfield $\boldsymbol{W'}$. We will denote by M the generic messenger mass scale, by which we suppress all interactions with $\boldsymbol{X}$ and $\boldsymbol{W'}$. Note that the μ-term is not forbidden by our R-charge assignments, so in order to solve the μ-problem, we also impose a discrete $\mathbb{Z}_2$ symmetry which is broken by the F-term of $\boldsymbol{X}$; the corresponding parities are given in Table 3.1. We will now proceed to discuss the interactions allowed by this structure.

[2]See below for why we omit the $U(1)_Y$ adjoint i.e. a singlet.

Field	Gauge rep.	R-charge	$\mathbb{Z}_2$-parity
$\boldsymbol{Q}$	$(\mathbf{3},\mathbf{2},\frac{1}{6})$	1	1
$\boldsymbol{U^c}$	$(\overline{\mathbf{3}},\mathbf{1},-\frac{2}{3})$	1	1
$\boldsymbol{D^c}$	$(\overline{\mathbf{3}},\mathbf{1},\frac{1}{3})$	1	-1
$\boldsymbol{L}$	$(\mathbf{1},\mathbf{2},-\frac{1}{2})$	1	1
$\boldsymbol{E^c}$	$(\mathbf{1},\mathbf{1},1)$	1	-1
$\boldsymbol{H}$	$(\mathbf{1},\mathbf{2},\frac{1}{2})$	0	1
$\boldsymbol{\eta}$	$(\mathbf{1},\mathbf{2},-\frac{1}{2})$	2	-1
$\boldsymbol{O}$	$(\mathbf{8},\mathbf{1},0)$	0	1
$\boldsymbol{T}$	$(\mathbf{1},\mathbf{3},0)$	0	1
$\boldsymbol{X}$	$(\mathbf{1},\mathbf{1},0)$	2	-1
$\boldsymbol{W'}$	$(\mathbf{1},\mathbf{1},0)$	1	1

Table 3.1: The chiral superfield matter content of the SOHDM. Gauge superfields are even under the $\mathbb{Z}_2$-parity, have R-charge 1, and are not shown. The fields $\boldsymbol{X}$ and $\boldsymbol{W'}$ are the spurion superfields parametrising SUSY breaking.

Due to its R-charge, η has no Yukawa couplings to SM fermions. Fermion masses therefore come entirely from Yukawa couplings to H, with the charged lepton and down-type quark couplings induced by supersymmetry breaking[3]

$$\mathcal{L}_{\text{Yuk}} = \int d^2\theta\, \lambda_U\, \boldsymbol{HQU^c} + \int d^4\theta\, \frac{\boldsymbol{X}^\dagger \boldsymbol{H}^\dagger}{M^2}(\lambda_D\, \boldsymbol{QD^c} + \lambda_E\, \boldsymbol{LE^c}) \ . \tag{3.2}$$

We therefore have a tree-level relation for the bottom-quark mass,

$$\frac{\lambda_b F_X}{M^2} 174\,\text{GeV} \simeq 5\,\text{GeV} \quad \Rightarrow \quad \frac{F_X}{M^2} \simeq \frac{1}{35\lambda_b} \ . \tag{3.3}$$

If we require that the bottom quark coupling is perturbative, say $\lambda_b \lesssim 1$, this gives a lower bound

$$\frac{F_X}{M^2} \gtrsim \frac{1}{35} \ . \tag{3.4}$$

In the Higgs sector, the μ-term is generated by a low-scale Giudice-Masiero mechanism, and $\boldsymbol{H}$ also has a renormalizable superpotential coupling to $\boldsymbol{T}$ and $\boldsymbol{\eta}$ generated after SUSY-breaking

$$\mathcal{L}_{\text{Higgs}} = \int d^4\theta\, \frac{\boldsymbol{X}^\dagger}{M}(\lambda_\mu \boldsymbol{H\eta} + \frac{\lambda_T'}{M}\, \boldsymbol{HT\eta}) \to \int d^2\theta\, (\mu \boldsymbol{H\eta} + \lambda_T\, \boldsymbol{HT\eta}) \ . \tag{3.5}$$

[3]For a model that generates this structure see [87].

The effective μ-term is therefore given by $\mu = \lambda_\mu F_X/M$; combining this with (3.3), we get

$$M \simeq 35\frac{\lambda_b}{\lambda_\mu}\mu \ , \quad F_X \simeq 35\frac{\lambda_b}{\lambda_\mu^2}\mu^2 \ . \tag{3.6}$$

The requirements of a weak-scale μ-term and natural couplings therefore dictate that the scale of SUSY breaking is low. Notice also that (3.5) implies that the $\boldsymbol{T}$ Yukawa coupling is small, $\lambda_T \lesssim \mathcal{O}(F_X/M^2) \sim 1/35$.

Dirac mass terms for the gauginos and their adjoint partners can be written as

$$\mathcal{L}_\text{D} = \int d^2\theta \, \frac{\boldsymbol{W}'_\alpha}{M}\big(\lambda_G \operatorname{Tr}(\boldsymbol{O}\boldsymbol{G^\alpha}) + \lambda_W \operatorname{Tr}(\boldsymbol{T}\boldsymbol{W}^\alpha)\big) \to M_3 \operatorname{Tr}(\widetilde{O}\widetilde{G}) + M_2 \operatorname{Tr}(\widetilde{T}\widetilde{W}) + \dots \ , \tag{3.7}$$

where $M_3 = \lambda_G D'/M$, and $M_2 = \lambda_W D'/M$.

Finally, soft scalar masses are given by Kähler terms of the form

$$\mathcal{L}_\text{soft} = \int d^4\theta \frac{\boldsymbol{X}^\dagger\boldsymbol{X}}{M^2}\big(\alpha_Q^2 \boldsymbol{Q}^\dagger\boldsymbol{Q} + \dots\big) \tag{3.8}$$

where after $\boldsymbol{Q}^\dagger\boldsymbol{Q}$ we insert analogous terms for all chiral fields, to generate soft masses for their scalars. Because the adjoint is a real representation, and our adjoint chiral fields have R-charge zero, there are also holomorphic terms for their scalars, i.e. for the triplet we get both $\operatorname{Tr}(\boldsymbol{T}^\dagger\boldsymbol{T})$ and $\operatorname{Tr}(\boldsymbol{T}^2)$. The second of these terms gives squared masses to the real and imaginary components of T which are of equal magnitude but opposite sign, but this is not a problem if such terms are sub-dominant.

3.2.1 Discussion

We are assuming a combination of F- and D-term SUSY breaking in the hidden sector, as the D-term SUSY breaking is necessary in order to generate large enough gaugino masses (see Section 3.3) and F-term SUSY breaking is required for large enough sfermion masses.[4] This is not unreasonable, as although dominant D-term breaking does not arise dynamically [120, 121] it is possible for a hidden sector to give rise to SUSY breaking satisfying $D \lesssim F$, even for non-Abelian D-terms [121]. Some examples of hidden sectors with mixed F- and D-term SUSY breaking can be found in [121–126].

Previous attempts to build models with an R-symmetry have required VEVs for both H_u and H_d, and can be split into two classes. In the first, R-charges of $\mathcal{R}_{\boldsymbol{H_u}} = 0$, $\mathcal{R}_{\boldsymbol{H_d}} = 2$ are assigned, and the R-symmetry is then broken at the level of a few GeV

[4] Given recent results on R-symmetric gauge mediation [107], it may in fact be possible to achieve the same effective softly broken Lagrangian purely from F-term SUSY breaking.

[127] in order to generate a small down-Higgs VEV and acceptable down-type fermion masses. In the second, the R-charges are taken to be $\mathcal{R}_{\boldsymbol{H_u}} = \mathcal{R}_{\boldsymbol{H_d}} = 0$, such that H_d can get a VEV with R-symmetry remaining unbroken. In this case it is necessary to extend the Higgs sector by adding two extra doublets, as in the MRSSM, in order to generate acceptable Higgsino masses [109]. The novelty herein is that, as a VEV for $H_d \equiv \eta$ is no longer required, we can assign it an R-charge of 2 and still get weak-scale chargino masses without the addition of extra $SU(2)$ doublets. Thus the particle content is more minimal than that of the MRSSM, but an unbroken R-symmetry is maintained.

The extra $\mathbb{Z}_2$ symmetry has been imposed in order to forbid a tree-level μ-term, thus solving the μ problem in the usual way [128], but we will see that it has other desirable consequences, in particular forbidding too-large neutrino masses.

The reader may wonder why we did not also add a singlet chiral field $\boldsymbol{S}$ of R-charge 0, in order to give the bino a weak-scale mass like the other gauginos. The reason is that Kähler potential terms such as $\boldsymbol{X}^\dagger \boldsymbol{X} \boldsymbol{S}$ and superpotential terms such as $\boldsymbol{W}'^\alpha \boldsymbol{W}'_\alpha \boldsymbol{S}$ would be allowed, leading to a large VEV for S, which causes problems for the breaking of both supersymmetry and electroweak symmetry. As we will discuss in Section 3.3.4, these troublesome tadpole terms can be avoided by imposing certain restrictions on the messenger couplings, but we find the simplest solution to this problem is to simply exclude the singlet from the model. This leads to the striking prediction of a very light neutralino, which nevertheless avoids all experimental bounds, as we explain in Section 3.3.3. In Section 3.3.4 we also discuss additional scenarios for making this neutralino more massive in order to re-introduce a cold DM candidate.

3.2.2 Electroweak symmetry breaking

Electroweak symmetry breaking is affected by the presence of the triplet $\boldsymbol{T}$ and the associated Dirac gaugino mass term. This gives new contributions to the D-terms of the $SU(2)$ gauge fields, which pick up pieces linear in the triplet scalars

$$\Delta D^j = -M_2(T^j + \overline{T^j}) \ . \tag{3.9}$$

We will see below that this leads to a small VEV for the neutral component T^0, but for now we will ignore this, a posteriori justifying this approximation.

We will assume that all squared soft masses are positive at the messenger scale, and appeal to radiative electroweak symmetry breaking. Indeed, if the top squark masses are $m_{\widetilde{Q},\widetilde{U}} \gtrsim 700$ GeV at the messenger scale (~ 100 TeV) then, upon running down to the weak scale, the squared soft mass of H is driven negative as a result of the large top Yukawa [129],[5] while all others remain positive. In the MSSM, this nevertheless leads to a VEV for H_d due to mixing induced by the $B\mu$ term, but here this and similar operators are forbidden by the symmetries of the model. So we may proceed in the knowledge that only H acquires a VEV due to radiative electroweak symmetry breaking.

With all other fields set to zero, the Higgs potential is in fact the same as in the SM, but with the coefficient of the quartic term determined at tree-level by the gauge couplings (by convention we take $\tilde{m}_h^2$ positive)

$$V_{\text{Higgs}} = \frac{1}{8}(g^2 + g'^2)|H|^4 + (|\mu|^2 - \tilde{m}_H^2)|H|^2 \ , \tag{3.11}$$

leading to a VEV

$$\langle H^0 \rangle = 2\sqrt{\frac{\tilde{m}_H^2 - |\mu|^2}{g^2 + g'^2}} = \frac{v}{\sqrt{2}} \simeq 174\text{GeV} \ , \tag{3.12}$$

where the last equality is fixed by experiment.

We now have to ask whether this is in fact a stable vacuum. The form of the soft masses guarantees that the Hessian of the potential will be positive definite, so an instability can only manifest as a non-vanishing linear term. Since $U(1)_{\text{EM}}$ remains unbroken, we cannot have linear terms in any charged fields, leaving only η^0 and T^0. Inspection of the F-terms following from (3.5) is enough to see that there is no linear term in η^0 (alternatively, note that η is charged under the unbroken R-symmetry, which therefore forbids a linear term). But with $\langle H^0 \rangle = v/\sqrt{2} = 174$ GeV and all other fields set to zero, the F-term for η^0 and the D-term for the neutral generator of $SU(2)$, along with the soft mass for T, give a potential for T^0, the non-constant part of which is[6]

$$V_T = \frac{v^2}{2}(\lambda_T \mu - \frac{1}{2} g M_2)(T^0 + \overline{T^0}) + (m_T^2 + \frac{1}{2}\lambda_T^2 v^2 + 2M_2^2)|T^0|^2 \ . \tag{3.13}$$

We see that there is a linear term in the real part of T^0, and that it acquires a VEV

$$\langle T^0 \rangle = \frac{\left(\frac{1}{2} g M_2 - \lambda_T \mu\right) v^2}{4M_2^2 + \lambda_T^2 v^2 + 2m_T^2} \ . \tag{3.14}$$

[5] The squared soft-mass for H at the weak scale is given approximately by;

$$\tilde{m}_H^2(m_{\tilde{t}}) \simeq \tilde{m}_H^2(M) - \frac{3}{8\pi^2}\lambda_t^2(m_{\tilde{t}_L}^2 + m_{\tilde{t}_R}^2)\log(M/m_{\tilde{t}}) \ , \tag{3.10}$$

where M is the messenger scale.

[6] All parameters can be taken real, as we will discuss in Section 3.4.2.

This naturally comes out at $\lesssim 1\,\text{GeV}$ which, as we discuss in Section 3.4, is compatible with precision electroweak measurements. The fact that this VEV is much smaller than $\langle H \rangle$ justifies our perturbative calculation.

3.3 Mass scales

Although we are considering an effective theory approach to TeV-scale model building, it is instructive to consider the scales of soft parameters in complete models of R-symmetric gauge mediation. Previous discussions of R-symmetric gauge mediation and/or Dirac gauginos in gauge mediation include [93, 96–99, 101, 103, 104, 107], however we focus here on the results of [103].

In [103] the messengers which mediate SUSY breaking have SM gauge charges, but also couple directly to the extra chiral adjoint fields through Yukawa couplings, which we denote λ. As a result the adjoint soft masses-squared arise at one-loop, along with the Dirac gaugino masses, and sfermion soft masses-squared arise at two loops. The generic prediction for soft masses in this model is given as [103]

- Gaugino masses $\sim \frac{\lambda g}{16\pi^2}\frac{D'}{M}$
- Sfermion masses $\sim \frac{g^2}{16\pi^2}\frac{F_X}{M}$
- Adjoint scalar masses $\sim \frac{\lambda}{4\pi}(\frac{D'}{M}, \frac{F_X}{M})$

Hence for $\lambda \sim g$, gaugino and sfermion masses are roughly equal and the adjoint scalars are more massive by a factor of $\sim 4\pi/g$. Thus the spectrum is similar to that of a gauge-mediation scenario, with the additional adjoint scalar masses an order of magnitude greater than the SM superpartners.

3.3.1 The Higgs

The Higgs sector in the SOHDM is the same as in the SM (up to a small mixing with the neutral component of the triplet T, which we ignore here and discuss further in Section 3.4), and in particular it is much simpler than in the MSSM. As usual, we fix the gauge so that the VEV of H is real and positive. If we package all contributions to the low-order Higgs potential into the effective parameters m_h and λ_h, we can write

$$V_{\text{Higgs}} = -\frac{m_h^2}{2}|H|^2 + \frac{\lambda_h}{4}|H|^4 \ . \tag{3.15}$$

Here m_h is the mass of the physical Higgs boson, and if we write the VEV as $\langle H \rangle = v/\sqrt{2}$, we obtain the relation

$$m_h^2 = \frac{\lambda_h v^2}{2} \ . \tag{3.16}$$

Since v is fixed, this is a relation between m_h and λ_h. To leading order, the coefficient λ_h is just $\frac{1}{2}(g^2 + g'^2)$,[7] and therefore we get $m_h = M_Z$, the same as the tree-level upper bound in the MSSM. In addition, the large contributions to the Higgs mass arising from loops involving stop squarks and top quarks saturate the MSSM correction. Thus the Higgs mass-squared is

$$m_h^2 = M_Z^2 + \frac{3}{4\pi^2}\lambda_t^2 m_t^2 \log\left(\frac{m_{\tilde{t}_L} m_{\tilde{t}_R}}{m_t^2}\right) , \tag{3.17}$$

whereas the MSSM correction is suppressed by a factor of $\cos^2(\alpha)$, where $\alpha = 0$ corresponds to the situation where the Higgs boson lives entirely in the H_u doublet. This feature is attractive from a fine-tuning perspective as both the tree-level Higgs mass and the one-loop correction are necessarily at the upper bounds of the MSSM values.

Depending on how SUSY breaking is mediated to the visible sector an additional reduction in fine-tuning might also be obtained from the following operator;

$$\int d^4\theta \frac{\boldsymbol{X}^\dagger \boldsymbol{X}}{M^4} (\boldsymbol{H}^\dagger \boldsymbol{H})^2 \ \to \ \frac{F_X^2}{M^4}|H|^4 \ , \tag{3.18}$$

as this operator increases the Higgs quartic coupling and, if sizeable, would lead to a greater Higgs mass.

3.3.2 Fermionic superpartners

The chargino mass matrix is

$$\begin{array}{c} \\ \widetilde{W}^- \\ \widetilde{\eta}^- \\ \widetilde{T}^- \end{array} \begin{array}{c} \begin{array}{ccc} \widetilde{T}^+ & \widetilde{H}^+ & \widetilde{W}^+ \end{array} \\ \left(\begin{array}{ccc} M_2 & \sqrt{2}M_W & 0 \\ -\frac{\lambda_T v}{\sqrt{2}} & \mu & 0 \\ 0 & 0 & M_2 \end{array} \right) \end{array} . \tag{3.19}$$

The zero entries are enforced by the unbroken R-symmetry. So there is one charged Dirac fermion of mass M_2, coming from the third rows and columns, while the other two mass states come from the upper left 2×2 block. In the limit $\lambda_T \ll 1$ there are two almost degenerate charginos with mass M_2, and one with mass μ.

[7] New contributions to the $SU(2)$ D-terms involving T lead to small reductions to the quartic coupling of $\mathcal{O}(\frac{\alpha}{4\pi})$.

The neutralino mass matrix is more interesting. We have one extra neutralino compared to the MSSM, coming from $\boldsymbol{T}$. Three of the neutralinos (the wino, the bino, and the neutral fermion in $\boldsymbol{\eta}$) have R-charge 1, while the other two (the neutral fermions from $\boldsymbol{H}$ and $\boldsymbol{T}$) have R-charge -1, so as for the charginos, all masses are Dirac-type, with mass matrix

$$\begin{array}{cc} & \begin{array}{ccc} \widetilde{\eta}^0 & \widetilde{W}^0 & \widetilde{B}^0 \end{array} \\ \begin{array}{c} \widetilde{H}^0 \\ \widetilde{T}^0 \end{array} & \begin{pmatrix} \mu & -M_Z\cos\theta_W & M_Z\sin\theta_W \\ -\frac{\lambda_T v}{\sqrt{2}} & M_2 & 0 \end{pmatrix} \end{array} . \tag{3.20, 3.21}$$

Clearly one linear combination of the R-charge 1 neutralinos remains massless;[8] explicitly, it is

$$\left(-1\ ,-\frac{\lambda_T v}{M_2\sqrt{2}}\ ,\ \frac{(\mu M_2-\lambda_T v M_Z\cos\theta_W)}{M_2 M_Z\sin\theta_W}\right) . \tag{3.22}$$

Compared to μ, M_2, we have $\lambda_T v \simeq 0$, so this is approximately

$$\left(-1\ ,0\ ,\ \frac{\mu}{M_Z\sin\theta_W}\right) . \tag{3.23}$$

Since $\mu \gtrsim 5M_Z\sin\theta_W$, this state is mostly bino, and therefore can avoid lower bounds on neutralino masses, as we will now discuss.

3.3.3 The light neutralino

The R-symmetry protects the, mostly bino, neutralino above from gaining a Majorana mass within the globally supersymmetric model discussed so far. However, we expect that SUGRA effects will violate the global R-symmetry, and when this is combined with SUSY breaking this could lead to an R-symmetry-violating Majorana mass for the gauginos. As X has non-zero R-charge, gaugino masses of the form

$$\int d^2\theta \frac{\boldsymbol{X}}{M_P}\boldsymbol{W^\alpha W_\alpha} = \frac{F_X}{M_P}\widetilde{W}^\alpha\widetilde{W}_\alpha \ , \tag{3.24}$$

are forbidden. This does not mean that Majorana masses are not generated, however, as there would likely exist anomaly-mediated contribution not greater than [130, 131]

$$m_\lambda = \frac{\beta(g^2)}{2g^2}m_{3/2} \ , \tag{3.25}$$

which, for the bino, implies a Majorana mass of

$$m_1 = \frac{11\alpha}{4\pi\cos^2(\theta_W)}m_{3/2} = 8.9\times 10^{-3}\, m_{3/2} \ . \tag{3.26}$$

[8] This prediction is relaxed if we introduce additional fields in order to raise the neutralino mass, as described in Section 3.3.4.

Now, as we are considering low-scale mediation of SUSY-breaking, such as gauge mediation, then for squark and slepton masses at the TeV scale we require $F_X/M \lesssim$ 100 TeV. Furthermore, for the single-Higgs generation of down-type fermion masses we require $F_X/M^2 \gtrsim 1/35$. Combining these relations we find that $F_X \lesssim 3.5 \times 10^5\,\mathrm{TeV}^2$, and thus the gravitino mass is of order $m_{3/2} \lesssim 83$ eV. Therefore we expect a Majorana bino mass of

$$m_1 \lesssim 0.67 \text{ eV} \quad . \tag{3.27}$$

Such a light neutralino, with SM couplings through sfermion-fermion-bino terms in the Lagrangian might make the reader uneasy. However, it has recently been shown that very light neutralinos can be compatible with cosmology and collider constraints, so long as the neutralino is mostly bino [132].

This can be understood quite simply. Interactions between the large bino component of the neutralino and SM fermions proceed via sfermion exchange. Thus if there exists a small hierarchy between soft scalar masses and the weak scale such that $\tilde{m} \gtrsim M_W$, then these interactions are suppressed in comparison with neutrino interactions, which proceed via electroweak boson exchange.

As the bino component carries no gauge charges, the only gauge interactions of the lightest neutralino arise due to its small Higgsino component. Regarding electroweak interactions, the lightest neutralino behaves in a similar manner to a neutrino, however vertices involved in physical processes are suppressed by the square of the small bino-Higgsino mixing angle. Thus it is clear that the lightest neutralino behaves very much like an additional neutrino, but with a suppressed SM-neutralino interaction strength.[9]

In order to demonstrate that such a particle is acceptable we summarise the results of a recent study on neutralino mass bounds in Appendix A, however for a thorough discussion we refer the reader to Ref. [132].[10]

3.3.4 Avoiding a light neutralino

Although a very light neutralino is compatible with current observations in particle physics, astrophysics and cosmology, it may be to the taste of some readers to remove any particles surplus to the SM with masses below the weak scale. For the bino this can be achieved with a little additional model building.

[9] Such a light neutralino cannot constitute the DM of the universe. It is reasonable that the DM could be made up of axions [133–135] or could originate from within some other hidden sector [136–139].

[10] For earlier work on light neutralinos/photinos see e.g. [140–145].

The simplest solution is to introduce a gauge singlet chiral superfield, $\boldsymbol{S}$, with R-charge $R_{\boldsymbol{S}} = 0$. In this way a TeV-scale Dirac bino mass can be generated through the operator

$$\int d^2\theta \frac{\boldsymbol{W'_\alpha}}{M}(\boldsymbol{S}\boldsymbol{B^\alpha}) \quad . \tag{3.28}$$

The problem that arises with the addition of this singlet is that, among other terms, a Kähler potential term $K \supset \boldsymbol{X}^\dagger \boldsymbol{X}\boldsymbol{S}/M$ cannot be forbidden by the imposed symmetries. This term leads to a large VEV for S, which depends on the SUSY breaking scale, and also the soft mass for S, as

$$|\langle S\rangle| \sim \frac{F_X^2}{M}\frac{1}{\tilde{m}_s^2} \ . \tag{3.29}$$

Thus this VEV potentially leads to a large μ-term, hypercharge D-term, or even destabilisation of the SUSY-breaking in the hidden sector. This is a common affliction of models involving singlet scalar fields. It is possible to build models of R-symmetric gauge mediation which avoid large tadpoles for S. In [97] a C-parity symmetry is imposed which forbids dangerous tadpole terms. In [103] particular structures in the couplings between the adjoints and the messengers are chosen and a large tadpole term is not generated. Finally in [107] it is demonstrated that these tadpole terms can be avoided if the adjoint-messenger couplings respect $SU(5)$ or if the singlet originates from a complete $SU(5)$ adjoint multiplet.

3.3.5 Neutrinos

Neutrino masses are straightforward to accommodate. The only dimension five operator which violates baryon or lepton number and is allowed by the symmetries is the Weinberg operator $\boldsymbol{H^2L^2}$, or more explicitly

$$\frac{1}{M_*}\int d^2\theta\, \epsilon_{ab}\epsilon_{cd}\boldsymbol{H}^a\boldsymbol{H}^c\boldsymbol{L}^b\boldsymbol{L}^d \supset \frac{1}{M_*}\int d^2\theta\, (H^0)^2(\nu_L)^2 \ , \tag{3.30}$$

where M_* is some mass scale. This is exactly what we need to generate neutrino masses after electroweak symmetry breaking. The obvious way for this term to come about is from a Kähler potential term

$$\int d^4\theta\, \frac{\boldsymbol{X}^\dagger}{M^3}\boldsymbol{H^2L^2} \ , \tag{3.31}$$

but fortunately this is forbidden by our $\mathbb{Z}_2$ symmetry, as it would give rise to Majorana masses of order $M_{\nu_L} \sim F_X v^2/M^3$, which are too large due to the low scale of SUSY breaking.

We can in fact implement a standard seesaw mechanism. We introduce singlet chiral superfields $\boldsymbol{N}$ which are even under the $\mathbb{Z}_2$ symmetry and have R-charge 1. These can then be given large supersymmetric masses, but the fermions can also get weak-scale Dirac masses with the left-handed neutrinos after electroweak symmetry breaking. The relevant Lagrangian is

$$\mathcal{L}_\nu = \int d^2\theta \left(M_R^2 \boldsymbol{N}^2 + \lambda_\nu \boldsymbol{HLN} \right) \ . \tag{3.32}$$

The mass scale suppressing the Weinberg operator is therefore the Majorana mass of these right-handed neutrinos, leading to acceptably small neutrino masses.[11]

3.4 Flavour, CP and precision electroweak

As we will see, the SOHDM is surprisingly robust against constraints from FCNCs, CP-violation, and precision electroweak observables.

3.4.1 Flavour-changing neutral currents

The largest potential source for FCNCs lies in the sparticle spectrum. Considering the flavour structure of (3.2) and (3.8), we see that, whilst remaining consistent with any flavour symmetries, the sparticle soft masses can originate from terms of the form

$$\begin{aligned}\mathcal{L}_{\text{soft}} = \int d^4\theta \frac{\boldsymbol{X}^\dagger \boldsymbol{X}}{M^2} \Big(& \boldsymbol{Q}^\dagger (\alpha_Q^2 + a_{Q1}\lambda_U\lambda_U^\dagger + a_{Q2}\lambda_D\lambda_D^\dagger)\boldsymbol{Q} + \boldsymbol{U^{c\dagger}}(\alpha_U^2 + a_U\lambda_U^\dagger\lambda_U)\boldsymbol{U^c} \\ & + \boldsymbol{D^{c\dagger}}(\alpha_D^2 + a_D\lambda_D^\dagger\lambda_D)\boldsymbol{D^c} + \boldsymbol{L}^\dagger(\alpha_L^2 + a_L\lambda_E\lambda_E^\dagger)\boldsymbol{L} + \boldsymbol{E^{c\dagger}}(\alpha_E^2 + a_E\lambda_E^\dagger\lambda_E)\boldsymbol{E^c} \Big) \ ,\end{aligned} \tag{3.33}$$

where we are suppressing flavour indices, and neglecting higher powers of the Yukawa matrices λ. It should be noted that in (3.2) both λ_D and λ_E come dressed with the SUSY breaking field X, thus one would expect on general grounds to generate the additional non-diagonal terms in (3.33), as well as the diagonal terms which may arise due to a low-scale mediation mechanism such as gauge mediation. It is also important to recall that, as a result of (3.2) the down-type quark Yukawas are of the form $(F_X/M^2)\lambda_D$, and similarly for the leptons. This implies that if $F_X/M^2 \sim 1/35$ then the Yukawa matrix λ_D can have large entries with $\lambda_D \sim \mathcal{O}(1)$ for the bottom quark entries. Thus the non-diagonal components of (3.33) involving λ_D are not necessarily small compared to the components involving λ_U.

[11] We make the reasonable assumption that there are no R-charge 1 fields at the messenger scale which have superpotential couplings to $\boldsymbol{HL}$.

We expect that FCNC processes within the SOHDM will be small and well within current bounds. This is due to the following three effective FCNC-suppressing ingredients of this model:

- Minimal flavour violation / flavour alignment.
- R-symmetry. This forbids A-terms that lead to left-right sfermion mixing after electroweak symmetry breaking, and also forbids Majorana gaugino masses.
- SM fermions couple at tree-level to a *single* Higgs doublet.

It can be seen from (3.33) that, by extending the flavour rotations that diagonalise the SM fermion mass matrices to act on the whole supermultiplets, the resulting sfermion mass-squared matrices $\tilde{m}^2_L, \tilde{m}^2_{E^c}, \tilde{m}^2_{U^c}$ and $\tilde{m}^2_{D^c}$ will be diagonalised automatically.[12] However, in order to diagonalise the mass-squared matrices $\tilde{m}^2_{Q_U}$ and $\tilde{m}^2_{Q_D}$ it will be necessary to perform a further rotation proportional to the CKM matrix, V_{CKM}. This further rotation will introduce FCNC interactions at squark-quark-gluino and squark-quark-neutralino vertices. However, the flavour structure at these vertices will be proportional to V_{CKM} and will thus satisfy 'Minimal Flavour Violation' (MFV) [146]. Thus within the SOHDM all FCNC processes are governed by the CKM matrix. Furthermore, the only relevant operators in the effective Hamiltonian below the weak scale are those relevant in the SM. This structure does not, however, require that the squark masses are degenerate.

It is possible that some other physics, beyond that described within this model, could lead to extra non-MFV terms in (3.33). However, the best-motivated source for such terms would be through gravity-mediation effects, which would be small ($\mathcal{O}(100\text{eV})$) in the SOHDM as the scale of supersymmetry breaking is low. The MFV assumption is therefore well-motivated within the current framework.

The R-symmetry plays a pivotal role in suppressing FCNC processes. In [109] it was shown that, when a supersymmetric model possesses an R-symmetry, the absence of Majorana gaugino masses and trilinear A-terms, which generate left-right sfermion mixing, leads to a strong suppression of FCNC processes. The suppression is effective enough that, with Dirac gaugino masses of order a few TeV, and vanishing left-right sfermion mixing, flavour violating sfermion masses (which violate MFV) of $\mathcal{O}(1)$ are allowed.

[12] As an example, we can see that if the quark rotation $\{d_R \to U^{d\dagger}_R d_R, d_L \to U^d_L d_L\}$ diagonalises λ_D then the same rotation for the squarks $\tilde{d}_R \to U^{d\dagger}_R \tilde{d}_R$ diagonalises the $\tilde{d}_R$ mass-squared matrix.

The detailed reasons for this extra suppression are described in [109], and we briefly summarise the results here. For the case of $\Delta F = 2$ flavour violation the strongest constraints come from $K - \overline{K}$ mixing, and next strongest from B mixing. The R-symmetry suppresses SUSY contributions to these processes as the usual troublesome dimension-five operators, such as;

$$\frac{1}{m_{\tilde{g}}} \tilde{d}_R^* \tilde{s}_L^* \overline{d}_R s_L \ , \tag{3.34}$$

are forbidden by the R-symmetry, and the leading operators are dimension six. In addition the Dirac gauginos lead to finite, rather than log-enhanced, radiative corrections to squark masses. The result is that the box diagrams leading to $K - \overline{K}$ mixing are suppressed sufficiently to allow $\mathcal{O}(1)$ non-MFV flavour violation in the squark sector. In [109] it is shown that phases in squark masses are still constrained by limits on ϵ_K. In particular, with $\mathcal{O}(1)$ non-MFV flavour violation in the squark sector, the phases are constrained to be $\theta < 0.15$. This constraint weakens if the first two generations of squarks are approximately degenerate, which is fortunately the case for the SOHDM if the dominant contributions to squark masses arise from flavour-diagonal gauge mediated terms.

For $\Delta F = 1$ flavour violation, such as $b \to s\gamma$, there is also a suppression due to the R-symmetry [109]. This is due to the fact that the Feynman diagrams for these processes involve a helicity flip, and this is not possible for an internal gaugino line as the opposite-helicity state has no tree-level couplings to SM fermions. The only contributing diagrams then involve a helicity flip on an external line. These contributions are sufficiently suppressed to allow $\mathcal{O}(1)$ non-MFV flavour violation in the sfermion sector. Similarly, constraints from ϵ'/ϵ do not lead to strong constraints on flavour violation [109].

Thus the R-symmetry acts to efficiently suppress flavour-violating processes, in addition to the MFV in the SOHDM.[13]

3.4.2 CP-violation

We have seen above that flavour violation imposes no significant constraints on the parameter space, but we must also consider new flavour-diagonal sources of CP-violation.

[13] It has recently been noted that in R-symmetric models $\mathcal{O}(1)$ mixing in the slepton sector is not allowed, and the allowed mixing is $\lesssim \mathcal{O}(0.1)$. This is due to limits on lepton flavour violation from processes such as $\mu \to e\gamma$ [147]. As we have the additional assumption of MFV then slepton mixing parameters will be small and the SOHDM is safe from these constraints.

First let us isolate physical phases in the Lagrangian. We can choose the phases of $\boldsymbol{O}$ and $\boldsymbol{T}$ so that the Dirac mass parameters M_2 and M_3 are real. A rotation of $\boldsymbol{\eta}$ can then make λ_T real. Finally, re-phasing $\boldsymbol{H}$ can make μ real, thereby removing all supersymmetric phases in our 'flavourless' sector. As a result, all new physical phases lie in the scalar soft masses.

At a typical point in MSSM parameter space, large electric dipole moments are generated at one-loop for leptons and quarks, whereas experimentally, such dipole moments are constrained to be small. In the SOHDM, the R-symmetry forbids all such one-loop diagrams.

The other contribution to the electric dipole moment of the neutron is the dimension-six three-gluon operator first discussed by Weinberg [148]. This obtains corrections from diagrams involving the Dirac gluinos, but it was argued in [109] that this imposes no strong constraints for TeV-scale masses.

3.4.3 Precision electroweak tests

Since the SOHDM has a significantly modified electroweak sector, one might worry that it is already ruled out by precision electroweak tests. In particular, we can ask what contributions are made to the parameters S and T.

At tree level, there is a contribution to T from the small VEV obtained by the triplet. As before, we will write v_T for this VEV; the tree level ρ parameter is then

$$\rho := \frac{M_W^2}{M_Z^2 \cos^2\theta_W} = 1 + \frac{2g^2 v_T^2}{M_Z^2 \cos^2\theta_W} \ . \tag{3.35}$$

The experimental upper bound is roughly $\rho \lesssim 1.0012$ [149], which implies $v_T \lesssim 3.6\,\text{GeV}$. The expression for the triplet VEV in the SOHDM was given in eq.((3.14)). As described in Section 3.2, λ_T is small, and if we take $\lambda_T \simeq 0$, we get

$$v_T \simeq \left(\frac{gM_2 v}{8M_2^2 + 4\tilde{m}_T^2}\right) v \ , \tag{3.36}$$

which for typical values of the parameters evaluates to $\lesssim 1\,\text{GeV}$, so this gives no significant constraints on the model.

In [150] the effects of an $SU(2)$ triplet superfield $\boldsymbol{T}$ on the S and T parameters at one-loop level are considered. The trilinear coupling

$$\mathcal{L}_{\text{Tri}} = \int d^2\theta \, \lambda_T \, \boldsymbol{H}\boldsymbol{T}\boldsymbol{\eta} \ , \tag{3.37}$$

breaks the custodial symmetry of the Higgs sector, however, in [150] it is shown that even for large Yukawa couplings the S and T parameters lie within the current 68 %

confidence level ellipse. In our model, this coupling is small ($\lambda_T \lesssim 1/35$) and one-loop corrections will remain within current bounds.

3.5 Gauge Couplings

Due to the addition of the $SU(3)$ octet superfield $\boldsymbol{O}$, the $SU(3)$ gauge coupling does not run at one-loop [150] at high scales. In addition, above the mass of the octet, asymptotic freedom is lost at two-loops. However, due to the two-loop suppression, the $SU(3)$ gauge coupling remains perturbative up to scales as high as 10^{18}GeV and no Landau pole problems arise.

It is also clear that, in comparison with the MSSM, there are no new contributions to the $U(1)_Y$ beta function, and $\boldsymbol{T}$ and $\boldsymbol{O}$ contribute differing amounts to the $SU(2)$ and $SU(3)$ beta functions, so that gauge coupling unification is lost.

One approach to recover unification is to add extra vector-like matter superfields $\boldsymbol{L', \overline{L}', E', \overline{E}', E', \overline{E}'}$, where the quantum numbers of the MSSM lepton doublet and right-handed electron are implied [93, 150]. These fields can be given weak-scale vector-like masses, and dangerous mixings with SM fields can be forbidden with the imposition of an appropriate discrete symmetry. If five singlets are also added then these new fields, in addition to the triplet and octet, would correspond to an adjoint representation of the GUT group $SU(3)_c \times SU(3)_L \times SU(3)_R \subset E_6$ [93, 150].[14] Additional vector-like matter falling in a complete representation of this gauge group must then be added in order to implement gauge mediation. This must contain at most two pairs of $\mathbf{3}, \overline{\mathbf{3}}$ under $SU(3)_c$ in order to maintain perturbativity up to the GUT scale.

An alternative approach based on $SU(5)$ would be to embed the triplet and octet in an adjoint of $SU(5)$ [93]. This requires the addition of a singlet and the vector-like 'bachelor' superfields $\boldsymbol{B, \overline{B}}$ with quantum numbers $(\mathbf{3}, \mathbf{2}, -5/6)$ and $(\mathbf{3}, \overline{\mathbf{2}}, 5/6)$. Again, these fields can be given vector-like masses and unification can be achieved [93]. For a gauge-mediated scenario it would be appealing to use these bachelor fields as messengers.

[14] One of these singlets would play the role of the adjoint $U(1)$ chiral superfield and three would take the place of right-handed neutrino superfields, leaving only one additional singlet superfield.

3.6 Collider Signatures

The SOHDM has a number of collider signatures which could be used to distinguish this model from the MSSM. Some of these features arise due to the R-symmetry and are common in R-symmetric models, whereas others arise as a result of the single-Higgs nature of the model.

One striking aspect of R-symmetric models is the presence of Dirac, rather than Majorana, gluinos and neutralinos, with restricted production and decay channels. The distinction between the Dirac and Majorana cases has been discussed in detail in [151–153], and processes which are allowed within the MSSM, but are forbidden in an R-symmetric model, have been enumerated in [151]. We summarise these processes below:

- Different-flavour quark-quark scattering: $\sigma[qq' \to \{\tilde{q}_L\tilde{q}'_L, \tilde{q}_R\tilde{q}'_R\}] = 0$
- Different-flavour quark-antiquark scattering: $\sigma[q\overline{q}' \to \{\tilde{q}_L\tilde{q}'_R, \tilde{q}_R\tilde{q}'_L\}] = 0$
- Squark-gluino production: $\sigma[qg \to \{\tilde{q}_L\tilde{g}_D, \tilde{q}_R\tilde{g}_D\}] = 0$
- Gluino pair production: $\sigma[q\overline{q} \to \{\tilde{g}_D\tilde{g}_D, \tilde{g}^c_D\tilde{g}^c_D\}] = \sigma[gg \to \{\tilde{g}_D\tilde{g}_D, \tilde{g}^c_D\tilde{g}^c_D\}] = 0$

Similar alterations to the electroweak sector occur. In [151] it is described how the differences in decay processes could be used to determine sfermion handedness through like-sign and unlike-sign dilepton signals at the LHC. If we ignore the small Yukawa interactions of the first two generations, and focus on the gauge interactions, then right-handed sfermions do not couple at tree-level to charginos, and thus decay dominantly to a bino-fermion pair. However, left-handed sfermions can decay to a chargino-fermion pair. Using this fact right- and left-handed sfermions can be discriminated. Combining this with the differences in sfermion production processes listed above it is in principle possible to separate a Dirac theory from a Majorana theory to a high level of statistical significance at the LHC [151].

Colour octet and weak triplet scalars also have a distinctive collider phenomenology [152–154]. However, as we require, and expect, that these extra scalars are heavy ($\gtrsim$ 7 TeV) we will not consider their phenomenology here.

Another feature of the SOHDM are the R-charge $\mathcal{R}_{\boldsymbol{\eta}} = 2$ scalars. In the MRSSM [109], in addition to the standard Higgs doublets, with $\mathcal{R}_{\boldsymbol{H_u}} = \mathcal{R}_{\boldsymbol{H_d}} = 0$, two R-charge $\mathcal{R}_{\boldsymbol{R_u}} = \mathcal{R}_{\boldsymbol{R_d}} = 2$ doublets are required. These extra particles have been found to have interesting collider signatures [155]. Although the particle content in the SOHDM is reduced, and only the two doublets with $\mathcal{R}_{\boldsymbol{H}} = 0$ and $\mathcal{R}_{\boldsymbol{\eta}} = 2$ are

Model	Scalar	Fermion
MSSM	$3^0_R, 2^\pm$	$4^0_M, 2^\pm$
MRSSM	$3^0_R, 2^0_C, 4^\pm$	$4^0_D, 4^\pm$
SOHDM	$1^0_R, 1^0_C, 2^\pm$	$2^0_D, 1^0_M, 3^\pm$

Table 3.2: Multiplicity of electroweak-charged particles originating from the Higgs and gauge sectors of related supersymmetric models. We only include particles with masses at the TeV scale, i.e. omitting adjoint scalars. Neutral and charged particles are discriminated by the superscript $(0, \pm)$. For neutral scalars the subscript denotes whether the scalar is real (1 d.o.f.) or complex (2 d.o.f.), and for neutral fermions the subscript denotes whether the fermion is Majorana or Dirac.

present, the main features of collider phenomenology for these sets of particles are similar; with a purely standard-model initial state any R-charged particles must be pair produced at colliders. For the $\mathcal{R}_{\boldsymbol{\eta}} = 2$ doublet this occurs dominantly at the LHC through Drell-Yan production mediated by electroweak gauge bosons [155], and for masses below 250 GeV the cross-section is $\mathcal{O}(10)$ fb. Since $|\mathcal{R}_{\boldsymbol{\eta}}| = 2$, in contrast to all other R-charged particles in the model, η-boson decay must result in a pair of light neutralinos, and four light neutralinos for any event involving the pair production of η-bosons.

The SOHDM could also be discriminated from the MSSM or the MRSSM at the LHC through the observation of particles originating from the Higgs and electroweak gauge sectors. We summarise the multiplicity of these particles in Table 3.2, where we exclude the adjoint scalars as we expect their masses to lie well above the TeV scale. One can see that, in particular, the charged particle multiplicities differ for all three models, and this could be used to distinguish between these models at the LHC.

Non-degenerate and non-diagonal flavour structure in sfermion masses would also hint at some underlying structure which protects the extra particles from generating unacceptable FCNCs in the SM sector, providing indirect evidence for the existence of a suitable extended R-symmetry.

At future colliders, precision Higgs physics could provide strong support for a single Higgs-doublet model. This is because the couplings of the Higgs to SM fermions would be the same as in the SM, which is not the case in commonly considered supersymmetric models. Finally, it is conceivable that a super-LHC (or 'SSC') running at $\sqrt{s} \sim 100$ TeV could uncover the messenger and SUSY-breaking sectors as, in the SOHDM, both sectors are required to exist at this scale.

3.7 Summary

We have described a supersymmetric model in which only a single Higgs doublet participates in electroweak symmetry breaking, this doublet providing mass to all SM fermions. The extra doublet superfield required for anomaly cancellation, $\boldsymbol{\eta}$, is merely a 'spectator' field, and does not acquire a VEV. The model has a number of distinctive features, such as an anomaly-free R-symmetry which is imposed to protect η from mixing with H, but also helps to ameliorate FCNC problems of supersymmetric models. This is particularly advantageous in models where fermion mass generation is tied to SUSY-breaking. Thus a non-degenerate or non-diagonal sfermion-mass flavour structure is allowed. The model *requires* a low scale of SUSY-breaking, and the simplest version predicts a very light neutralino with mass $\mathcal{O}(0.7)$ eV.

The many attractive features of the SOHDM mean its implications for the LHC need to be seriously considered. It also motivates further exploration of models of low-scale mediation of SUSY-breaking which not only maintain an R-symmetry, but also generate the flavour structure of the down-type fermions as in (3.2).

Chapter 4

Multiple SUSY-breaking and even more Goldstini

In this chapter we study the 'goldstini' scenario of Cheung, Nomura, and Thaler, in which multiple independent supersymmetry (SUSY) breaking sectors lead to multiple would-be goldstinos, changing collider and cosmological phenomenology. In supergravity, potentially large corrections to the previous prediction of twice the gravitino mass for goldstini masses can arise when their scalar partners are stabilised far from the origin. If the sequestered hidden sector is a metastable SUSY-breaking sector of the Intriligator-Seiberg-Shih (ISS) type then multiple goldstini can originate from within a single sector, along with many supplementary 'modulini', all with masses of order twice the gravitino mass. These fields can couple to the Supersymmetric Standard Model (SSM) via the 'Goldstino Portal'. Collider signatures involving SSM sparticle decays can provide strong evidence for the ISS mechanism of SUSY breaking. Along with axions and photini, the Goldstino Portal gives another potential window to the hidden sectors of string theory.

4.1 Introduction

If the Standard Model is UV completed by string theory – consistent with the hypothesis of supersymmetry (SUSY) – the topological complexity of compactification manifolds suggests the existence of many additional sectors sequestered from the fields of the Standard Model. The dimensional reduction of form fields may result in a proliferation of light axion-like scalar fields [156], or weak-scale abelian vector fields and their superpartners [157]. Moreover, the presence of stacks of spacetime-filling branes may lead to nonabelian gauge sectors with fundamental matter in the four-dimensional theory. The mere observation that such supersymmetric nonabelian gauge theories possess metastable SUSY-breaking vacua [158] suggests that supersymmetry may be broken in these different (purely field-theoretic) sectors. Furthermore, there are numerous additional ways in which supersymmetry may be broken by intrinsically stringy objects – e.g., nonsupersymmetric flux backgrounds or the presence of both D- and anti D-branes in the compactification manifold. On a topologically complex compactification manifold with various nonabelian gauge sectors, fluxes, branes, and antibranes, it is not unreasonable to expect a rich variety of SUSY-breaking dynamics to coexist. Thus, the existence of multiple (likely metastable) SUSY-breaking sectors is not merely a theoretical novelty, but rather a well-motivated consequence of physics in the ultraviolet.[1]

Historically, however, the study of SUSY breaking and its phenomenology has focused on a single sector additional to the Supersymmetric Standard Model (SSM), whose dynamics give rise to a nonsupersymmetric ground state. Recently it has been shown [74, 75, 162] that relaxing this assumption to include multiple sources of SUSY breaking can lead to interesting and appealing scenarios in which the conventional phenomenology of single-sector SUSY breaking is significantly modified. In this chapter we wish to extend the results of [74, 75] with an eye towards the underlying physical context in which multiple SUSY breaking is likely to arise.

The mediation of this multiple-sector supersymmetry breaking to the Standard Model may occur in any of the customary ways, leading to weak-scale soft masses and the usual successes of the SSM. However, the multiple breaking of supersymmetry gives rise to couplings between additional 'goldstini' and SSM fields. In this fashion, the existence of new sectors may be revealed via what we may call the 'Goldstino Portal'. In this sense the goldstini and their companions are further distinguished from moduli, whose masses are likewise around $m_{3/2}$ but whose couplings are Planck-suppressed.

Specifically, in [74, 162] it was argued that the presence of multiple sequestered sectors that break SUSY spontaneously gives rise to multiple 'goldstini' in addition to the true global goldstino which provides the extra degrees of freedom of the gravitino of mass $m_{3/2}$, and in [74] it was shown that these additional goldstini would have mass $2m_{3/2}$. It was further shown [74, 75] that such a set-up can lead to exciting new signatures at the LHC which could confirm not only the validity of the supergravity framework but also the presence of multiple sequestered SUSY breaking sectors,

[1] Indeed, the fact that cosmological evolution preferentially populates the metastable vacua of SQCD rather than the supersymmetric vacua [159–161] provides a strong argument that the mere existence of multiple (reheated) nonabelian gauge sectors with light fundamental matter implies the existence of simultaneous SUSY breaking in multiple sectors.

providing indirect, but striking, evidence for the complexity of the string compactification. Subsequently it was shown that this scenario can also lead to solutions of the cosmological problems with a heavy gravitino LSP [75].

These considerations come with two caveats. The first is purely experimental; the smallness of flavour-changing neutral currents (FCNCs) and other signs of Standard Model flavour violation imply that the flavour-violating contributions to SSM soft masses from all SUSY-breaking sectors must necessarily be small. In particular, this requires that all SUSY breaking communicated via intrinsically flavour-violating mediation mechanisms such as (the non-anomaly-mediated part of) gravity mediation must be many times smaller than that communicated via flavour-preserving mechanisms. Although this is possible if all such contributions to SUSY breaking are conveniently small to begin with, it seems much more plausible that the smallness of flavour violation arises from locality and warping [130] or conformal sequestering [163, 164]. Once again, this is a well-motivated consequence of physics in the ultraviolet. Sequestering is known to arise readily in the presence of strongly warped backgrounds such as warped throats, e.g., type IIB string theory [165], and the ubiquity of warped throats on realistic compactification manifolds is well-known [166–168]. The pairing of multiple SUSY breaking and sequestering via warped throats is suggested by more than just FCNC considerations alone; the very existence of multiple goldstini requires it as multiple *unsequestered* SUSY breaking sectors simply lead to one ur-breaking of supersymmetry. But if sequestering and multiple SUSY breaking are so closely intertwined, it is then natural to consider what implications sequestering may have on the spectrum and phenomenology of the resulting goldstini. In particular, it was shown in [4] that warping and sequestering lead to substantial deviations from the goldstino mass prediction of $2m_{3/2}$, and hence the spectrum of goldstini – and resulting collider phenomenology – are richer than previously thought.

The second consideration is largely theoretical. Weak-scale supersymmetry in the SSM favours *dynamical* means of SUSY breaking in order to explain the hierarchy between the Planck and SUSY-breaking scales [169]. In turn, dynamical SUSY breaking in general requires a SUSY-breaking sector to possess a rich set of gauge dynamics and fields. It is therefore instrumental to consider whether common classes of dynamical SUSY-breaking theories might modify or alter the goldstino spectrum, perhaps by the presence of additional light states. At the very least, the corresponding goldstino mass depends on how the SUSY breaking vacuum is stabilised. Moreover, we will argue that it is quite common that a *single* dynamical SUSY-breaking sector gives rise to *multiple faux goldstini*. Such additional states may then couple to MSSM fields through the Goldstino Portal, and their observation would shed further light on the nature of the supersymmetry breaking sector(s).

In short: the potential observability of multiple SUSY breaking has been well established. However, it is instrumental to ask whether the additional physics that naturally accompanies multiple SUSY breaking may enrich and expand the goldstino spectrum and phenomenology.

In particular, in Section 4.2 we compute the goldstino mass for a general class of effective supersymmetry breaking Lagrangians using the conformal compensator formalism. We will find that important corrections to the goldstino mass arise from the effects related to the stabilisation of the SUSY-breaking vacuum. In Section 4.3 we study the particle content of a hidden Intriligator-Seiberg-Shih-type (ISS) [158] sector preserving a (discrete) R-symmetry. We show that such a sector would give rise to N_c goldstini and $N_c(N_c-1)$ 'modulini' of mass $\geq 2m_{3/2}$ (in the absence of warping or conformal sequestering), where N_c is the number of colours in the asymptotically free UV gauge group. A simple example of this set-up is schematically illustrated in Figure 4.1. Although such a discrete R-symmetry preserving sector is incapable of generating gaugino masses, in the context of multiple SUSY breaking sectors this poses no problem. In particular, since there is no phenomenological reason to require more than one of the independent SUSY-breaking sectors to break R-symmetry.[2]

Figure 4.2 provides a schematic illustration of the new possibilities that arise for the mass spectrum of goldstini/modulini. Such states are typically grouped into sets with a goldstino (or goldstini) at a lower limit point at $\beta m_{3/2}$ with modulini sitting relatively tightly spaced above this limit. For unsequestered or unwarped sectors, $\beta = 2$ (modulo potentially large corrections related to the stabilisation of the SUSY-breaking vacuum as explained in Section 4.2). Otherwise, any value $2 \geq \beta \geq 0$ is possible, so some subset of the goldstini/modulini may be lighter then the gravitino, while the lightest observable-sector supersymmetric partner (LOSP) may either sit above all the goldstini and modulini, or may be in the middle of the spectrum of states [4]. The true LSP may be the gravitino, one of the limit point goldstini, or yet another state, such as a hidden photino.

In Section 4.4 we briefly discuss the couplings of the goldstini and modulini of our scenario, and among other topics, present a potential 'smoking gun' collider signature

[2]We note in passing that such R-symmetry-preserving sequestered SUSY breaking sectors can also lead to attractive phenomenological features, such as, *e.g.*, cosmologically acceptable thermal leptogenesis [75].

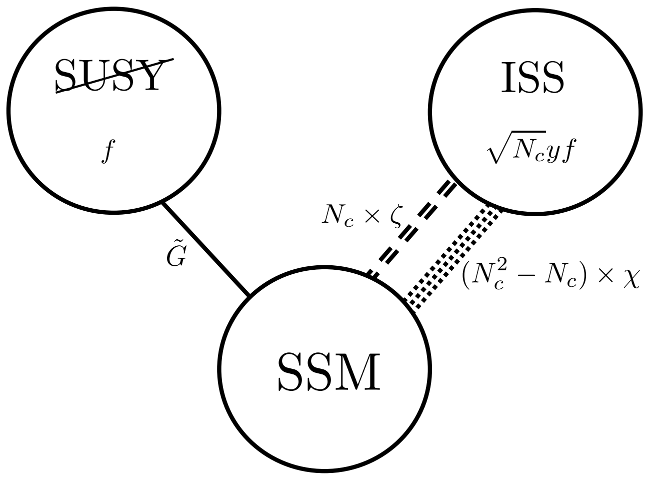

Figure 4.1: A schematic example of multiple sequestered SUSY-breaking. In this set-up there are two SUSY breaking sectors: The first sector is a SUSY breaking sector with one F-term of magnitude f. This sector need not preserve an R-symmetry and could thus generate gaugino masses. The second sector is an R-symmetry preserving $SU(N_c)$ ISS sector where all non-zero F-terms are of magnitude yf, implying this sector has an overall effective-SUSY-breaking-scale of $\sqrt{N_c}yf$. The overall effective SUSY breaking scale that determines the gravitino mass is $f_{eff} = f\sqrt{1+N_c y^2}$. If $y \ll 1$, N_c goldstini, ζ, and $N_c(N_c-1)$ modulini, χ, all arise from the ISS sector, as shown in Section 4.3, while the longitudinal mode of the gravitino dominantly arises from the first sector.

that can give evidence for the physical realisation of the ISS mechanism of SUSY-breaking. In general the goldstini of multiple SUSY breaking sectors, including those within a hidden ISS sector, couple to SSM chiral multiplets through the Goldstino Portal as [74]

$$\mathcal{L}_{int} \supset \sum_{i=1}^{N}\sum_{a=1}^{N-1} \frac{\tilde{m}_i^2 V_{ia}}{f_i}\zeta_a \psi \phi^\dagger \tag{4.1}$$

where N is the total number of F-terms, f_i, in all sectors, $\tilde{m}_i^2$ is the soft mass contribution from the i'th hidden sector F-term, $\tilde{m}_i^2 = -f_i^2/\Lambda_i^2$, the effective mediation scale of the i'th hidden sector to the SSM is Λ_i, and V_{ia} is the rotation matrix that diagonalises the goldstini mass matrix.[3] The ζ_a are the $N-1$ goldstini mass eigenstates and the true global goldstino that forms the longitudinal component of the gravitino is the N^{th} eigenstate with zero mass in this basis. If we make the reasonable assumption that SUSY breaking from all sectors is not communicated in an identical way, *i.e.*, if not *all* Λ_i are equal, then couplings of the SSM to all goldstini are generated by the interaction of eq.(4.1). These goldstini-SSM couplings distinguish the goldstini

[3]To avoid confusion, note that the f_i have mass-dimension two.

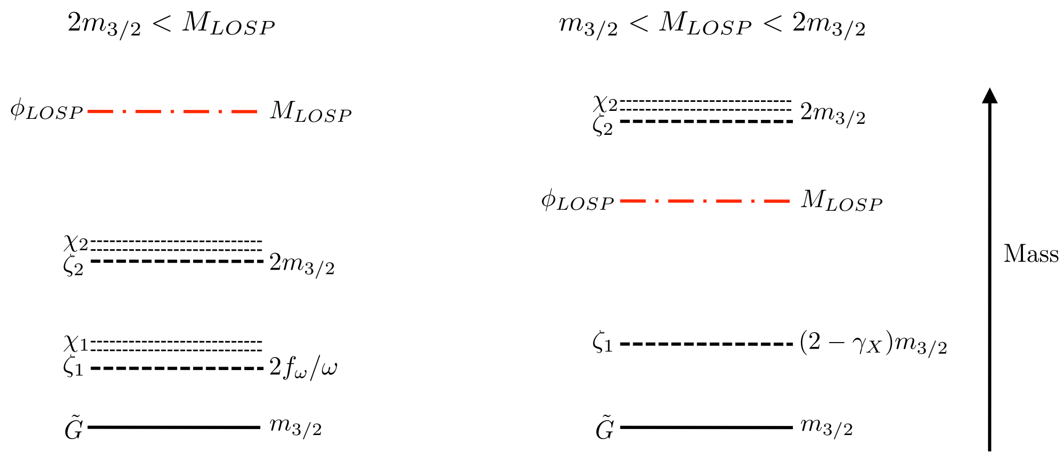

Figure 4.2: A diagram depicting a subset of the possible spectra. The left panel shows the SSM LOSP, the gravitino and goldstini/modulini from two ISS sectors, one at the end of a warped throat (so with mass spectrum at $2f_\omega/\omega$ as shown in [4]), and one just gravitationally sequestered from the SSM. The right panel shows a possible spectrum where the SSM LOSP is lighter than $2m_{3/2}$, but, however, could still decay to a goldstino originating in a conformally sequestered (or warped) sector, here chosen not to be of ISS type, so there is only a single goldstini state, and no modulini. An interesting variant of this scenario occurs if the anomalous dimension of the SUSY-breaking field satisfies $\gamma_X > 1$, in which case LOSP decays could occur to a goldstino which is lighter than the gravitino [4]. The resulting collider and cosmological phenomenology can depend strongly on which of these patterns is realised. Unlike for the various goldstini, decays to the modulini of a hidden ISS sector depend on the couplings in that sector, and are thus not guaranteed. Three different sectors are shown in order to elucidate a range of possibilities, though any number ≥ 2 of independent SUSY-breaking sectors implements the goldstini scenario.

from other $m_{3/2}$-scale fermions such as, e.g., derivatively-coupled modulini, whose couplings to SSM states at a scale E are suppressed relative to those of goldstini by $E\Lambda_i/f_i$.[4]

For the field-theoretic breaking of global SUSY, it is reasonable to expect that the distribution of breaking scales is roughly log-flat since, assuming SUSY is unbroken at tree level, breaking only occurs via non-perturbative effects (modulo technicalities involving Fayet-Illiopoulos terms), which scan over an exponentially large range of scales as UV couplings and beta-function coefficients are linearly changed [169, 170]. In the context of multi-sector SUSY breaking, there should be a lower cut-off on this distribution of SUSY-breaking scales, implied by the (at least gravi-

[4]Though this is true of conventional, derivatively coupled modulini, there are of course exceptions – for example, the fermionic components of moduli superfields involved in supersymmetry breaking, whose couplings to SSM states are goldstino-like. We particularly thank Joe Conlon for discussions on related issues.

tational strength, *i.e.*, anomaly-mediated) communication of breaking from the dominant SUSY-breaking sector to the sub-dominant ones. In Chapter 5 we show that spontaneous SUSY-breaking can, in fact, be triggered in a sub-dominant sector as a result of the SUSY-breaking felt from the dominant SUSY-breaking sector. If we require SUSY to solve the hierarchy problem, and we assume the dominant SUSY breaking sits at the intermediate scale, the lowest independent SUSY-breaking sector should have scale $\sim$ TeV. In Section 4.2 we will see how such a scenario leads to a strong modification of the goldstino mass when arising from a sector with such a very low SUSY-breaking scale.

In fact, in the landscape of string theory, one might naively expect 'tree-level' breaking due to the presence of fluxes or anti-D-branes in the vacuum not to be distributed at all scales, but instead concentrated at the string scale. Nevertheless, because of the presence of warped throats (caused by the back reaction from fluxes or branes), an approximately log-flat distribution of SUSY-breaking scales can still apply due to the approximately log-flat distribution of throat lengths expected in string compactifications[166–168].

Having discussed our view of the overall scene in which the goldstini scenario is set and motivated, we now turn to our specific results, starting with the changes to the goldstini mass spectrum related to the stabilisation of SUSY breaking vacua.

4.2 Goldstini Masses in Supergravity

Perhaps the clearest way to study the goldstino mass spectrum in supergravity is through the use of the conformal compensator formalism [171–173], in which a 'spurion' superfield $\mathbf{\Sigma}$ is introduced with conformal weight 1 assigned to the lowest component. The conformal compensator can then be used to track the breaking of a superconformal gravity theory down to normal supergravity. In addition, if supersymmetry is also broken, then the conformal compensator can be used in an analogous way to keep a track of the generation of soft-terms. The relevant physics may be captured by considering a single chiral superfield $\boldsymbol{X}(y) = x(y) + \sqrt{2}\psi_X(y)\theta + f_X(y)\theta^2$ with a Polonyi-type superpotential and Kähler terms necessary for stabilising the vacuum at finite $\langle x \rangle$. The Lagrangian is given by

$$\mathcal{L} = \int d^4\theta\, \mathbf{\Sigma}^\dagger \mathbf{\Sigma} \left(\boldsymbol{X}^\dagger \boldsymbol{X} - \frac{c(\boldsymbol{X}^\dagger \boldsymbol{X})^2}{M^2} + ... \right) + \int d^2\theta \mathbf{\Sigma}^3 f \boldsymbol{X} + h.c. \qquad (4.2)$$

where $\mathbf{\Sigma} = \sigma + f_\Sigma \theta^2$ is the conformal compensator and $c > 0$. Such a Lagrangian naturally arises as an effective description of SUSY breaking valid below the scale

M (e.g., an O'Raifeartaigh model with fields of mass M)[5]. The quartic stabilising term in the Kähler potential is absolutely necessary in the context of supergravity; its absence would induce a runaway to large field values. If $\boldsymbol{X}$ were the only source of supersymmetry breaking, we would identify ψ_X as the true longitudinal goldstino G that is eaten by the gravitino. Indeed, in this case the zero momentum equation of motion for x may be solved to yield $x = \frac{\psi_X^2}{2f_X}$. Thus in the far infrared we may write X as a non-linear superfield,

$$\boldsymbol{X} = \frac{G^2}{2f_X} + \sqrt{2}G\theta + f_X\theta^2 \tag{4.3}$$

which corresponds to the usual non-linear parameterisation of the goldstino $G \equiv \psi_X$ [174].

Now let us consider the effects of multiple SUSY breaking on the fermion ψ_X. We assume the dominant contribution to SUSY breaking comes not from $\boldsymbol{X}$, but from other sectors sequestered from $\boldsymbol{X}$, so that $\langle f_\Sigma/\sigma\rangle = m_{3/2}$. Clearly, it is now necessary to keep careful track of the dependence on the conformal compensator. We may analyse the effects of SUSY breaking on $\boldsymbol{X}$ by going to the canonical basis via the re-scaling $\boldsymbol{X} \to \boldsymbol{X}/\boldsymbol{\Sigma}$ and solving the auxiliary equation of motion to find

$$f_X = -\frac{2c(f_\Sigma/\sigma)|x|^2 x + 2cx^\dagger\psi_X^2 + fM^2}{M^2 - 4c|x|^2}. \tag{4.4}$$

By minimising the resulting scalar potential for x, we may then extract the mass for the would-be goldstino $\eta \equiv \psi_X$,

$$m_\eta = 2m_{3/2}\left(1 - \frac{M^2 m_{3/2}^2}{2cf^2} + ...\right) \tag{4.5}$$

where additional correction terms are $\mathcal{O}\left(\frac{M^4 m_{3/2}^4}{c^2 f^4}\right)$. This expansion is valid in the regime $m_{3/2}^2/c \ll f^2/M^2 \lesssim m_{3/2}M_P$. One can see that as $\sqrt{f}$ (and M) approaches $m_{3/2}$ these corrections become significant and a different expansion is necessary. From a numerical study we find that for $\sqrt{f} < m_{3/2}$ these large corrections can drive the goldstini mass much smaller than $2m_{3/2}$. Such corrections are to be expected as in this case the SUSY-breaking communicated to a sector becomes larger than the breaking within the sector itself and there is no SUSY to be spontaneously broken within the sector from the outset!

[5] Note that here, for simplicity, we have assumed an R-symmetry is preserved. Inclusion of Kähler terms such as $c'\boldsymbol{X}^\dagger\boldsymbol{X}^3/M^2$ allow the study of R-breaking cases, with similar results to the R-preserving case.

A few remarks are in order. As can be seen clearly in eq.(4.5), the goldstino mass in a given SUSY-breaking sector depends on both the overall scale of SUSY breaking and the scales within the sector itself; the interplay of supersymmetry breaking, gravitational effects and vacuum stabilisation leads to important corrections to the goldstino mass - whenever the SUSY breaking field $\boldsymbol{X}$ gains a large vacuum expectation value linear terms in the Kähler potential lead to mixing between $\boldsymbol{X}$ and the gravity multiplet, and thus corrections to the goldstino mass[6]. Of course, the generalisation of this set-up to N SUSY-breaking sectors is straightforward, resulting in N goldstini η_i; in the mass eigenbasis these become the eaten longitudinal goldstino and $N-1$ uneaten goldstini ζ_a (related to the η_i by $\eta_i = V_{ia}\zeta_a$, where V_{ia} is the rotation matrix that diagonalises the goldstini mass matrix).

In this case it may seem that if one makes a unitary transformation such that there is only one Polonyi field $\boldsymbol{G} = \sum_i f_i X_i / f_{eff}$ all other orthogonal combinations $\tilde{\boldsymbol{X}}_i$ might remain massless by this derivation. However, in this new basis the stabilising Kähler term will lead to mixed interactions between $\boldsymbol{G}$ and the other fields $\tilde{\boldsymbol{X}}_i$. The non-zero vev of $\boldsymbol{G}$ then leads to masses for the fermionic components of $\tilde{\boldsymbol{X}}_i$ and the same results are recovered.

In the subsequent section we will omit the corrections due to mixing with the gravity multiplet. Such a simplifying assumption will make the effects of new physics more transparent, with the understanding that corrections from stabilisation have been suppressed.

4.3 Multiple Goldstini and Modulini from ISS Sectors

The notion of multiple SUSY breaking sectors prompts us to consider how SUSY may be broken within each sector. The ISS models [158] demonstrate that SQCD with massive flavours exhibits a metastable SUSY breaking ground state. Further, the simplicity of such models would suggest that spontaneously broken SUSY is generic in SUSY field theory. Therefore it is natural to consider, in the context of multiple SUSY breaking sectors, that some number may well be of the ISS type, without the addition of any of the singlets or deformations that are absent in the original ISS models, and that are needed only to break R-symmetries. Here we show that such

[6] We thank Clifford Cheung and Jesse Thaler for discussions concerning this interpretation and for correcting a numerical factor in the original version of eq.(4.5). Corrections due to mixing with the gravity multiplet are also discussed in the Appendix A of [74].

a sector would give rise to multiple goldstini fields along with many more 'modulini' fields of mass $\geq 2m_{3/2}$.[7] These extra states could potentially lead to a smoking gun signature of an ISS hidden sector by determining missing energy in LOSP decays to the gravitino, goldstini and modulini.

4.3.1 ISS models at low energies

To illustrate the essential physics we concentrate on the classic ISS-model of SQCD with N_c colours and $N_c + 1 \leq N_f < \frac{3}{2}N_c$ flavours in the free magnetic range [175–177]. The generalisation to other gauge groups should be straightforward. A simple, intuitive understanding of why such an ISS sector gives rise to multiple goldstini fields comes from the fact that, in the far IR, it flows to multiple de-coupled O'Raifeartaigh-like models as we now show.

Using Seiberg duality [176] the IR-free description of the theory is described by an $N_f \times N_f$ gauge singlet meson matrix $\mathbf{\Pi}_{ij}$ and N_f flavours of magnetic quarks $\boldsymbol{\varphi}_i$ and $\tilde{\boldsymbol{\varphi}}_j$ in the fundamental (respectively anti-fundamental) of a $SU(\tilde{N} = N_f - N_c)$ magnetic gauge theory. This theory is weakly coupled at low energies and has a superpotential given by

$$W = h\,\mathrm{Tr}\left[\boldsymbol{\varphi} \cdot \mathbf{\Pi} \cdot \tilde{\boldsymbol{\varphi}} - \mu^2 \cdot \mathbf{\Pi}\right]. \tag{4.6}$$

We assume a generic, non-hierarchical, matrix μ^2_{ij} which can be diagonalised without loss of generality. Among other symmetries this theory exhibits a $U(1)_R$ symmetry where the $\boldsymbol{\varphi}$ fields have zero R-charge and $\mathbf{\Pi}$ has R-charge 2.

Considering the F-components of the meson superfields

$$-F^{\dagger}_{\Pi_{ij}} = h\varphi_i \cdot \tilde{\varphi}_j - h\mu^2_{ij} \quad , \tag{4.7}$$

the first term in this matrix equation is of rank $N_f - N_c$ whereas the second term is of rank $N_f > N_f - N_c$, therefore it is impossible to have $F_{\Pi_{ij}} = 0$ for all $\{i, j\}$ and SUSY is broken. This is the famous ISS 'rank condition'. The minimum of the potential is

$$V = \sum_i^{N_c} (h\mu_i^2)^2 \quad , \tag{4.8}$$

where μ_i^2 are the N_c smallest eigenvalues of μ^2_{ij}. This minimum occurs in field space

$$\mathbf{\Pi} = \begin{pmatrix} \boldsymbol{Y} & \boldsymbol{Z} \\ \tilde{\boldsymbol{Z}} & \mathbf{\Phi} \end{pmatrix}, \quad \boldsymbol{\varphi} = \begin{pmatrix} \varphi_0 + \boldsymbol{\chi}, & \boldsymbol{\rho} \end{pmatrix}, \quad \tilde{\boldsymbol{\varphi}} = \begin{pmatrix} \tilde{\varphi}_0 + \tilde{\boldsymbol{\chi}} \\ \tilde{\boldsymbol{\rho}} \end{pmatrix}, \quad \mu^2 = \begin{pmatrix} \tilde{\mu}_0^2 & 0 \\ 0 & \mu_0^2 \end{pmatrix} \tag{4.9}$$

[7] Purely for typographical clarity we ignore, throughout this section, the possibility of the warping or conformal sequestering considered in [4].

with $\varphi_{\mathbf{0}}\cdot\tilde{\varphi_{\mathbf{0}}} = \tilde{\mu}_0^2$. Also, $\mathbf{\Phi}$ is an $N_c \times N_c$ matrix of fields, $\boldsymbol{Y}$ is $(N_f - N_c)\times(N_f - N_c)$, $\boldsymbol{\rho}$ is $N_c \times N_c$ and the dimensionality of the other terms is apparent from these assignments. Upon rewriting the superpotential in terms of these fields it splits into three pieces $W = W_1 + W_2 + W_3$ with

$$\begin{aligned} W_1 &= h\,\mathrm{Tr}[\boldsymbol{\rho}\cdot\mathbf{\Phi}\cdot\tilde{\boldsymbol{\rho}} + \boldsymbol{\rho}\cdot\tilde{\boldsymbol{Z}}\cdot\tilde{\varphi}_0 + \varphi_0\cdot\boldsymbol{Z}\cdot\tilde{\boldsymbol{\rho}} - \mu_0^2\cdot\mathbf{\Phi}] \\ &= -h\,\mathrm{Tr}[\mu_0^2\cdot\mathbf{\Phi}] + h\sum_{i=1}^{N_f - N_c}(\boldsymbol{\phi}_{1_i}\cdot\mathbf{\Phi}\cdot\boldsymbol{\phi}_{2_i} + \tilde{\mu}_{0_i}(\boldsymbol{\phi}_{1_i}\cdot\boldsymbol{\phi}_{4_i} + \boldsymbol{\phi}_{2_i}\cdot\boldsymbol{\phi}_{3_i})) \end{aligned} \quad (4.10)$$

Here the $\boldsymbol{\phi}$ are N_c dimensional vectors, and the $\tilde{\mu}_{0_i}$ are the first $N_f - N_c$ diagonal components of the $\tilde{\mu}_0^2$ matrix. In the first line we recognise W_1 as an O'Raifeartaigh-like model and in the second line the fields $\boldsymbol{\rho}, \tilde{\boldsymbol{\rho}}, \tilde{\boldsymbol{Z}}$, and $\boldsymbol{Z}$ have been written as matrices made up of row and column vectors to demonstrate explicitly how the superpotential W_1 decomposes into $N_f - N_c$ O'Raifeartaigh-like sectors. The remaining pieces of the superpotential are

$$W_2 = h\,\mathrm{Tr}[\boldsymbol{\chi}\cdot\boldsymbol{Y}\cdot\tilde{\boldsymbol{\chi}} + \boldsymbol{\chi}\cdot\boldsymbol{Y}\cdot\tilde{\varphi}_0 + \varphi_0\cdot\boldsymbol{Y}\cdot\tilde{\boldsymbol{\chi}}] \quad (4.11)$$

$$W_3 = h\,\mathrm{Tr}[\boldsymbol{\rho}\cdot\tilde{\boldsymbol{Z}}\cdot\tilde{\boldsymbol{\chi}} + \boldsymbol{\chi}\cdot\boldsymbol{Z}\cdot\tilde{\boldsymbol{\rho}}] \ . \quad (4.12)$$

W_2 comprises a sector which doesn't break SUSY and contains massive chiral superfields along with the Goldstone superfields of the spontaneously broken symmetries. The Goldstone fields of the spontaneously broken $SU(N_f - N_c)$ are eaten by the gauge superfields through the supersymmetric Higgs mechanism. These SUSY-preserving fields are only coupled to the SUSY-breaking sector through the cubic terms in W_3 and can therefore be consistently neglected when considering the first sector.

It is clear that $\mathbf{\Phi}$ remains massless at tree level, and the diagonal component of $\mathbf{\Phi}$ contains the goldstino. The pseudo-moduli of this field become massive at one-loop level through their interactions with the heavy $\boldsymbol{\phi}$ fields and these masses can be calculated to all orders in the SUSY breaking parameters with the use of the Coleman-Weinberg potential [178]. However, as we would later like to embed this theory in SUGRA, and the Coleman-Weinberg approach is not manifestly supersymmetric, we choose instead to work in terms of the effective Kähler potential which arises when the heavy superfields are integrated out. This agrees with the Coleman-Weinberg potential to second order in the SUSY breaking F-terms and in the limit where SUSY is unbroken this is exact at one-loop.[8]

[8]Including higher order corrections in the SUSY breaking parameters would necessitate including supercovariant derivatives. The effective Kähler potential is sufficient for our needs.

In general for a superpotential of the form

$$W = \frac{1}{2} M_{ij} \boldsymbol{\varphi}_i \cdot \tilde{\boldsymbol{\varphi}}_j \quad , \tag{4.13}$$

where M_{ij} includes mass terms and the pseudo-moduli fields, the exact one-loop Kähler potential is given by

$$K^{(1)} = -\frac{1}{32\pi^2} \operatorname{Tr}\left[M^\dagger M \log\left(\frac{M^\dagger M}{|\Lambda|^2} \right) \right] \quad . \tag{4.14}$$

Reading off the matrix M from eq.(4.10) one finds that the theory describing the light fields contained in $\boldsymbol{\Phi}$, after integrating out the heavy fields contained in $\boldsymbol{\phi}$, is described by the superpotential

$$W = h \operatorname{Tr}[\mu_0^2 \cdot \boldsymbol{\Phi}] \quad , \tag{4.15}$$

and the effective Kähler potential $K_{eff} = K^{(0)} + K^{(1)}$, where $K^{(0)}$ is the canonical Kähler potential, and $K^{(1)}$ is given by

$$K^{(1)} = -\frac{h^2}{32\pi^2} \sum_{i=1}^{N_f - N_c} \operatorname{Tr}\left[2\left(2 + \log\left(\frac{|\tilde{\mu}_{0_i}|^2}{\Lambda^2} \right) \right) \boldsymbol{\Phi}^\dagger \cdot \boldsymbol{\Phi} + \frac{1}{3|\tilde{\mu}_{0_i}|^2} (\boldsymbol{\Phi}^\dagger \cdot \boldsymbol{\Phi})^2 + ... \right] \quad . \tag{4.16}$$

Here the ellipses denote higher order terms which we can ignore as we are studying the theory near the origin of field space, $\langle \Phi \rangle \ll \tilde{\mu}_0$. (The first logarithmic correction to the terms quadratic in Φ corresponds to one-loop wavefunction renormalization of the fields.) Eqs.(4.15) and (4.16) are sufficient for studying the low-energy phenomenology of the ISS model. One can see from the quartic term in the Kähler potential that, once the diagonal components of $\boldsymbol{\Phi}$ develop F-terms, a scalar potential for all pseudo-moduli in $\boldsymbol{\Phi}$ is generated, and in these (global) SUSY ISS models all scalars are stabilised at the origin $\langle \Phi \rangle = 0$.

Most importantly for our purposes, this low energy theory respects the R-symmetry detailed earlier, forbidding the fermions in $\boldsymbol{\Phi}$, hereafter called 'modulini', from gaining mass. This can also be understood by considering the ISS model before integrating out the massive fields: As there are more fermions with R-charge $Q_R = 1$ than with $Q_R = -1$, then, if the vacuum is R-symmetry preserving, not all fermions can obtain a Dirac mass, implying some remain massless.

One may worry that sub-leading corrections spoil this result. There exist corrections to the Kähler potential of the form $\delta K \sim \operatorname{Tr}[\boldsymbol{\Phi}^\dagger \cdot \boldsymbol{\Phi}]^2/|\Lambda|^2$ where Λ is the strong coupling scale of the theory. These corrections have interesting consequences when the theory is embedded in SUGRA, however as they respect the R-symmetry, we conclude that, in the global limit, they do not contribute to the modulini masses. There is also a non-perturbative explicit R-symmety-breaking superpotential term

$$W = N_c(h^{N_f}\Lambda^{-(3N_c-2N_f)}\det[\mathbf{\Pi}])^{1/(N_f-N_c)} \tag{4.17}$$

generated by gaugino condensation [177, 179–181]. However it preserves a discrete R-symmetry subgroup larger than $\mathbb{Z}_2$, and thus the modulini remain protected from gaining a mass. We will return, in the next section, to a discussion of these operators in the context of SUGRA .

In summary, one sees that in the global SUSY limit the metastable supersymmetry-breaking vacuum of SQCD with N_c colours and $N_c+1 \leq N_f < \frac{3}{2}N_c$ massive flavours contains N_c^2 massless modulini (of which N_c are goldstini). In the next section we show that in local supersymmetry these modulini acquire a mass $\geq 2m_{3/2}$ (ignoring warping and/or conformal-sequestering).

4.3.2 ISS modulini masses in Supergravity

In SUGRA with spontaneously broken SUSY, one requires a constant term in the superpotential to cancel the cosmological constant from the non-zero scalar potential. This constant breaks any continuous R-symmetry and we would expect this to manifest itself in a hidden ISS sector by displacing the minimum of the scalar potential for the pseudo-moduli from the origin, and in turn generating masses for the modulini.

First, by considering eq.(4.16) we see that when $\langle\Phi\rangle \neq 0$ modulini masses are indeed generated. As long as $\langle\Phi\rangle \ll \tilde{\mu}_0$ the dominant contribution comes from the quartic operator, higher order terms leading to subdominant corrections suppressed by higher powers of $\langle\Phi\rangle/\tilde{\mu}_0$. For $f_a \sim \mu^2 \ll M_P^2$ for all a, we show in Appendix B.1 that the condition $\langle\Phi\rangle \ll \tilde{\mu}_0$ is satisfied. Thus our SUGRA analysis is valid whenever the scale of supersymmetry breaking is parametrically below the Planck mass.

Moreover, as also detailed in Appendix B.1, we find, for fields, $\boldsymbol{X}_i$, with super- and Kähler-potentials of the form,

$$\begin{aligned} W &= W_0 + f_a\boldsymbol{X}_a \qquad (4.18)\\ K &= \boldsymbol{X}_a\boldsymbol{X}^\dagger_{a^\star} + \frac{1}{\mu^2}A_{ab^\star cd^\star}\boldsymbol{X}_a\boldsymbol{X}^\dagger_{b^\star}\boldsymbol{X}_c\boldsymbol{X}^\dagger_{d^\star} \quad , \qquad (4.19)\end{aligned}$$

and under the same conditions, that the fermion masses are given by

$$m_{ab} = 2m_{3/2}\left(A_{(ad^\star bl^\star)}(A_{(ij^\star kl^\star)}f_if_{j^\star})^{-1}f_{d^\star}f_k - \frac{f_af_b}{f_{eff}^2}\right) \quad , \tag{4.20}$$

once the goldstino direction has been rotated away. (The goldstino direction is the zero eigenvector of this mass matrix which can clearly be seen as $f_a m_{ab} = 0$.)

Armed with eq.(4.20) we can apply these results to modulini from the ISS sector. In Section 4.3 we identified two quartic operators in the Kähler potential that may lead to modulini masses: $\mathrm{Tr}[(\mathbf{\Phi}^\dagger\mathbf{\Phi})^2]$ and $\mathrm{Tr}[(\mathbf{\Phi}^\dagger\mathbf{\Phi})]^2$, and in both cases the tensor A can be written in terms of the identity matrix. First we consider just the operator $\frac{1}{\mu^2}\mathrm{Tr}[(\mathbf{\Phi}^\dagger\mathbf{\Phi})^2]$ and diagonalise the F-terms as in Section 4.3. In this basis one finds for the mass matrix

$$m_{ab,cd} = 2m_{3/2}\left(\frac{f_a^2+f_b^2}{2f_af_b}\delta_{ad}\delta_{bc} - \frac{f_af_c}{f_{eff}^2}\delta_{ab}\delta_{cd}\right) \quad , \tag{4.21}$$

where the f_a are the diagonal elements of the $h\mu_0^2$ matrix in the superpotential. We can now split $\mathbf{\Phi}$ into two sets of fields to study the masses.

First, focusing on the diagonal elements, i.e. $a=b, c=d$, we find a mass matrix

$$m_{aa,bb} = 2m_{3/2}\left(\delta_{ab} - \frac{f_af_b}{f_{eff}^2}\right) \quad , \tag{4.22}$$

which has N_c eigenvalues of $2m_{3/2}(1,1,1,...,1,0)$. The field with zero mass is the true goldstino field $G = f_i\Phi_{ii}/f_{eff}$ that mixes with the gravitino and is eaten leading to a gravitino of mass $m_{3/2}$. In the presence of multiple SUSY breaking sectors this field is in general a mixture of the goldstini from all sectors and from the ISS sector, in this case, we would then expect N_c 'goldstini' fields, ζ, of mass $2m_{3/2}$.

Now considering the off-diagonal fields, i.e. $a \neq b, c \neq d$, we find that the only non-zero terms in the mass matrix have $c=b, d=a$ and are of the form

$$m_{ab,ba} = 2m_{3/2}\left(\frac{f_a^2+f_b^2}{2f_af_b}\right) \quad . \tag{4.23}$$

These fields in general have $m \geq 2m_{3/2}$, with a lower limit, $m = 2m_{3/2}$, in the case with all F-terms equal (again ignoring warping and/or conformal sequestering). These off-diagonal fields are the (now massive) modulini, χ, which accompany the goldstini.

In summary, in the context of multiple sequestered SUSY breaking sectors, from each metastable ISS-type SUSY-breaking sector one expects N_c goldstini of mass $2m_{3/2}$ and $N_c(N_c-1)$ modulini with mass $m \geq 2m_{3/2}$. We emphasise that this result is valid in the absence of extra singlet fields or other deformations of the global-SUSY-limit of the ISS sector that spoil the discrete R-symmetry outlined in Section 4.3.1. Nevertheless, there is no reason to require *all* of the independent SUSY-breaking sectors to break their discrete R-symmetries.

4.3.3 Sub-leading corrections

There are a number of operators that might alter these results. We first consider those we expect to arise within the ISS sector itself. Naïvely, a cause for concern is the fact that by using the effective Kähler potential we are omitting higher order terms in an expansion in $f/\mu^2 \lesssim 1$. We have, however, calculated the full one-loop diagram for the modulini masses, which includes these corrections to all orders and where the effects of SUGRA are included, and we find that the goldstini masses remain unaltered and the modulini masses remain bounded below by $2m_{3/2}$, so do not change the qualitative results from the previous section. The full results of this calculation are contained in Appendix B.2.

Next, as discussed in [158] and in Section 4.3.1, there are corrections due to the underlying microscopic theory of the form $\delta K \sim \mathrm{Tr}[\mathbf{\Phi}^\dagger \cdot \mathbf{\Phi}]^2/|\Lambda|^2$ where Λ is the strong coupling scale of the theory. As highlighted in [158] the effects from these operators are expected to be small as $|\Lambda| \gg \mu$. Including this operator we find that the masses of the fermions are altered slightly. In particular if we set all F-terms equal we find that for

$$K = \mathrm{Tr}[\mathbf{\Phi}^\dagger \cdot \mathbf{\Phi}] - \frac{a}{|\mu|^2}\mathrm{Tr}[(\mathbf{\Phi}^\dagger \cdot \mathbf{\Phi})^2] - \frac{b}{|\Lambda|^2}\mathrm{Tr}[\mathbf{\Phi}^\dagger \cdot \mathbf{\Phi}]^2 \quad , \tag{4.24}$$

and the superpotential in eq.(4.15) the fermion masses are

$$m = 2m_{3/2}\frac{1}{1 + \frac{bN_c|\mu|^2}{a|\Lambda|^2}} \quad . \tag{4.25}$$

As $|\Lambda| \gg |\mu|$ then unless $b \gg a$ corrections from the microscopic theory are small (though possibly phenomenologically interesting). The sign of b is unknown and so these small corrections to the goldstini and modulini masses can potentially be positive or negative.

As mentioned earlier gauge interactions also lead to an explicit breaking of the R-symmetry through the generation of the low energy superpotential [158, 177, 179–181]

$$W = N_c(h^{N_f}\Lambda^{-(3N_c-2N_f)}\det[\mathbf{\Pi}])^{1/(N_f-N_c)} \quad . \tag{4.26}$$

Corrections due to this term should be small, though. First, this operator leads to a superpotential term proportional to $\mathbf{\Phi}^{N_f/(N_f-N_c)}$; however we know that $N_f > 3(N_f - N_c)$ so the discrete R-symmetry remaining after the inclusion of this operator will forbid majorana masses for the modulini in $\mathbf{\Pi}$ in the global SUSY limit. On the other hand, once the theory is embedded in SUGRA, we know the R-symmetry is broken and this leads to vacuum expectation values for the scalar components of

$\langle \Pi \rangle \sim m_{3/2}$ [182]. As with the corrections to the Kähler potential we would then expect this operator to lead to masses for the modulini. We can estimate these corrections as

$$\delta m \sim N_c h^{N_f/(N_f-N_c)} \Lambda^{-(3N_c-2N_f)/(N_f-N_c)} \langle \Phi \rangle^{N_f/(N_f-N_c)} \tag{4.27}$$

$$\sim m_{3/2} \left(\frac{m_{3/2}}{\Lambda} \right)^{(3N_c-2N_f)/(N_f-N_c)} \tag{4.28}$$

and as $\Lambda \gg \mu \gg m_{3/2}$ and also $3N_c > 2N_f$, these corrections should be small unless $(3N_c - 2N_f)/(N_f - N_c) < 1$.

Other operators may arise from outside the ISS sector which lead to R-symmetry breaking and would modify these masses. Such scenarios have been discussed in detail in [74] and thus we direct the interested reader to this work for a through discussion. We note that if the ISS sector(s) is/are sequestered from other SUSY breaking sectors, and only couple to them via the SSM, then corrections to these masses should be at least a loop factor smaller than $m_{3/2}$. If the ISS sector only couples to the SSM and other SUSY breaking sectors gravitationally then we expect the masses not to deviate from the calculation above.

4.4 Couplings and Phenomenology

We now turn briefly to collider phenomenology. For definiteness throughout this section, we will take as a working assumption the set-up described in detail in Refs.[74, 75], namely, the goldstino and gravitino masses are $\geq \mathcal{O}(10\text{GeV})$, and the SUSY-breaking scales are such that the goldstini have comparable, or greater couplings to the SSM than the gravitino. In such a set-up all SUSY collider events will terminate in a cascade decay to the LOSP which may further decay to the goldstino or gravitino within the detector. Such an event can lead to striking signatures at the LHC [183] such as monochromatic electrons or muons in the case of a selectron or smuon LOSP [184]. The lifetime of the LOSP could be determined by observing decays of stopped LOSPs within the detector [185, 186] or within a proposed stopper detector [187–189] which could be constructed after the observation of long-lived charged particles. Further, when observing these decays it may be possible to determine the masses of the gravitino and goldstino using the methods discussed in [190–192]. Therefore, under these assumptions, it may be possible to measure the gravitino and goldstino masses and couplings to the SSM LOSP and we will take this to be the case throughout the remainder of this work.

Let us begin with a few brief remarks on the coupling of goldstini to the SSM. The couplings of the goldstini to Standard Model fields in this case come from interactions of the form

$$\mathcal{L} \supset \sum_i \frac{1}{\Lambda_i^2} \int d^4\theta \boldsymbol{X}_i^\dagger \boldsymbol{X}_i \boldsymbol{\Phi}^\dagger \boldsymbol{\Phi} = \sum_{i,a} \frac{\tilde{m}_i^2 V_{ia}}{f_i} \zeta_a \psi \phi^\dagger \quad . \tag{4.29}$$

As mentioned in Section 4.1, V_{ia} is the rotation matrix that diagonalises the goldstini mass matrix:

$$m_{ij} = 2m_{3/2} \left(\delta_{ij} - \frac{f_i f_j}{f_{eff}^2} \right) \quad , \tag{4.30}$$

where the ζ_a are the $N-1$ goldstini mass eigenstates and the true goldstino that forms the longitudinal component of the gravitino is the N^{th} eigenstate with zero mass in this basis. We see that as $\sum_i f_i V_{i,a\neq N} = 0$ then if SUSY breaking from all sectors is communicated in an identical way, i.e. all Λ_i are equal, then the goldstini couplings to the SSM would be zero, and we would only interact with the true goldstino that forms the longitudinal mode of the gravitino. However, it is a reasonable assumption that in general not all Λ_i are equal, and if even one of these effective mediation scales is different then couplings to all goldstini are generated.

4.4.1 Distinguishing ISS SUSY-breaking

An important question is how we could possibly distinguish if we were coupled to N_c goldstini from one hidden ISS sector, multiple goldstini from many different sectors or just one goldstino with a different effective SUSY breaking scale. We will see that making this distinction is in principle possible, however we will first consider some moral differences between these scenarios. First of all for a hidden ISS sector one would expect a larger coupling of goldstini to sfermion-fermion pairs than gaugino-gauge boson pairs. This would imply a hidden SUSY breaking sector that preserves an R-symmetry. Secondly the F-terms of a hidden ISS sector should be roughly the same magnitude whereas there is no a priori reason to expect the SUSY breaking scale in multiple sequestered sectors to be similar. Finally the SUSY breaking F-terms of a hidden ISS sector would be mediated in a similar way, and therefore couplings to goldstini arising within a single ISS sector should be of the same order of magnitude.

We illustrate the possibility of making this distinction with the example given in Section 4.1 of two sequestered SUSY breaking sectors which couple to the SSM differently as illustrated in Figure 4.1. Considering the decay of a scalar LOSP to the goldstini via the Goldstino Portal, if we ignore details of phase-space factors, the partial width for this process is

$$\Gamma_{\phi^\dagger \to \zeta\psi} \;\simeq\; \frac{1}{16\pi} m_\phi \sum_{a=1}^{N-1} |C_a|^2 \quad , \tag{4.31}$$

where C_a is the dimensionless coupling of the goldstini to ϕ and ψ given in eq.(4.1). As detailed in Appendix B.3, if the sfermion masses are generated through a Kähler potential term of the form

$$K_{soft} = \frac{\mathrm{Tr}[\mathbf{\Phi}^\dagger \cdot \mathbf{\Phi}] \boldsymbol{\phi}^\dagger \boldsymbol{\phi}}{x\Lambda^2} \quad , \tag{4.32}$$

where $\boldsymbol{\phi}$ is an MSSM superfield, we find that the respective decay widths to goldstini and the gravitino are

$$\Gamma_{\phi^\dagger \to \zeta\psi} \;\simeq\; \frac{m_\phi}{16\pi} \left(\frac{(x-1)f}{x\Lambda^2} \right)^2 \frac{N_c y^2}{1 + N_c y^2} \tag{4.33}$$

$$\Gamma_{\phi^\dagger \to G\psi} \;\simeq\; \frac{m_\phi}{16\pi} \left(\frac{f}{x\Lambda^2} \right)^2 \frac{(x + N_c y^2)^2}{1 + N_c y^2} \quad . \tag{4.34}$$

As expected we see that in the limit $x \to 1$ the decay channel to goldstini vanishes and we recover the usual decay width to the gravitino. More importantly however we see that N_c from the ISS sector always appears in combination with y^2 which parameterises the overall scale of the SUSY breaking in the ISS sector. Therefore in this scenario with Goldstino Portal couplings alone one could not distinguish the N_c goldstini in an ISS sector from a SUSY breaking sector with one goldstino and a higher SUSY breaking scale.

However, there is in principle no reason for the couplings to be of the form in eq.(4.32) and the more general coupling

$$K_{soft} = \frac{B_{ijkl} \mathbf{\Phi}^\dagger_{ij} \mathbf{\Phi}_{kl} \boldsymbol{\phi}^\dagger \boldsymbol{\phi}}{x\Lambda^2} \quad , \tag{4.35}$$

where B takes some unknown values, allows not only the goldstini to couple to the SSM fields but the off-diagonal modulini fields also couple with similar strength. This arises through the non-zero F-terms of the SUSY breaking fields.[9] This coupling then

[9]We note that the coupling of hidden sector SUSY-preserving fields to the SSM through their interactions with the SUSY breaking fields can therefore be of the same strength as goldstino couplings to the SSM and this could have phenomenological consequences for other models of SUSY breaking. This mechanism of SUSY-preserving fields 'hitching' through the Goldstino Portal could be useful in scenarios where small renormalizable couplings to gauge-invariant combinations of SSM fields are desired.

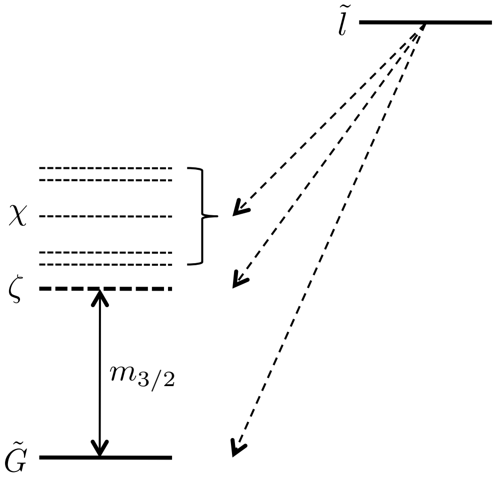

Figure 4.3: LOSP decays to the gravitino, goldstini and modulini of a hidden ISS sector. The modulini masses are bounded below by $2m_{3/2}$ and the observation of such a decay pattern would provide strong support for the physical realisation of the ISS mechanism of SUSY breaking.

allows for a 'smoking gun' collider signature of a hidden ISS sector as LOSP decays will occur to the goldstini and modulini of the hidden ISS sector. If not all F-terms are identical then the modulini masses are all greater than $2m_{3/2}$ (in the absence of warping or conformal sequestering), but bounded below by this value and the long-lived LOSP decay spectrum would be observed to be of the form depicted in Figure 4.3. This decay pattern would give strong support for the ISS mechanism of SUSY breaking if observed and the number of colours in the hidden ISS sector could, in principle, be deduced from the number of decay lines.

This signature is distinct from, say, a LOSP decaying to many gravitino-mass-scale moduli or modulini. This is because the couplings to the ISS sector particles are not simply Planck-scale but depend on a combination of the SUSY-breaking scale in the ISS sector and the messenger scale, which needn't necessarily bear any relation to the Planck scale. Therefore, although one would generically expect many $O(m_{3/2})$ mass particles in top down constructions such particles would not typically lead to the LOSP decay signatures as could arise from a hidden ISS sector.

4.5 Summary

As the LHC continues to explore the electroweak scale, it is timely to consider what experimental indications may be found regarding physics at much higher scales. Certainly the discovery of Standard Model superpartners would be a great breakthrough in itself, but there also exists the potential to learn much more about the mechanism of supersymmetry breaking and its communication to our sector. The observation of LOSP decays to a gravitino would tell us about the quantum nature of gravity [193], while the goldstini proposal [74] shows both that such an observation could be consistent with a standard cosmology [75] and that the observation of LOSP decays to additional goldstini would imply the existence of other sequestered SUSY breaking sectors.

Considering the consequences of multiple sequestered SUSY breaking sectors in light of theoretical considerations (e.g., the structure of calculable models of dynamical SUSY breaking) leads to a surprisingly rich spectrum of fields with masses $\mathcal{O}(2m_{3/2})$ and whose interactions with Standard Model fields may be much stronger than the naive mediation scales suggest. The presence of such goldstini and modulini spanning a range of masses would significantly alter conventional supersymmetric phenomenology. Moreover, measuring their masses and couplings at the LHC would lend insight into not merely the mechanism of supersymmetry breaking, but also the existence and dynamics of additional sectors coupled to the Standard Model through the Goldstini Portal. In this fashion, various features of ultraviolet physics, such as metastable supersymmetry breaking, may become evident in the infrared via the mass spectrum and interactions of goldstini and modulini.

Chapter 5

Stimulated Supersymmetry Breaking

In this chapter we show that small soft terms can create a supersymmetry breaking minimum along a pseudo-flat direction of a hidden sector which would otherwise be incapable of spontaneous supersymmetry breaking. As this minimum lies along a pseudo-flat direction, with non-zero F- or D-terms, the resultant supersymmetry breaking in the hidden sector can be orders of magnitude greater than the soft terms which created the minimum. This opens new avenues for building models of gauge mediation, has consequences for the cosmology of hidden sectors, and strengthens the case for multiple supersymmetry breaking sectors.

5.1 Introduction

As described in Chapter 2, if we wish to employ weak scale supersymmetry (SUSY) as a remedy to the hierarchy problem then, in addition to the supersymmetric standard model (SSM), a supplementary sector which spontaneously breaks SUSY becomes a necessity.

Extending this, if one entertains the idea of multiple sectors, with dynamics over a range of scales then, once supersymmetry has been broken in at least one sector, this raises the possibility of another hidden sector which may have soft masses well below the typical supersymmetric mass scales in the sector. Such a sector would therefore be approximately supersymmetric; the soft supersymmetry breaking a small perturbation on the potential and dynamics of the sector.

In this chapter we are concerned with an effect peculiar to approximately supersymmetric hidden sectors, where, in analogy with approximate global symmetries, we define an ‘approximately’ supersymmetric sector as one in which SUSY is broken softly at scales much lower than the supersymmetric mass scales in the sector.

One would expect such a small perturbation on the sector to have correspondingly small effects, however we comment here on a scenario whereby small soft parameters can have a pronounced effect, enabling a sector which has no stable SUSY breaking vacuum in the absence of the small soft terms to break SUSY spontaneously at typical mass scales of the sector, much greater than the SUSY breaking due to the soft terms.

The basic mechanism is as follows: Consider a supersymmetric hidden sector, containing multiple superfields, which possesses a supersymmetric vacuum. However, along the minimum of the scalar potential, far from the supersymmetric minimum, there also exists a tree-level flat direction with non-zero SUSY breaking. Due to the SUSY breaking this flat direction is lifted radiatively, rendering it pseudo-flat, sloping gently towards the supersymmetric minimum. Such a scalar potential is depicted in Figure 5.1, and we call this sector the ‘secondary’ sector.

Now we consider perturbing this secondary sector by adding a soft potential with scalar masses, $\tilde{m}$, much smaller than the typical supersymmetric mass scales in the secondary sector. These soft terms could be generated due to supersymmetry breaking in another sector, the ‘primary’ sector. This soft potential only modifies the full scalar potential of the secondary sector in a minor way. However, if the symmetry structure of the secondary sector superpotential is different from that of the soft potential, it is possible that the minimum of the supersymmetric scalar potential does not coincide with the minimum of the soft potential.

In this scenario, if the minimum of the soft potential coincides with a point along the pseudo-flat direction then, owing to the extremely flat potential, a local minimum can appear. Thus the small parameters in the soft potential are important in the context of the secondary sector as it possesses a flat direction.

The consequences of a local minimum along a pseudo-flat direction now become important, as along such a direction the SUSY breaking is non-zero, and even more importantly this SUSY breaking occurs at scales much larger than the soft masses that induced the local minimum. Thus we have ‘stimulated’ supersymmetry breaking.

In this way approximately supersymmetric secondary sectors can exhibit a rather curious phenomenon, spontaneously breaking the approximate SUSY, even when the exactly supersymmetric counterpart has no SUSY breaking minimum.

This is amusing, but seems rather contrived - breaking supersymmetry in order to break supersymmetry. However stimulated SUSY breaking may have a place in BSM physics.

The first obvious application is in theories of gauge-mediated SUSY breaking, in particular in the framework of 'ordinary gauge mediation' (OGM), which we now summarise. For a recent general treatment of OGM see [194], and a recent review of gauge mediation [195]. In this scenario the details of the hidden SUSY breaking sector are considered irrelevant, and the SUSY breaking in the hidden sector is parameterised by a singlet 'spurion' superfield, $\boldsymbol{X}$, with $\langle \boldsymbol{X} \rangle = \theta^2 F$. The singlet is then coupled to N pairs of messenger superfields $\boldsymbol{Q}$, $\overline{\boldsymbol{Q}}$, transforming in the $\mathbf{5} \oplus \overline{\mathbf{5}}$ of $SU(5) \supset G_{SM}$.

The superpotential, including messenger masses and couplings to the SUSY breaking singlet, is then taken to be;

$$W_{OGM} = \lambda \boldsymbol{X} \overline{\boldsymbol{Q}} \boldsymbol{Q} + M \overline{\boldsymbol{Q}} \boldsymbol{Q} \quad , \tag{5.1}$$

and from this starting point SUSY breaking is communicated to the supersymmetric standard model (SSM) via gauge interactions, yielding a distinctive SSM spectrum. Note that in eq.(5.1) we have not taken the canonical assumption of $\langle X \rangle = M + \theta^2 F$ as the messenger masses could, in principle, arise from a different supermultiplet, especially when the scales of M and F are greatly separated.

We can see that the details of the hidden sector are necessarily non-trivial by considering the simplest model of SUSY breaking, a Polonyi model, with a hidden sector superpotential $W_h = f\boldsymbol{X}$. Coupling this to the messenger sector we have the combined superpotential

$$W_T = \boldsymbol{X}(\lambda \overline{\boldsymbol{Q}} \boldsymbol{Q} + f) + M \overline{\boldsymbol{Q}} \boldsymbol{Q} \quad . \tag{5.2}$$

Now, even if λ is small, this theory possesses a supersymmetric minimum, and the previously flat X directions are lifted by the messenger interactions. These pseudo-flat directions tilt towards the supersymmetric minimum and the theory is rendered redundant for the purposes of SUSY breaking.

However, in the standard scenario the hidden sector involves couplings between $\boldsymbol{X}$ and some extra superfields which generate radiative corrections to the potential for X, a long-lived SUSY breaking minimum can be achieved, and we can proceed with models of OGM.

With the aid of stimulated SUSY breaking we can proceed along an alternative avenue. We start by positing the existence of an extra primary SUSY breaking sector which generates a soft mass $\tilde{m}$ for X, satisfying $\tilde{m}^2 < f \lesssim M^2$.[1] This soft mass can

[1] In fact $\tilde{m}^2$ can only be a loop factor smaller than f for this mechanism to work, as we discuss in Section 5.2.

stabilise X along a SUSY breaking pseudo-flat direction, possibly near the origin, with $\langle \boldsymbol{X} \rangle = \theta^2 f$.

The extra primary SUSY breaking sector need only break SUSY spontaneously, and is not lumbered with any of the necessary properties of a sector required for gauge mediation. The strongest such requirement being that of significant R-symmetry breaking, along with SUSY breaking, in order to generate comparable gaugino and sfermion masses.[2]

Hence a new recipe for building models of gauge mediation is to construct a secondary sector, including messengers, which possesses a tree-level flat direction along which there is comparable SUSY and R-symmetry breaking. Even if this sector is incapable of spontaneous SUSY breaking in isolation, if we introduce small soft masses for the fields in this sector it may be possible to create a SUSY breaking minimum somewhere along the flat direction. These small soft masses come at the price of a supplementary primary SUSY breaking sector, however this sector needn't also break R-symmetry. Further, this primary SUSY breaking sector can be very weakly coupled to the secondary sector. Finally the stimulated SUSY breaking in the secondary sector can be gauge-mediated to the SSM.

A novel feature of this set-up is that the gravitino mass is no longer set by the SUSY breaking in the sector which contributes dominantly to SUSY breaking in the SSM.

The mechanism of stimulated SUSY breaking also has some more general consequences, in particular in the context of multiple SUSY breaking sectors, whose phenomenology has been a subject of recent interest [4, 74, 75, 162]. If there exist multiple sequestered sectors then some of these may have been stimulated into breaking SUSY, even if they are incapable of spontaneous SUSY breaking in isolation. Or, in other words, if there exist multiple SUSY breaking sectors then many of them need not take the form of a successful SUSY breaking sector in isolation.

Another consequence follows from the observation that the gravitino mass, and thus soft SUSY breaking parameters, are of the order of the Hubble parameter, i.e. $m_{3/2} \sim H$, in the early Universe [196]. It therefore follows that, due to larger soft-masses, additional sectors may have experienced stimulated SUSY breaking in the early Universe, and, when $m_{3/2}$ fell below a critical value, such sectors could have experienced a SUSY-restoring phase transition.

[2]This applies to the MSSM, however the model described in Chapter 3 has a continuous R-symmetry, and thus doesn't require any R-symmetry breaking in the SUSY breaking sector.

In this chapter we focus mainly on the mechanism of stimulated SUSY breaking and comment briefly on the model building applications and cosmological consequences. In Section 5.2 we construct both F-term and D-term examples of stimulated SUSY breaking. We calculate the details of the F-term model for specific parameters, explicitly demonstrating stimulated SUSY breaking. In Section 5.3 we discuss some general features of the mechanism, including the required properties of a candidate stimulated SUSY breaking sector. Finally, we conclude in Section 5.4.

5.2 Some Illustrative Examples

Before discussing the mechanism of stimulated SUSY breaking in more generality in Section 5.3, we first focus on specific examples, in order to illustrate the mechanism as clearly as possible.

5.2.1 An F-term Model

The model contains two sectors;

- The 'primary' sector, which breaks SUSY spontaneously and has dimensionful parameters of order Λ_p. We denote the primary SUSY breaking superfield $\boldsymbol{P}$.
- The 'secondary' sector, which experiences stimulated SUSY breaking. We denote the secondary SUSY breaking superfield $\boldsymbol{S}$. The dimensionful parameters in the secondary sector are of order Λ_s, and satisfy $\Lambda_s \ll \Lambda_p$. In isolation this secondary sector does not possess a local SUSY breaking minimum, and relies on couplings to the primary sector in order to achieve stimulated SUSY breaking.

In this model we work in the limit of rigid SUSY, with $M_P \to \infty$. We also assume a minimal Kähler potential for all fields, with the exception of the interaction term, which we introduce later.

We denote the superpotential for the primary sector W_p, and for the secondary sector W_s. Thus the complete superpotential is $W = W_p + W_s$, where

$$W_p = \boldsymbol{P}(y_p \boldsymbol{\phi}_1 \boldsymbol{\phi}_2 - h_p \Lambda_p^2) - \Lambda_p(\boldsymbol{\phi}_1 \boldsymbol{\phi}_3 + \boldsymbol{\phi}_2 \boldsymbol{\phi}_4) \tag{5.3}$$

$$W_s = \boldsymbol{S}(y_s \overline{\boldsymbol{Q}} \boldsymbol{Q} - h_s \Lambda_s^2) - \Lambda_s \overline{\boldsymbol{Q}} \boldsymbol{Q} \quad . \tag{5.4}$$

We now describe the origin, and motivation, for each sector.

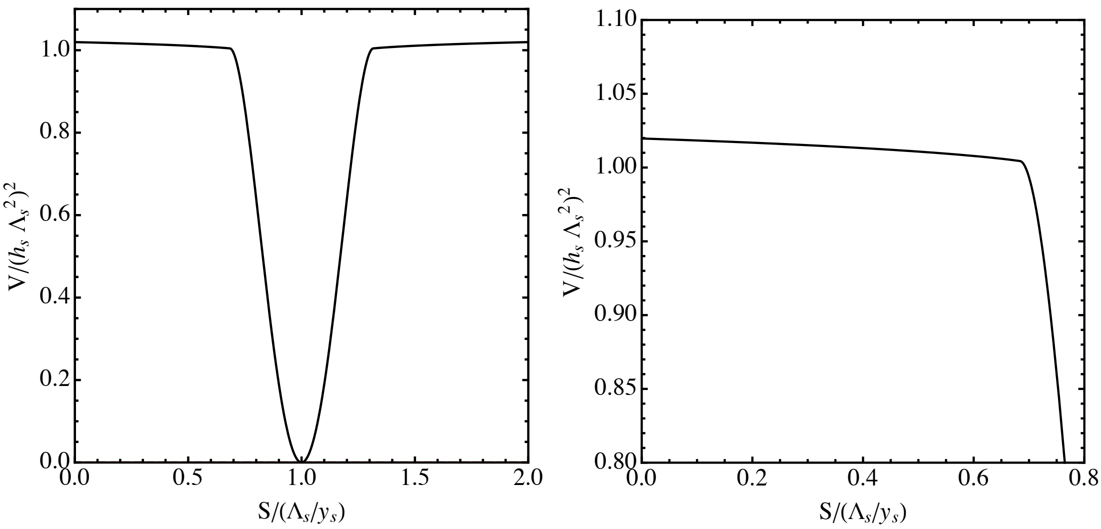

Figure 5.1: The scalar potential for the secondary sector in isolation, i.e. in the limit $\lambda \to 0$. The potential has been minimised in the $\overline{Q}$ and Q directions, and is plotted as a function of S. The relevant parameters are $h_s = 0.1$, $y_s = 1$, $\Lambda_s = 1$. In the left panel one can see the pseudo-flat directions either side of the supersymmetric minimum. In the right panel we zoom in on the left panel to see the lifting of these pseudo-flat directions due to radiative corrections.

W_p takes the form of the low energy limit of a well-known model of dynamical SUSY breaking, namely the Intriligator-Seiberg-Shih models [158]. In [158] it was shown that SUSY QCD, with N_f massive quark flavours, N_f being in the range $N_c < N_f < 3/2N_c$, exhibits a metastable, SUSY breaking vacuum if the quark masses are hierarchically smaller than the IR strong-coupling scale of the theory, i.e. $m_f \ll \Lambda_{IR}$. This theory can be studied using the Seiberg dual [176] theory with N_f flavours and $\tilde{N} = N_f - N_c$ colours. Discarding supplementary massive, SUSY-preserving superfields, at low energies one is left with an O'Raifeartaigh-like superpotential of the form in W_p. In this case W_p is a simplified version of the model, and realistic scenarios with $\tilde{N} > 1$ contain $\tilde{N}$ copies of the dual quark superfields $\boldsymbol{\phi}$. Radiative corrections stabilise $\boldsymbol{P}$ at the origin, and the dimensionful scales Λ_p and $h_p\Lambda_p^2$ can be generated dynamically. For our purposes W_p is a well-motivated spontaneous SUSY breaking model, with dynamically generated scales [197], and for more details on the ISS models we refer the reader to the original work [158].

W_s is inspired by the form of the OGM set-up, and by early models of hybrid supersymmetric inflation [198–201]. It does not respect an R-symmetry, and is incapable of spontaneous SUSY breaking on its own. $\boldsymbol{S}$ is a gauge-singlet and we identify the standard model messengers, $\boldsymbol{Q}$ and $\overline{\boldsymbol{Q}}$, with a 5 and $\overline{5}$ of $SU(5)$, with the intention of gauge-mediating to the supersymmetric standard-model (SSM).

This superpotential is not generic, however we can justify this form with selection rules from the spontaneous breaking of an R-symmetry due to gaugino condensation, as well as attempting to generate the parameters dynamically, along the lines of e.g. [202, 203]. We introduce a pure SUSY QCD sector which becomes strongly coupled at a scale Λ. The gauge fields are contained in the chiral superfield $\boldsymbol{W}_\alpha$ and the massive quark superfields in this sector are $\overline{\boldsymbol{q}}$, $\boldsymbol{q}$. If we allow non-renormalizable couplings of this sector to the messengers through physics at some higher scale $M_\star$, we can replace W_s with an R-symmetric superpotential

$$W_{s_R} = \left(\frac{\overline{\boldsymbol{Q}}\boldsymbol{Q}}{M_\star} - m_q\right)\overline{\boldsymbol{q}}\boldsymbol{q} + \mathrm{Tr}(\boldsymbol{W}_\alpha^2)\left(\frac{1}{g_{SYM}^2} - \frac{\overline{\boldsymbol{Q}}\boldsymbol{Q}}{M_\star^2}\right) \tag{5.5}$$

Thus if the extra SUSY Yang-Mills sector exhibits gaugino condensation we can identify $\langle \mathrm{Tr}(\boldsymbol{W}_\alpha^2)\rangle \sim \Lambda^3$. Further, below the strong coupling scale Λ we can treat $\overline{\boldsymbol{q}}\boldsymbol{q}$ as a meson superfield, making the identification $\overline{\boldsymbol{q}}\boldsymbol{q} \sim \Lambda\boldsymbol{S}$. Hence we arrive at the form of W_s given in eq.(5.4), where the parameters can be retrofitted as

$$y_s \sim \Lambda/M_\star \tag{5.6}$$

$$h_s\Lambda_s^2 \sim m_q\Lambda \tag{5.7}$$

$$\Lambda_s \sim \Lambda^3/M_\star^2 \quad . \tag{5.8}$$

We also assume that the quark masses m_q can be similarly retrofitted. Although we have discussed a possibility for explaining the structure of W_s, alternatively, one should note that non-generic superpotentials can be maintained from high scales due to the perturbative non-renormalization of superpotentials. We have also attempted to generate scales in this model dynamically, however one may alternatively choose to remain agnostic about the origin of the various terms, as the purpose of this model is mainly demonstrative.

For interactions between each sector we assume a Kähler potential term of the form

$$K_{ps} = -\frac{\lambda^2}{M_M^2}(\boldsymbol{P}^\dagger\boldsymbol{P})(\boldsymbol{S}^\dagger\boldsymbol{S}) \quad . \tag{5.9}$$

K_{ps} is the only interaction between the primary and secondary sectors, in particular between the stimulated SUSY breaking superfield $\boldsymbol{S}$ and the primary SUSY breaking superfield $\boldsymbol{P}$. We assume that K_{ps} arises after integrating out messenger interactions between the primary and secondary sectors. For the specific case of gravity mediation $M_M \sim M_P$, although lower mass messengers are also possible.

This completes the model. Although the complete model does not exhibit an R-symmetry, it still breaks SUSY spontaneously and has no SUSY-preserving vacuum, even with kinetic mixing between $\boldsymbol{P}$ and $\boldsymbol{S}$ taken into account.[3] At first this appears at odds with the general theorem of Nelson and Seiberg [204], however this is not the case, as although there is no continuous R-symmetry the superpotential is not generic and the primary and secondary sectors are not coupled through superpotential terms. In fact, the primary sector still breaks SUSY in the same vacuum that would be realised if the primary sector were isolated.

5.2.2 Sectors in Isolation, $\lambda = 0$

To build a complete picture of stimulated SUSY breaking it is necessary to first consider the sectors in isolation.

The primary sector, W_p, is an O'Raifeartaigh model, and with $h_p y_p < 2$ the minimum of the tree-level potential lies at $\langle \phi_i \rangle = 0$, with $\langle P \rangle$ undetermined, and a non-zero F-term of $F_P = h_p \Lambda_p^2$. Although there exists a flat direction along P at tree-level this is lifted radiatively. Integrating out the massive $\boldsymbol{\phi}_i$ superfields to find the Coleman-Weinberg potential [178] one finds a one-loop soft mass for P. Expanded to second order in the small parameter h_p this is

$$\tilde{V}_p = \frac{h_p^2 y_p^4}{24\pi^2} \Lambda_p^2 |P|^2 \quad . \tag{5.10}$$

Thus P is stabilised at the origin, and the low energy effective theory for the primary sector is given by eq.(5.10) and the superpotential

$$W_{p_{\text{eff}}} = h_p \Lambda_p^2 \boldsymbol{P} \quad . \tag{5.11}$$

The story for the secondary sector, W_s, is somewhat different. There exists a supersymmetric minimum at $\langle y_s S \rangle = \Lambda_s$ and $\langle \overline{Q} Q \rangle = h_s \Lambda_s^2 / y_s$.

Writing $\tilde{S} = y_s S - \Lambda_s$, which is zero at the supersymmetric minimum, then for $|\tilde{S}|^2 > y_s h_s \Lambda_s^2$ the scalar potential is minimised with $\langle \overline{Q} Q \rangle = 0$ and $\langle \tilde{S} \rangle$ is a flat direction at tree-level. However in this region $F_S \neq 0$ and radiative corrections lift this flat direction. Including these corrections by integrating out the massive $\overline{Q}$ and Q superfields, the potential for $\tilde{S}$ is

$$\begin{aligned} V_s &= h_s^2 \Lambda_s^4 + \frac{1}{32\pi^2} (2 y_s^2 h_s^2 \Lambda_s^4 \log(|\tilde{S}|^2/\mu^2)) \\ &+ (|\tilde{S}|^2 + y_s h_s \Lambda_s^2)^2 \log(1 + y_s h_s \Lambda_s^2 / |\tilde{S}|^2) \\ &+ (|\tilde{S}|^2 - y_s h_s \Lambda_s^2)^2 \log(1 - y_s h_s \Lambda_s^2 / |\tilde{S}|^2)) \quad , \end{aligned} \tag{5.12}$$

[3] We thank Graham Ross for bringing this to our attention.

where μ is the UV cut-off and we have written $\tilde{S} = y_s S - \Lambda_s$.

Whenever $|\tilde{S}|^2 \leq y_s h_s \Lambda_s^2$ the potential is minimised with $\langle \overline{Q} Q \rangle = (y_s h_s \Lambda_s^2 - |\tilde{S}|^2)/y_s^2$ and there are similar one-loop corrections. These corrections are, however, subdominant in this region as $\tilde{S}$ becomes massive at tree level. Although we don't give these corrections here they are included in all Figures.

In the left panel of Figure 5.1 we show the scalar potential for S, having minimised in the $\overline{Q}$ and Q directions. One can see the supersymmetric minimum and in the right panel of Figure 5.1 we focus on the pseudo-flat direction to show the gentle slope generated by the radiative corrections.

This concludes the study of the primary and secondary sectors in isolation. We now go on to consider the case where $\lambda \neq 0$ and the SUSY breaking from the primary sector is mediated to the secondary sector.

5.2.3 Stimulated SUSY breaking, $\lambda \neq 0$

Once we turn on the coupling, λ, between the primary and secondary sectors the SUSY breaking from the primary sector is mediated to the secondary sector. In this case a soft mass for the scalar component of $\boldsymbol{S}$ is generated, and, to second order in h_p, the soft potential for S is

$$\tilde{V}_S = \tilde{m}^2 |S|^2 = \frac{\lambda^2 h_p^2 \Lambda_p^4}{M_M^2} |S|^2 \quad . \tag{5.13}$$

This soft mass works to stabilise S at the origin. On the contrary we see from the lower panel of Figure 5.1 that the potential from the secondary sector alone leads to a shallow gradient at the origin, preferring to stabilise S at the supersymmetric minimum $\langle y_s S \rangle = \Lambda_s$. It is the interplay between the behaviour of these two terms that can lead to stimulated SUSY breaking.

In order to introduce a minimum near the origin the soft mass must be great enough to overcome the slope of the pseudo-flat direction. In this model this corresponds to the requirement that

$$\tilde{m} \gtrsim \frac{h_s y_s^2}{4\pi} \Lambda_s \quad . \tag{5.14}$$

Thus for relatively natural values of $h_s \sim y_s \sim 0.1$ the soft mass can be up to four orders of magnitude below the typical mass-scales in the secondary sector. Smaller soft masses can lead to stimulated SUSY breaking if the couplings in the secondary sector are reduced.

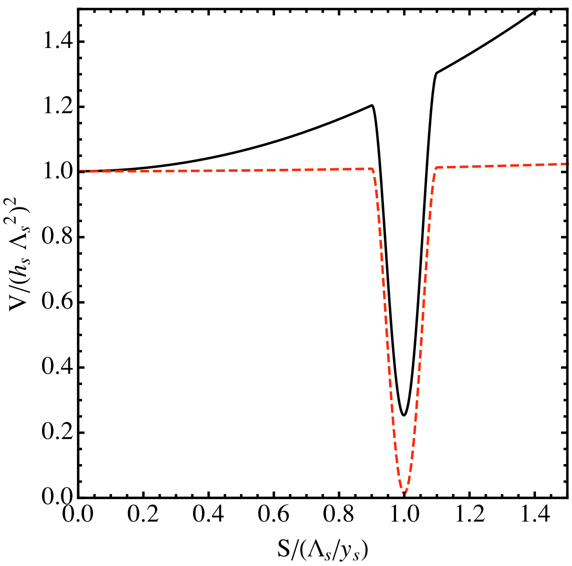

Figure 5.2: The potential in the secondary sector, minimised in the $\overline{Q}$ and Q direction, as a function of the scalar field S. We have included the soft potential for S, generated through interactions with the primary sector, with $\lambda \neq 0$. One can see that the soft mass has introduced a metastable minimum near the origin which would not exist otherwise. The parameters chosen are $\Lambda_s = 10^4$ TeV, $h_s = 0.1$, $y_s = 0.1$ and $\tilde{m} = 50$ TeV (solid black), $\tilde{m} = 10$ TeV (dashed red). If we identify $\overline{\boldsymbol{Q}}$ and $\boldsymbol{Q}$ as messenger superfields, the metastable minimum gives the phenomenologically appealing value of $F_Q/M_Q = 100$ TeV, where $F_Q = h_s y_s \Lambda_s$ is the SUSY breaking experienced by the messengers and $M_Q = \Lambda_s$ is the messenger mass. Thus acceptable gaugino and sfermion masses can be generated from such a sector.

In Figure 5.2 we plot the scalar potential for S with the soft mass included. One can see that a metastable minimum appears near the origin. In this minimum, for the parameters we have chosen, the ratio of the soft masses to the stimulated SUSY breaking is

$$\begin{aligned} F_{soft}/F_S &= \frac{\tilde{m}^2}{h_s \Lambda_s^2} \\ &= 2.5 \times 10^{-4} \quad , \end{aligned} \tag{5.15}$$

where the parameters used are detailed in the caption of Figure 5.2. The soft terms have 'stimulated' SUSY breaking in the secondary sector.

The soft mass of $\tilde{m} = 50$ TeV can be achieved with couplings of order $h_p \sim \lambda \sim 0.1$, messenger masses of $M_M \sim 10^9$ TeV, and a primary SUSY breaking scale of $\Lambda_p \sim 10^6$ TeV, below the limit at which one expects to generate dangerous flavour-changing neutral-currents from gravity mediated soft-terms.

In the scenario where the stimulated SUSY breaking is metastable one would like to make this vacuum cosmologically acceptable. The first concern is whether after reheating one expects to settle in the metastable or stable minimum. At high temperatures, $T \gg \Lambda_s$, the masses of the messengers, $\overline{\boldsymbol{Q}}$ and $\boldsymbol{Q}$, are irrelevant and the coupling between the messengers and $\boldsymbol{S}$ will dominate the dynamics. Thus the thermally generated mass should drive $\langle S \rangle \to 0$. As the temperature falls we then expect to settle in the metastable, rather than the stable minimum. One might also worry about the lifetime of the metastable minimum. Approximating the potential with a triangle, the bounce action is

$$B \approx \frac{2\pi^2}{3} \left(\frac{\Lambda_s}{y_s \tilde{m}} \right)^2 \gg 1 \quad , \tag{5.16}$$

where we have utilised the results of [205]. Thus the metastable SUSY breaking state can also be made cosmologically long-lived.

Therefore, with $\overline{\boldsymbol{Q}}$ and $\boldsymbol{Q}$ identified as messengers charged under the standard model gauge group, one could mediate the stimulated SUSY breaking to the SSM, generating gaugino and sfermion masses at the same order of magnitude as a result of the comparable R-symmetry breaking and SUSY breaking scales in this model. In such a manner stimulated SUSY breaking can be utilised in building models of low-scale gauge mediation.

5.2.4 A D-term Model

It is also possible to build models of stimulated SUSY breaking where the SUSY breaking arises from D-terms. A simple example appears in an adapted form of a D-term inflation model [206]. We assume the same primary and interaction sectors as in eq.(5.4), and simplify the secondary sector superpotential to

$$W_s = y_s \boldsymbol{S}\overline{\boldsymbol{Q}}\boldsymbol{Q} - \Lambda_s \overline{\boldsymbol{Q}}\boldsymbol{Q} \quad , \tag{5.17}$$

which is invariant under an R-symmetry. We introduce charges of ± 1 for $\boldsymbol{Q}$ and $\overline{\boldsymbol{Q}}$ under an extra $U(1)_s$ gauge symmetry. If we include a Fayet-Iliopoulos D-term, $h_s \Lambda_s^2$, the full tree-level scalar potential is

$$\begin{aligned} V_s &= |y_s \overline{Q} Q|^2 + |y_s S - \Lambda_s|^2 (|Q|^2 + |\overline{Q}|^2) \\ &\quad + \frac{g^2}{2} (|Q|^2 - |\overline{Q}|^2 + h_s \Lambda_s^2)^2 \quad . \end{aligned} \tag{5.18}$$

Both dimensionful parameters in this model can also be retrofitted to dynamically generated scales, following the examples in [202].

The scalar potential in eq.(5.18) has a similar behaviour to the F-term model described previously. There is a supersymmetric minimum at $\langle y_s S\rangle = \Lambda_s$, $\langle Q\rangle = 0$, $\langle|\overline{Q}|^2\rangle = h_s\Lambda_s^2$, and for large values of S, when $|y_s S - \Lambda_s|^2 > h_s g^2\Lambda_s^2$, the scalar potential is minimised for $\langle Q\rangle = \langle\overline{Q}\rangle = 0$ and is tree-level flat in the S direction. Along this flat direction the SUSY breaking is

$$D_s = g h_s \Lambda_s^2 \quad . \tag{5.19}$$

Again, as SUSY is broken, this flat direction is lifted by radiative corrections. For large $|\tilde{S}|^2 = |y_s S - \Lambda_s|^2 > h_s g^2 \Lambda_s^2$ the potential behaves as

$$\begin{aligned} V_s &= \frac{g^2}{2} h_s^2 \Lambda_s^4 + \frac{1}{32\pi^2}(2g^4 h_s^2 \Lambda_s^4 \log(|\tilde{S}|^2/\mu^2)) \\ &+ (|\tilde{S}|^2 + g^2 h_s \Lambda_s^2)^2 \log(1 + g^2 h_s \Lambda_s^2/|\tilde{S}|^2) \\ &+ (|\tilde{S}|^2 - g^2 h_s \Lambda_s^2)^2 \log(1 - g^2 h_s \Lambda_s^2/|\tilde{S}|^2)) \quad , \end{aligned} \tag{5.20}$$

where μ is a UV-cut-off.

Thus, once again, if we include the coupling of this secondary sector to the primary sector then soft terms for S, generated as a result of the SUSY breaking in the primary sector, can stabilise S somewhere along this pseudo-flat direction. In this case the overall SUSY breaking in the secondary sector is

$$D_s = g h_s \Lambda_s^2 \gg \tilde{m}^2 \quad , \tag{5.21}$$

and the SUSY breaking in the primary sector has stimulated SUSY breaking in the secondary sector.

Having considered some simple models of stimulated SUSY breaking we now go on to consider the mechanism in more general terms.

5.3 Some General Features of Stimulated SUSY breaking

Considering the mechanism in general, we can identify the key ingredients of a stimulated SUSY breaking set-up, as well as some generic properties.

First we consider the tree-level scalar potential of the secondary sector alone, and simply denote this potential V. It is commonplace for supersymmetric theories to possess tree-level flat directions, where $V' = \partial V/\partial\phi = 0$ and $V'' = \partial^2 V/\partial\phi^2 = 0$, with ϕ a scalar field. Usually such flat directions are supersymmetric, with $V_{\text{flat}} = 0$, however it is possible that flat directions arise which have non-zero F- or D-terms, giving

$$V_{\text{flat}} = F_i^\dagger F_i + \frac{1}{2}D^a D^a \neq 0 \quad , \tag{5.22}$$

where the sum over fields is implied.

Denoting the superfields corresponding to the scalar flat directions $\boldsymbol{X}_i$, and denoting any additional superfields which are charged under gauge and global symmetries $\boldsymbol{\phi}_j$, then a renormalizable theory of the following form may possess such flat directions

$$W = f_i \boldsymbol{X}_i + (\lambda_{ijk}\boldsymbol{X}_i + M_{jk})\boldsymbol{\phi}_j \boldsymbol{\phi}_k \quad , \tag{5.23}$$

where λ_{ijk} is a trilinear coupling constant. Depending on the nature of λ_{ijk} and M_{jk} it may be possible to justify the form of the superpotential with an R-symmetry, under which the singlet superfields have R-charges of $Q_{X_i} = 2$. Otherwise, if the theory does not possess an R-symmetry, quadratic and cubic terms in $\boldsymbol{X}_i$ can be forbidden with selection rules from spontaneous R-symmetry breaking.[4]

Studying the F-terms from the superpotential in eq.(5.23) one can see that for very large field values, where $\sqrt{f_i}\langle\lambda_{ijk}X_i + M_{jk}\rangle \gg f_i$, the scalar potential is minimised with $\langle\phi_i\rangle = 0$, and is tree-level flat in the $\langle X_i\rangle$ direction. Thus any theory of the form in eq.(5.23) may be a candidate for stimulated SUSY breaking, even if it possesses a SUSY-preserving minimum.

As the flat directions in such theories are not supersymmetric they are typically lifted radiatively, generating a potential for the flat direction. If this is the case we call this direction 'pseudo-flat'. We now correct the tree-level potential with the full one-loop Coleman-Weinberg [178] potential

$$V_F = V + V_l \quad . \tag{5.24}$$

Pseudo-flat directions are usually considered in the context of theories which break SUSY at tree-level. In such a case, once radiative corrections are taken into account, a local minimum with non-zero vacuum energy exists, i.e. $V > 0$, $V_F' = 0$ and $V_F'' > 0$, where only the tree level vacuum energy is included in the first inequality. Attempting to stimulate SUSY breaking in a theory which already possesses a local SUSY breaking minimum would be rather pointless, therefore we focus our attention on theories which 'almost' break SUSY.

We define an 'almost' SUSY breaking theory as one in which there exists a supersymmetric minimum, but, far from the supersymmetric minimum, also exhibits

[4]A further term, $A_{ijk}\boldsymbol{\phi}_i\boldsymbol{\phi}_j\boldsymbol{\phi}_k$, may also be added. However, depending on the form of A_{ijk}, this may allow for cancellations between terms which spoil the stimulated SUSY breaking.

a tree-level flat direction along the local minimum of the scalar potential, where the conditions

$$V > 0, \quad V' = 0, \quad V'' = 0 \ \ , \tag{5.25}$$

are satisfied. Although this looks promising for spontaneous SUSY breaking, in an almost-SUSY breaking theory the full potential, including radiative corrections, has no stable points where

$$V > 0, \quad V_F' = 0, \quad V_F'' > 0 \ \ . \tag{5.26}$$

Two examples of such a theory were discussed in the previous section and the upper panel of Figure 5.1 demonstrates such a potential. In an almost-SUSY breaking theory, rather than stabilising the fields at a local SUSY breaking minimum, the radiative corrections lift the flat direction so as to gently slope towards the supersymmetric minimum.

Now, if SUSY breaking occurs in the primary sector then soft masses, and in general a soft scalar-potential, can be generated in the secondary sector, along with supersymmetric superpotential terms generated via the Giudice-Masiero mechanism [128]. We assume that all such dimensionful terms are of order $\tilde{m} \sim F_P/M_M$, and coupling constants of order $c \sim \tilde{m}/M_M$, where F_P parameterises the SUSY breaking in the primary sector and M_M is the scale of the messengers between the primary and secondary sectors.

These terms will alter the scalar potential for the secondary sector and we call the additional terms in the scalar potential $\tilde{V}$, all terms vanishing in the limit $\tilde{m} \to 0$. If $\tilde{m}$ is much smaller than the typical scales in the secondary sector then this additional soft scalar potential can be considered as a small deformation of the scalar potential, and the secondary sector becomes approximately supersymmetric.

In most cases such a small perturbation on the scalar potential is of little interest. However, if V contains a tree-level flat direction where $F \neq 0$, and $\tilde{V}$ possesses a stable minimum somewhere along this flat direction, it is possible for the scalar fields to be stabilised in a metastable, or even stable, state with SUSY breaking $F \gg \tilde{m}^2$. This is 'stimulated' SUSY breaking.

If a tree-level flat direction with non-zero F-terms were exactly flat at all orders then stimulated SUSY breaking could be achieved with arbitrarily small soft terms. However, tree-level flat directions are typically lifted due to the SUSY breaking within the secondary sector. Therefore in order to realise stimulated SUSY breaking in a realistic scenario the soft terms of order $\tilde{m}$ must overcome the gradient of the full one-loop potential. This places a lower limit on the magnitude of SUSY breaking that must be transmitted to the secondary sector in order to stimulate SUSY breaking. A rule-of-thumb is that soft terms should be greater than the typical scales in the secondary sector suppressed by a loop factor.

Finally we come to some general conditions for stimulated SUSY breaking. If V is the tree-level scalar potential for a secondary sector, V_l is the one-loop correction to this potential, and $\tilde{V}$ is the soft scalar potential generated from SUSY breaking in the primary sector, then the full scalar potential is $V_T = V + V_l + \tilde{V}$. To realise stimulated SUSY breaking we require that at some point in field space the conditions

$$V \neq 0, \qquad V' = 0, \qquad V'' = 0, \tag{5.27}$$

$$\tilde{V}' + V_l' = 0 \tag{5.28}$$

$$\tilde{V}'' + V_l'' > 0 \tag{5.29}$$

are satisfied. Thus, a stable local minimum of the soft-plus-loop-level scalar potential must coincide with a point along a SUSY breaking tree-level flat direction.

5.3.1 A Pseudo-Goldstino

Although stimulated SUSY breaking is spontaneous, the presence of the soft terms implies that it is only an approximate SUSY that is broken spontaneously. Thus, in the rigid SUSY limit, we expect a pseudo-goldstino, as opposed to an exactly massless goldstino. One can see that in the limit $\tilde{m} \to 0$, from eq.(5.27) we still have $V \neq 0$ and $V' = 0$, and consequently a massless goldstino. Therefore any correction to the mass must be of order $\tilde{m}$. These corrections can arise at tree-level from SUSY-preserving superpotential terms which are generated via the Giudice-Masiero mechanism [128], or, if such terms are absent, then one would also expect a mass $m_{PG} < \tilde{m}$ to be generated at loop-level.

Therefore a ‘smoking gun’ consequence of stimulated SUSY breaking would be the existence of a light fermion, with mass a few orders of magnitude below the scale of SUSY breaking in a hidden sector. The mass of this pseudo-goldstino would give an estimate of the soft SUSY breaking terms which are stabilising the stimulated SUSY breaking. If $\tilde{m} \sim m_{3/2}$, corresponding to gravity mediation from the primary sector, one would expect the pseudo-goldstino to acquire mass $2m_{3/2}$ [4, 74]. However, if the mediation from the primary to secondary sector occurred at lower scales, and $\tilde{m} \gg m_{3/2}$, the pseudo-goldstino mass would bear no relation to the gravitino mass.

5.3.2 Non-minimal Kähler Potential

Although in Section 5.3 the description of potential stimulated SUSY breaking scenarios was fairly general, in the individual sectors of Section 5.2 we assumed minimal Kähler potential terms. However we also assumed that scales in each sector were generated dynamically, explaining the hierarchy between these scales and the Planck scale. However, one typically expects non-renormalizable operators when considering effective descriptions of strongly coupled theories.

Non-renormalizable operators in the primary sector are not a concern for this work, as all we require of the primary sector is that it breaks SUSY spontaneously and dynamically, and we are not concerned with the details of how this occurs here, although we note that higher order Kähler terms in the ISS model used in Section 5.2 are under control [158].

The important consideration is whether higher-order terms, in particular Kähler terms, which can be consistent with imposed symmetries, may spoil the flatness of the pseudo-flat direction in the secondary sector. A particularly troublesome operator is

$$\Delta K_S = \frac{(\boldsymbol{S}^\dagger \boldsymbol{S})^2}{\Lambda^2} \quad . \tag{5.30}$$

If the unknown scale Λ is of order the typical scales in the secondary sector, i.e. $\Lambda \sim \Lambda_s$, this operator generates a soft mass of order $\Lambda_s \gg \tilde{m}$ along the flat direction, thus spoiling stimulated SUSY breaking. However, we expect that such an operator would arise from integrating out modes of mass Λ_s and would come suppressed by at least a loop factor, so should not spoil the stimulated SUSY breaking. It is in fact such corrections that we calculated in eq.(5.12).

If $\Lambda \gg \Lambda_s$, arising from integrating out unknown heavier modes associated with some strong-coupling scale, we require that $\Lambda_s^2 \ll \tilde{m}\Lambda$ in order for stimulated SUSY breaking to be possible.

5.3.3 Gravity Mediated Soft Terms

A particularly appealing scenario for stimulated SUSY breaking would be if the primary sector were to break SUSY at scales $F_P \lesssim (10^{10}\ \text{GeV})^2$, generating soft masses of order $\tilde{m} \sim 10$ GeV in the secondary, and SSM, sectors via gravity mediation. These soft masses could in principle stimulate SUSY breaking in a hidden sector up to scales as high as ~ 100 TeV, which would correspond to four orders of magnitude between the soft terms and the SUSY breaking.

This gravity-mediated stimulated SUSY breaking can be realised with the secondary sector model of Section 5.2.1. For $\tilde{m} \sim 10$ GeV we find that with the parameters $\Lambda_s = 10^6$ TeV, $h_s = 1$ and $y_s = 10^{-4}$, a metastable SUSY breaking vacuum appears near the origin. The small value of y_s implies that the secondary SUSY breaking field and the messengers are very weakly coupled, and this small coupling requires explanation. In addition, for these parameters, the ratio of SUSY breaking experienced by the messengers to the messenger masses is $F_Q/M_Q = 100$ TeV, suitable for gauge mediation. Summarising this set-up; a primary SUSY breaking sector generates soft terms in all sectors via gravity mediation. These soft terms go on to stimulate SUSY breaking in a secondary sector at a much higher scale, and this stimulated SUSY breaking is subsequently gauge mediated to SSM.

Such a scenario would also correspond to a neat realisation of the 'Goldstini' scenario [74], with both the gravitino, from the primary sector, and goldstino, from the secondary sector, with masses potentially measurable at the LHC, along with an appealing cosmology [75]. All arising from one fundamental SUSY breaking in the primary sector.

5.4 Summary

We have demonstrated the mechanism of stimulated SUSY breaking, both in the context of specific models and in more general terms. It may be that this mechanism is merely a technical novelty; allowing approximately supersymmetric sectors to break SUSY spontaneously, even though their exactly supersymmetric counterparts cannot. However, if one is willing to pay the price of an extra SUSY breaking sector, stimulated SUSY breaking can open new possibilities for building models of gauge mediation, by utilising models that, alone, are incapable of breaking SUSY spontaneously. Such an example is demonstrated in the Introduction.

As a sector which experiences stimulated SUSY breaking need not exhibit an R-symmetry, it may be possible to avoid some of the problems faced in building models of gauge mediation which relate to the necessity of R-symmetry breaking. One such difficulty lies in generating gaugino masses comparable to the sfermion masses.

Stimulated SUSY-breaking may also have interesting cosmological consequences as large soft masses, arising due to thermal effects in the early Universe [196], may have led to stimulated SUSY breaking in sectors which have subsequently evolved to a SUSY-preserving minimum. Further, if there exist multiple sequestered sectors, stimulated SUSY breaking lends support to the concept of multiple SUSY breaking sectors

[74, 162]. This is because, even if the extra sectors are not capable of spontaneous SUSY breaking in isolation, these sectors may have been stimulated into spontaneous SUSY breaking by the existence of a single original SUSY breaking sector.

Recently the apparently similar, but essentially different model of 'cascade SUSY breaking' was proposed [207]. This model also relies on SUSY breaking from a primary sector which is mediated to a secondary sector, generating soft terms of order $\tilde{m}$. The ultimate difference, however, is that in cascade SUSY breaking the eventual SUSY breaking in the secondary sector is $F_S \propto \tilde{m}^2$, corresponding to the global minimum in Figure 5.2. Whereas, in stimulated SUSY breaking we have $F_S \propto \Lambda_s^2 \gg \tilde{m}^2$ and the soft terms stimulate the secondary sector to break SUSY at much higher scales. Thus, although the overall set-up is rather similar, cascade, and stimulated SUSY breaking mechanisms both constitute appealing, although rather different, scenarios for model building.

Part II

Dark Matter and Baryogenesis

Chapter 6

Overview of Baryogenesis and Dark Matter

6.1 Baryogenesis

It is in everyday experience that we learn of a local preponderance of matter over antimatter, and thus baryons over antibaryons. However, in the last century we have learned that this asymmetry between abundances extends to the whole Universe. We define η, a measure of the asymmetry, as the cosmological average of

$$\eta = \frac{n_B - n_{\overline{B}}}{n_\gamma} \quad , \tag{6.1}$$

where n is denotes number density. If the Universe were baryon-symmetric at temperatures of a few keV the remaining value of η would be zero, and the remaining baryon density would be $n_B/n_\gamma \approx 10^{-20}$ due to the efficient annihilation of baryons with antibaryons [55]. Thus the remaining abundances of nuclei are very sensitive to η, and the relative abundances of particular nuclei are also sensitive to this quantity. The process by which various elements form in the early Universe is called 'Big Bang Nucleosynthesis', (BBN), and it is possible to calculate with some accuracy how much of each element should remain after BBN. In performing these calculations η is a free parameter, and it is found that these calculations agree with observation whenever $\eta \approx 6 \times 10^{-10}$ [55]. This is strong evidence for the presence of a cosmological baryon asymmetry.

Recently additional evidence for a baryon asymmetry has been found by measuring temperature anisotropies in the cosmic microwave background radiation. The magnitude, or power, of these anisotropies on a given angular scale is dependent on η, and thus this parameter can be determined by measuring the size of the peaks [52]. This independent measurement corroborates the value predicted by BBN calculations.

There is clearly a non-zero value of η, but is this really a problem? If one believes in inflationary cosmology then it is, because even if we assume the Universe formed with a non-zero value of η this asymmetry would have been diluted by many orders of magnitude during inflation, and the pre-inflationary value of η required would have been enormous. Even if one was comfortable with such an unnatural scenario, the explanation for a baryon asymmetry would still be lacking. Therefore the correct question to ask is: how could the baryon asymmetry have formed after, or at the end of, inflation?

There are a plethora of theories attempting to explain the value of the baryon asymmetry, and all require the existence of some physics beyond the SM (see e.g. [208]). One commonly studied example is 'electroweak baryogenesis' (for a recent review see [209]), where the baryon asymmetry is created in the walls of expanding bubbles of broken electroweak phase which arise during a strongly first-order electroweak phase transition. In this case an additional source of CP-violation is required. Another example is 'leptogenesis' [210], where a lepton asymmetry is created by the out-of-thermal-equilibrium decay of right-handed neutrinos, and this asymmetry is transferred to baryons through electroweak sphalerons. However, when one notes that the Baryon and DM abundances are quite similar, it is natural to investigate theories that generate both a baryon and DM asymmetry at the same time. This line of investigation has recently garnered much attention, and still comparatively few models that attempt to *generate* the asymmetries exist, whereas the sharing, and thus linking, of the two asymmetries has gained more attention. In Chapter 8 we present a novel model in which a shared DM and baryon asymmetry is generated.

6.2 Dark Matter

In 1934 Fritz Zwicky postulated the existence of DM in galaxy clusters in order to explain the orbital velocities of galaxies within those clusters [48]. This was not the first time the DM hypothesis had been proposed. As early as the 1840s John Couch Adams and Urbain Le Verrier proposed the existence of an unseen, dark, planet in order to account for the anomalous motion of Uranus. In this instance the DM hypothesis proved fruitful. The current guise of the DM hypothesis takes its form in the existence of particles somewhat more microscopic than the, now discovered, planet Neptune, however much of the evidence follows from similar reasoning.

Robust evidence for DM arises on many scales and we will review this evidence briefly here, however recent, more thorough reviews are contained in [42, 211]. On the galactic scale it is seen that the rotational velocities of stars about the center of their host galaxies have a distribution that is flat at large radii, however the distribution of observed matter within the galaxy suggests that the rotational velocity should fall off at large radii [43]. This behaviour is most pronounced in 'Low Surface Brightness' galaxies, which are likely dominated by DM at all radii. Another method for determining the local matter density is to measure the dispersion of velocities within a galaxy. The magnitude of the dispersion is linked to the gravitational potential, and hence matter abundance. Measurements of velocity dispersions in dwarf spheroidal, and spiral, galaxies indicate the presence of DM [44–47].

Evidence on the scale of galaxy clusters arises again in measurements of velocity dispersions [48, 49], and also in how light travels through and past galaxy clusters. Einstein's GR predicts that light is bent when travelling through a gravitational potential well. This effect is known as 'Gravitational Lensing', and can also be used to determine the local matter density in objects such as galaxy clusters [50]. The presence of gravitational lensing can be observed whenever double images of a galaxy in the background appear on either side of a large object along the line of sight. Measurements of the total mass of galaxy clusters made in this way corroborate the existence of DM. Convincing additional evidence came with the gravitational lensing studies of the bullet cluster [51] and recently Abell 2744 [212]. In these observations of the merging, or collision, of galaxy clusters, it is observed that a significant DM component has continued to travel unhindered, while hot gas has clumped together at the point of collision, lending further support to the assumption that DM interacts weakly with both baryons and with itself.

Evidence arises on cosmological scales through the observation of temperature anisotropies in the CMB. These anisotropies arise as a result of acoustic oscillations of the photon-baryon plasma before the CMB forms (see e.g. [53]). The angular scale and magnitude at which the first peak arises depends on the total amount of matter present, however the second peak depends on the amount of DM present. Observation of these peaks suggests the presence of a significant component of DM in the early Universe [52]. Additional evidence arises through measurements of structure through the observation of the 'Lyman-alpha' forest [213].

Evidence for DM on a hierarchy of scales is found by considering the formation of structure in the Universe. Cold (non-relativistic) DM aids structure formation, and hot (relativistic) DM suppresses the formation of structure on scales less than the free-streaming scale of the DM [54]. Baryonic matter was too hot after the big bang to form the observed structure in the Universe [55], thus cold DM provides a good explanation for the formation of structure on most scales. However, it should be noted that objects on smaller, sub-galactic, scales are predicted by the cold DM paradigm and there is, as yet, a lack of observation of these structures. This is sometimes referred to as the 'Missing Satellites' problem (see e.g. [214]).

It is clear that the evidence for particle DM is strong, but what might the DM be? There is a cornucopia of suggestions for the nature of DM in the literature, however the most popular usually involve a stable particle with mass in the range 1 GeV − 10 TeV. These particles should interact weakly in order to explain the behaviour of DM, and the lack of any observations of DM interactions. If the particle is in thermal equilibrium with the SM particles in the early Universe, and if there is no asymmetry in the number of DM particles versus antiparticles, then it will annihilate into SM particles at a rate greater than the expansion rate of the Universe. The reverse process will also be equally efficient. However, when the rate for this process falls below the expansion rate of the Universe, this process falls out of thermal equilibrium and leaves behind some relic density of DM particles. For a DM particle with a weak-scale mass, and a weak-scale interaction rate, roughly the correct relic abundance is left behind [55, 215–220]. This is sometimes called the 'WIMP Miracle'. Many theories using this mechanism of DM production have been constructed, and are usually tied to new physics at the TeV scale. As a result the LSP in a SUSY theory [143, 144], and the lightest neutral Kaluza-Klein particle in extra-dimensional scenarios [221], can satisfy these requirements.

Alternatively, one can link the DM abundance to the baryon abundance by postulating that the DM relic abundance is a result of an asymmetry in DM particle versus anti-particle [222]. This usually implies the existence of an operator which breaks the symmetry in the dark sector, and baryon-number symmetry, down to some subgroup. Also, efficient annihilation of the symmetric component of the DM requires operators which are more efficient than those which lead to the WIMP miracle discussed above. It is possible to tie this scenario to new physics at the weak scale, and one finds that it can naturally arise in theories of Technicolor [222]. Quite a few models which generate such an asymmetry have been considered, and this scenario will be the focus of Chapter 8, so we do not dwell on it any more here.

As most models of DM require some form of coupling between the DM and SM particles, then additional non-gravitational interactions between the two are implied. There are a number of experimental methods proposed for detecting these interactions, and they generally come under two banners: direct and indirect detection.

Direct detection experiments are based on the principle that, at our position in the galaxy, there is a local density of DM from the galactic DM halo. The sun revolves around the center of the galaxy at a speed of $v_{Sun} \simeq 220$ km s^{-1}, and if the distribution of DM in the halo is, on average, stationary then this means that in our rest frame there is a flux of DM particles travelling at roughly this velocity. If these particles possess some interactions with SM particles, (e.g. quarks), then every so often they should scatter off an atom (nucleus) and deposit some energy by giving the atom a kick [223]. For this reason highly radio-pure detectors have been built underground in order to try and detect this process. These detectors are, however, limited by background energy deposits due to radiation, and thus events that look like DM scattering can occur due to SM physics. Ingenious techniques have been developed to veto against these processes, and most detectors use two complimentary detection methods out of ionisation, scintillation, or phonon signals. As yet no detectors constructed along these lines have unambiguously detected signals of DM scattering.

An additional effect which can be used in order remove events due to background is to look for an annual modulation in event rates. This is expected to arise for DM scattering as, while the Sun is orbiting the center of the galaxy at a constant speed, the Earth is orbiting the Sun at close to 30 km s^{-1}. This means that we expect the flux of DM particles is a little greater in June, and a little lower in December. Thus, if observed events in a detector are arising as a result of DM scattering, the rate should modulate over the year [224, 225]. The DAMA/LIBRA experiment has observed an annual modulation at a significance exceeding 8σ [226], and recently the CoGeNT experiment has shown some indication of a modulation [227]. If interpreted in terms of simple DM elastic scattering these signals appear in conflict with the null observation of other direct detection experiments. However, if one is willing to consider more exotic scenarios such as inelastic scattering DM (iDM [228–230]), DM with different couplings to neutrons than to protons (IVDM [231]), or DM with low mass, $M_{DM} \sim 10$ GeV, then it may be possible to reconcile the results of these two observations with the null experiments [7].

These potential signals of DM have prompted much model building by theorists. In particular, the possibility that the scattering may be due to light DM particles, with mass close to the proton mass, has led to much recent attention focussed on the possibility of asymmetric DM with shared dark-sector to visible-sector asymmetries. In Chapter 8 this is discussed further and a simple model is proposed.

Indirect detection methods rely on the possibility that DM particles can annihilate with themselves, or decay. One method, which doesn't involve scattering of DM on SM particles is to look for the end products of DM annihilation or decay in the DM halo of our galaxy, and in some nearby dwarf galaxies. If the relic abundance is due to the WIMP miracle then, for a given DM mass, the annihilation cross-section is naïvely known.[1] Thus, once one assumes a particular DM model and a distribution for the DM in the galaxy, one can predict the annihilation rate, and subsequently the flux of gamma-rays, electrons, positrons, neutrinos, protons and antiprotons in the vicinity of the Earth. Detectors either on the surface of the Earth, or orbiting the Earth can then look for these signals, or similar signals which might arise from DM decay. In the past few years there have been some tentative signals along these lines from experiments such as the PAMELA and FERMI satellites [233–239], which have resulted in a flurry of activity in DM model building, see e.g. [232], and in searching for SM physics explanations, e.g. [240, 241]. These possible signals are not, however, a subject of study in this thesis, and so we do not consider them any further here.

Another method for indirect detection relies on the assumption of DM-nucleon scattering and DM annihilation or decay. It was suggested some time ago, [242–250], that if DM scatters off SM particles then, due to this scattering, DM particles could build up in astrophysical objects such as the Earth, the Sun, and other more compact objects like neutron stars and white dwarfs. If the DM does not annihilate or decay then the residual DM in the core of an object could significantly alter the dynamics within the object, such as in the Sun [251–253]. Alternatively, if the DM does annihilate or decay, then these processes might result in a flux of high-energy neutrinos from within the astrophysical object. These neutrinos could propagate relatively freely from within the Sun or the Earth and then be detected by neutrino detectors. Large scale experiments have been built along these lines, and null observations severely restrict the class of models of DM for which this is a possibility, see e.g. [254].

An interesting signal can also arise if the energy released due to DM annihilations leads to significant heating of a star. This effect would be most pronounced for dense objects without their own internal source of energy, such as white dwarfs or neutron stars. These processes are the subject of Chapter 7.

Finally, it should be noted that certain DM candidates have been proposed which are very difficult to detect, such as axions or gravitinos in SUSY models (for a review see e.g. [136]). These particles could in principle be indirectly detected through their

[1]Naïvely, as scenarios involving additional sub-GeV particles in the dark sector can enhance the annihilation cross-section in the halo at low velocities (see e.g. [232]).

production in stars or colliders, however it is very difficult to detect any such particles in the galactic halo.

Clearly, DM is both coy and ubiquitous, posing a unique puzzle for both experimental and theoretical physicists. In this part of the thesis we touch on two different aspects of DM phenomenology. In Chapter 7 we investigate new ways to indirectly look for the presence of DM, by observing its effect on white dwarf stars. Then in Chapter 8 we present an attractive model that generates the observed DM relic abundance, as well as the observed baryon asymmetry, thus linking the two.

Chapter 7

Capture of Inelastic Dark Matter in White Dwarfs

We saw in the previous chapter that one popular model of DM that aims to explain the annual modulation observed by DAMA and CoGeNT is so-called 'Inelastic DM', (iDM). In this chapter we consider the capture of iDM in white dwarfs by inelastic spin-independent scattering on nuclei. We show that if the DM annihilates to SM particles then, under the assumption of primordial globular cluster formation (hence DM densities greater than one expects due to the surrounding galactic halo density), the observation of cold white dwarfs in the globular cluster M4 appears inconsistent with explanations of the observed DAMA/LIBRA and CoGeNT annual modulation signals which are based on spin-independent inelastic DM scattering. Alternatively, if the inelastic DM scenario were to be confirmed and it was found to annihilate to SM particles then this would imply a much lower DM density in the core of M4 than would be expected if it were to have formed in a DM halo. Finally we argue that cold white dwarfs constitute a unique DM probe, complementary to other direct and indirect detection searches.

7.1 Introduction

It has been pointed out in [250, 255] that as white dwarfs (hereafter WDs) have no internal energy source, and many cold WDs have now been observed, it is possible that, due to a non-zero DM-nucleon cross-section, the energy released by the annihilation of DM particles in WD cores could contribute significantly to the luminosity of the star.

An interesting possibility for DM-nucleon interactions is that the DM could predominantly scatter off nucleons inelastically to an excited energy state, so-called iDM.

This idea has been proposed as a possible explanation [228–230] for the annual modulation signal observed by the DAMA [226, 256, 257] and also, now, CoGeNT [227] collaborations. The key feature in iDM is the mass splitting, δ, between DM particles that scatter off nuclei. For iDM explanations of the DAMA/LIBRA annual modulation δ is of the order $10 - 130$ keV (depending on DM mass and couplings).

The main physical consequence of the inelastic splitting is that the minimum velocity for a DM particle to scatter off a nucleus and impart an energy E_R is increased. This can severely weaken the sensitivity of direct detection experiments as the number of particles in the halo with a large enough velocity to scatter can be very small, or even zero in some cases. As a consequence the allowed DM-nucleon cross-sections can be orders of magnitude larger than for elastic scattering.

Limits on iDM from capture in the Sun [258–260] are promising as the escape velocity of the Sun, $v_{esc} \sim 600 - 1300$ km s^{-1}, is large enough to provide sufficient energy to in-falling DM particles to overcome inelastic splittings $\delta \sim 100$ keV. Although these limits are hampered by the difficulty of detecting neutrinos, progress in neutrino telescope exposure means strong limits exist on particular models of iDM, for example, limits on sneutrino iDM have been studied in [2]. However, models of iDM that annihilate predominantly to e^+e^-, $\mu^+\mu^-$, $\gamma\gamma$, light hadrons or gluons are immune to these limits as these particles either stop before decaying and producing neutrinos or don't produce neutrinos at all. In these cases the energy deposited in the Sun from DM annihilations is swamped by the internal energy due to fusion. Therefore models of the class described in [232] can evade limits from solar capture.

The converse is true for capture in WDs as it is the deposited energy that is used to set the limits, and annihilation to neutrinos will only deposit a small amount of energy in the WD. Therefore models of DM that attempt to explain the DAMA annual modulation observation with the iDM mechanism, in particular models that also aim to offer an explanation of recent PAMELA [235] and Fermi LAT [238] observations through DM annihilation, are subject to limits from capture in WDs.

In this chapter we investigate limits on the iDM scenario by considering the temperature and luminosity of observed WDs in our closest globular cluster M4. Throughout we assume that the DM annihilates to standard model particles.

7.2 White dwarfs in M4

White dwarfs are compact objects made up of a core comprised almost entirely of carbon and oxygen nuclei, and degenerate electrons. The electron degeneracy prevents any contraction and the temperature of this core is too low to ignite nuclear fusion reactions. As a result, WDs have no internal energy source and release only the thermal energy of the non-degenerate ions in the core. For these reasons the evolution of WDs can be described as a cooling process and the age of a globular cluster such as M4 can be estimated by observing a cut-off at low magnitudes in the WD cooling sequence. This has motivated observations of WDs in globular clusters down to very low magnitudes.

Recently this low magnitude cut-off has been observed in the globular cluster M4 [261]. We use the best-measured set of data from these observations, subject to all of the selection processes detailed in [261], including the use of proper motion measurements, to produce a decontaminated sample.

We take the data in the form of magnitudes in the F606W and F775W Hubble Space Telescope filters and convert the colour $m_{606W} - m_{775W}$ to an effective temperature under the assumption that the WD is radiating as a black-body. To do this we numerically shine a black-body spectrum through the HST filter transmission curves, convert magnitudes to the ACS/WFC Vega-mag system [262] and correct for reddening and extinction as detailed in Section 9 of [261]. We then use the m_{606W} magnitude, the M4 distance modulus, and the effective temperature of each star and compare with Vega[1] to calculate the luminosity for each star. This data is plotted later in Figure 7.4.

Having obtained the luminosity and temperature it is possible to calculate the radius of each WD (under the assumption of black-body radiation). Then, using the Salpeter equation of state [263], which gives an approximate mass-radius relationship, we determine an approximate mass for each star.

7.3 DM in M4

In order to set limits on the iDM-nucleon cross-section it is necessary to estimate the DM density surrounding the WD's at the center of M4. Although it is currently impossible to do this to with any great accuracy, recent developments in the observation and simulated evolution of globular clusters embedded in galactic halos now allow an estimate of the DM content. Some time ago Peebles [264] suggested that globular clusters may be formed in sub-halos of DM before falling into galactic halos. However observations of $\mathcal{O}(1)$ mass-to-light ratios [265] and the tidal stripping of stars from

[1] We use the parameters $T_{eff} = 9550$ K, $R_V = 2.52\ R_\odot$ and $L_V = 37\ L_\odot$ for Vega.

some globular clusters[2] suggest a significant DM component cannot reside within or without the observed stellar distribution [267]. These observations set an upper limit on the DM content of globular clusters.

Recent simulations have shed light on how these results can be reconciled with a primordial scenario of globular cluster formation through the process of tidal stripping. In fact, the presence of globular clusters has been suggested as a clue towards a resolution of the 'missing satellite problem' of cold DM simulations [268]. In [269] it was found that once a sub-halo falls into a larger halo mass-loss occurs continually through tidal stripping and the orbit of the sub-halo decays down towards the centre of the larger halo. Further it was found that the mass-loss can be significant, resulting in only $\sim 2\%$ (8%) of the mass of a sub-halo accreted at $z = 2$ (1) surviving, and this result appears to be independent of the masses of the halo and sub-halo. The tidal stripping of DM from primordial globular clusters has been investigated with several N-body simulations (see e.g. [266, 270–272]). Results suggest that globular clusters can be formed naturally within DM sub-halos which are subsequently tidally stripped by the host galaxy, resulting in a baryon-dominated core with a small mass-to-light ratio, resembling observed globular clusters. In particular a recent analysis of the Aquarius simulation [272] lends support to this scenario, and an approximate relation between the current mass of a globular cluster and the mass of the initial sub-halo it was embedded within is given as $M_{GC} = 0.0038\ M_{DM,0}$.

A recent review [273] also argues that metal-poor globular clusters formed in low-mass DM halos in the early universe.

The observed cold WDs reside in the dense core of M4, which has survived previous tidal stripping until now. Therefore it is reasonable to assume that the majority of the DM in the core of M4, well within the tidal radius, will also have survived from the early sub-halo. This assumption is supported by the results of [266] where it is found that the presence of the stellar core makes the sub-halos more resilient to tidal stripping, and for NFW sub-halo profiles the DM density in the innermost regions of the sub-halo is not modified by the external tidal field. Outside of the star dominated region the DM sub-halo is stripped back to the tidal radius, thus resulting in a mass-to-light ratio close to the purely baryonic value.

Similar reasoning has led to recent consideration of indirect DM signals from DM annihilation in other globular clusters, [274, 275].

[2]It should be noted that obvious tidal tails have only been observed in a fraction of the total ~ 150 globular clusters residing in our galaxy [266].

Motivated by these developments we follow similar methods to those used in [250], to which we refer the reader for details. The mass of baryonic matter in M4 is estimated to be $M_b \sim 10^5 M_\odot$ and the core radius of $0.83'$ in arc-minutes implies $r_c = 0.531$ pc when combined with a distance to the cluster of 2.2 kpc. The tidal radius is estimated using a concentration parameter of $\log(r_t/r_c) = 1.59$ giving $r_t = 20.66$ pc. These parameters set the baryon density distribution, which we model with a King profile [276, 277].

Using cosmological data and taking mass loss during stellar evolution into account, the amount of DM in the original M4 sub-halo is estimated to be $M_{DM} \sim 10^7 M_\odot$. For details of this estimation see [250]. The virial radius, which sets the initial DM distribution is estimated using the fitted form of the spherical collapse over-density [278]

$$\Delta = \frac{18\pi^2 + 82(\Omega_m(z) - 1) - 39(\Omega_m(z) - 1)^2}{\Omega_m(z)} \quad , \tag{7.1}$$

where the matter density is given by [279]

$$\Omega_m(z) = \left[1 + \frac{1 - \Omega_m}{\Omega_m(1+z)^3}\right]^{-1} \quad . \tag{7.2}$$

We take $\Omega_m(0) = 0.273$ giving $\Delta = 357$. The concentration of low mass halos is given in [279] as

$$c(z) = \frac{27}{1+z} \left(\frac{M_{DM}}{10^9 M_\odot}\right)^{-0.08} \quad , \tag{7.3}$$

and combining this expression with those for the virial radius, scale radius and central density from [250] the original DM sub-halos are completely determined by the parameters

z	R_{vir} [pc]	a [pc]	ρ_c [$M_\odot\ pc^{-3}$]
0	3597	92	0.37

We model the original DM halo with an NFW profile [280]. As discussed in [250] the core density is a very weak function of the total mass of the sub-halo, changing only by a factor of three for halo masses between $10^6 M_\odot$ and $10^8 M_\odot$.

It remains to consider the effects of the baryonic core on the DM distribution. Although the DM density may be enhanced in the core due to the presence of the baryonic core [281–283] the heating of DM particles due to interactions with stars may tend to wipe out this enhancement. Therefore by estimating the time-scale over which this process occurs with eq.(3a) of [284] we can find the radius at which this time-scale is equal to the age of the universe. We find that this radius lies at $r_{heat} = 1.4$ pc and, as this is smaller than the radius where the WDs are observed, we expect heating effects to be small here. The possible important effect is therefore the contraction of the DM core due to conservation of angular momentum when the gas in the original halo which eventually forms the globular cluster loses energy and falls into the core. We use the algorithm of Gnedin [282] to perform this baryonic contraction. Finally as mentioned earlier, to take account of the likely tidal stripping of the stars and DM halo we truncate the density distribution at the tidal radius.

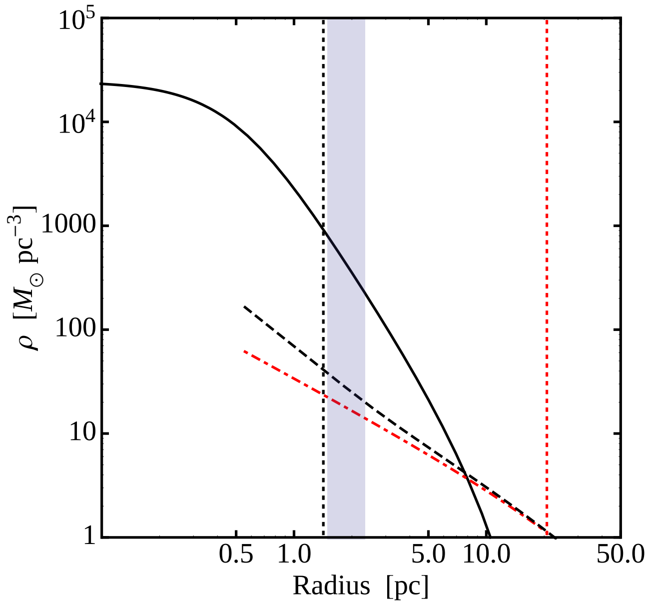

Figure 7.1: Densities of stars (solid line) and the DM halo with and without baryonic contraction effects in dashed black and dot-dashed red respectively. The region from which the observed WD data is taken is indicated in shaded blue. The vertical dotted lines denote the radius at which heating effects start to become important (dotted black) and the tidal radius (dotted red).

The estimated DM and star densities for the halos are plotted in Figure 7.1. One can see that this estimate for the DM density is much smaller than the baryonic density, and in fact, for the contracted (uncontracted) halo, DM makes up less than 43% (41%) of the total mass of the cluster, consistent with the observed lack of DM in globular clusters. Further, the total estimated DM content is $7.7 \times 10^4 M_\odot$, less than 1% of the original $10^7 M_\odot$ halo.

We assume a DM density at the largest radius within which the WD data is observed, $r_{max} = 2.3$ pc, giving $\rho_{DM,0} = 21$ M$_\odot$ pc^{-3} = 798 GeV cm^{-3} for the contracted halo[3].

[3]The DM density for the uncontracted halo is $\rho_{DM,0} = 14$ M$_\odot$ pc^{-3}, not much smaller than the contracted halo.

7.4 Capture of iDM in white dwarfs

The capture of DM by scattering in stars or planets has been studied for some time, see e.g. [242–250], and recently the capture of iDM in the Sun has been studied [258–260]. It is this work which we extend to include capture in WDs and we follow the formalism first set out in [258], which was subsequently extended to include spin-dependent scattering as well as spin-independent scattering in [260].

Recently spin-dependent inelastic scattering has been suggested as a viable alternative to the standard spin-independent iDM scenario [285], where it is shown that spin-dependent couplings to protons, and not neutrons, can give a good fit to the DAMA data whilst remaining consistent with other experiments. This scenario is subject to limits from scattering in the Sun [260] however limits from capture in WDs should be weak as WDs are mostly composed of ^{12}C and ^{16}O which have no nuclear spin. It is tempting to consider limits from scattering on ^{13}C which makes up $\sim 1\%$ of all carbon and has nuclear spin $I = 1/2$, however this spin is carried by an unpaired neutron and thus the scenario described in [285] will lead to negligible capture rates in WDs. Therefore we only consider spin-independent scattering iDM in this work.

To calculate the capture rate in a WD we use the equations contained in Section II of [260]. To take account of the incoherent scattering of DM in the nucleus we also use the Helm form factor[4] and follow [250] in making the assumption that the WDs are entirely composed of carbon. We also assume the DM couplings to neutrons and protons are the same. This can be corrected for specific models by re-scaling the cross-section accordingly.

To find the DM velocity dispersion we make the assumption of hydrostatic equilibrium and integrate the hydrostatic equation for spherical geometry using the baryon and DM distributions shown in Figure 7.1. We find that the DM velocity dispersion does not exceed 8 km s^{-1} and, as the capture rate decreases with increasing dispersion, we set v_0 to this value. Similarly the WD velocity through the DM is likely to be of the order of the velocity dispersion and we find this doesn't exceed 6 km s^{-1}, however to set conservative limits we set $v_\star = 20$ km s^{-1} which is the escape velocity at the inner radius at which the WDs are observed.

We calculate the escape velocity and density of nuclei within a given WD using the Salpeter equation of state [263]. Due to the large escape velocity of a WD the typical kinetic energy of an in-falling DM particle is $\mathcal{O}(1)$ MeV. Therefore all of

[4]We use the same form factor as in [260] for consistency, however there is some uncertainty in which form factor is best and care should be taken for processes at high momentum transfer [286].

the in-falling particles easily have enough kinetic energy to overcome the inelastic splitting and scatter. This makes the inelastic splitting relatively unimportant up to splittings $\delta \sim 1$ MeV, where the capture rate starts to decrease. This is shown in Figure 7.2. Although the splittings associated with iDM are much too small to decrease the capture rate significantly we include them in our calculations for the sake of thoroughness.

The capture rate typically falls as the inverse of the DM mass, therefore the luminosity should be largely independent of the DM mass. However there is a subtle interplay between two factors which leads to a dependence not only on the DM mass but also on the WD mass. The first factor is due to the conversion between a DM-nucleon and DM-nucleus cross-section at zero momentum transfer, which results in a factor of $\sigma_{\chi N} \propto (\mu_{\chi N}/\mu_{\chi n})^2$ where μ is the reduced mass and N (n) subscripts denote the nucleus (nucleon). This factor has a preference for heavy DM particles. However there is also suppression due to the nuclear form factor.[5] Therefore, although heavier DM particles have a larger range of scattering energies, the higher energy events are suppressed. This effect therefore discriminates against heavy DM particles.

Which of these two factors wins out depends on the WD mass. As heavy WDs have greater escape velocities ($\sim (7-12) \times 10^3$ km s^{-1}), heavy DM particles feel the form factor suppression more and light DM particles lead to greater luminosities. For light WDs the escape velocities are lower ($\sim (2-3) \times 10^3$ km s^{-1}) the form factor suppression is subdominant and heavier DM particles lead to a greater luminosity. The mass dependence for two different WDs is illustrated in Figure 7.3.

As described in [250] the time-scale for equilibrium between the capture and annihilation of DM in WDs is roughly $\mathcal{O}(1)$ year, and therefore we can safely assume that the capture rate is twice the annihilation rate. We also assume that all of the energy of the annihilating particles contributes to the black-body luminosity of the WDs, however specific DM models could be investigated by calculating the fraction of energy lost as neutrinos per annihilation and weakening the limits accordingly.

7.5 Uncertainties

We will now discuss some of the assumptions that have gone into this calculation. The greatest source of uncertainty is the estimation of the DM density. It is known that young, metal-rich globular clusters form in mergers, and it should also be noted that

[5]Due to the form factor suppression energy transfers of $E_R > 4$ MeV contribute very little to the capture rate, even if kinematically possible.

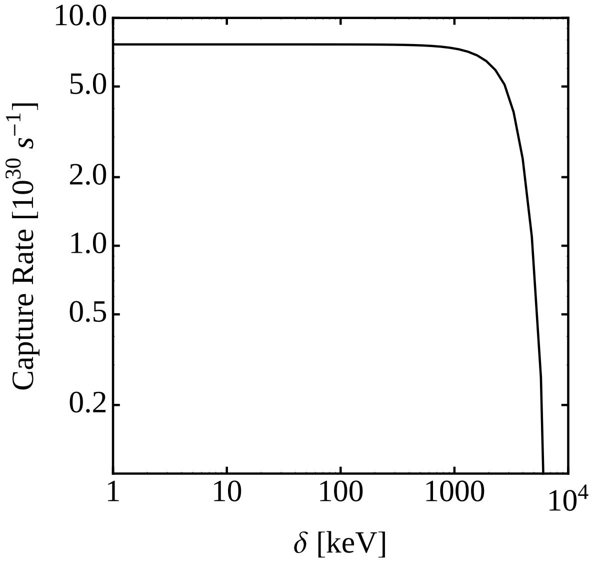

Figure 7.2: The DM capture rate for a solar mass WD as a function of inelastic splitting δ. The DM parameters are $m_\chi = 50$ GeV and $\sigma_n = 10^{-41}$ cm^2. The capture rate is largely independent of the inelastic splitting up to $\delta \sim 1$ MeV, when it starts to fall off rapidly. A DM density of $\rho_{DM,0} = 21$ M$_\odot$ pc^{-3} = 798 GeV cm^{-3} is assumed.

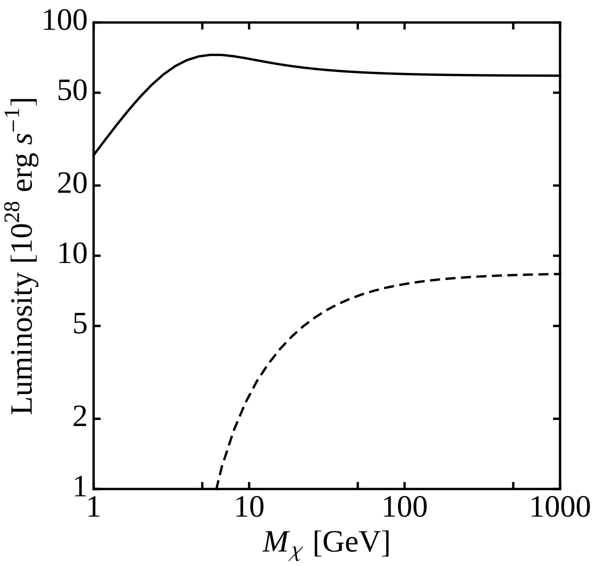

Figure 7.3: The luminosity of a WD due to capture and annihilation of DM as a function of DM mass for WDs of mass $M_\star = M_\odot$ (solid line) and $M_\star = 0.2\ M_\odot$ (dashed). The DM parameters are $\delta = 130$ keV and $\sigma_n = 10^{-41}$ cm^2. There is a slight enhancement around $m_\chi \sim 10$ GeV for the solar mass WD and the luminosity is suppressed for small DM masses. This behaviour is discussed in the text. A DM density of $\rho_{DM,0} = 21$ M$_\odot$ pc^{-3} = 798 GeV cm^{-3} is assumed.

there are some models where the old, metal-poor, globular clusters are not formed due to the collapse of a DM dominated halo. In particular, the observations made by Gilmore and collaborators have lead them to argue that low mass star clusters are fundamentally different to higher mass galaxies rather than both being members of a continuous family [287]. The explanation for this scenario typically requires some kind of modification of DM such as warm DM, a cold/hot admixture or a non-zero self-interaction cross section such that there is a minimum size for DM halos in the Universe. Since we are trying to put constraints on models of cold DM, it is a consistent assumption that the old, metal poor, globular clusters do form in the centre of DM halos in the early Universe but we note that this is a large uncertainty.

It has been shown that for direct detection experiments the details of the DM velocity distribution can have a significant impact on detection rates [288], particularly for iDM [1, 289]. However, due to the large escape velocity of the WDs all in-falling DM particles will have a large enough velocity to scatter and the details of the velocity distribution will be unimportant.

We have made the estimate that the WDs are travelling at the local escape velocity, however a more realistic (but less conservative) assumption would be that they are travelling at a speed closer to the local velocity dispersion, which is roughly a factor of 3 smaller. As the capture rate is inversely proportional to this speed we may have underestimated the capture rate by the same amount.

Due to the large escape velocity the energy transfer in scattering events can be large ($\sim$ 1 MeV), and the scattering is thus significantly suppressed by the nuclear form factor. We use the Helm form factor, which for light nuclei can be up to $\sim 20\%$ greater than more realistic form factors at these high energy transfers [286]. Therefore a conservative estimate of the uncertainty due to the choice of form factor is of the order 20%.

For considerations relating to errors in WD observations we refer the reader to [261].

7.6 Results

In Figure 7.4 we show the observed WDs in the Temperature-Luminosity plane. On the same plot we show curves for WDs whose sole energy source is due to DM annihilation in the core for WDs ranging in mass from 0.1 $M_\odot$ to 1.35 $M_\odot$. These curves correspond to two benchmark points

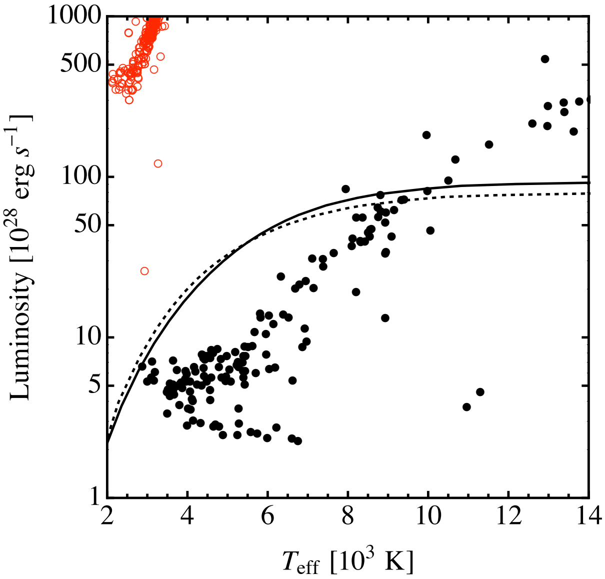

Figure 7.4: Observed WDs (black dots) and main-sequence stars (open red circles). Also plotted are the luminosity and temperature of WDs in the mass range $0.1 - 1.35$ $M_{\odot}$ for the two benchmark points i1 and i2 (dashed) described in the text. For both curves a DM-nucleon cross-section of 10^{-41} cm^2 is assumed. The luminosity from DM capture is greater than a significant number of the observed WD luminosities. A DM density of $\rho_{DM,0} = 21$ M$_{\odot}$ pc^{-3} = 798 GeV cm^{-3} is assumed.

	M_χ [GeV]	δ [keV]	σ_n [10^{-41} cm^{-1}]
i1	10	40	1
i2	100	130	1

The mass and splitting for the point i1 corresponds roughly to best-fit points for light DM scenarios [7]. The mass and splitting in point i2 corresponds to the conventional quenched scattering iDM scenario. This scenario is considered ruled out by other direct detection experiments, however, for demonstrative purposes we still include this choice of parameters in our analysis. We choose a cross-section of $\sigma_n = 10^{-41}$ cm^2 as this is below the cross-section at which the optically thick limit applies and the capture rate becomes independent of the scattering cross-section. This occurs because the scattering rate becomes so great that every DM particle which passes through the WD will scatter multiple times and become captured. This important point was first emphasised in the context of inelastic DM capture in [290].

The temperature of a black-body is related to the luminosity as $T \propto L^{1/4}$, so Figure 7.4 can be misleading, as a change in cross-section does not correspond to a simple re-scaling of the luminosity. Therefore in Figure 7.5 we estimate the observed WD masses as described in Section 7.2, and plot curves showing the luminosity due to DM capture and annihilation for a given WD mass.

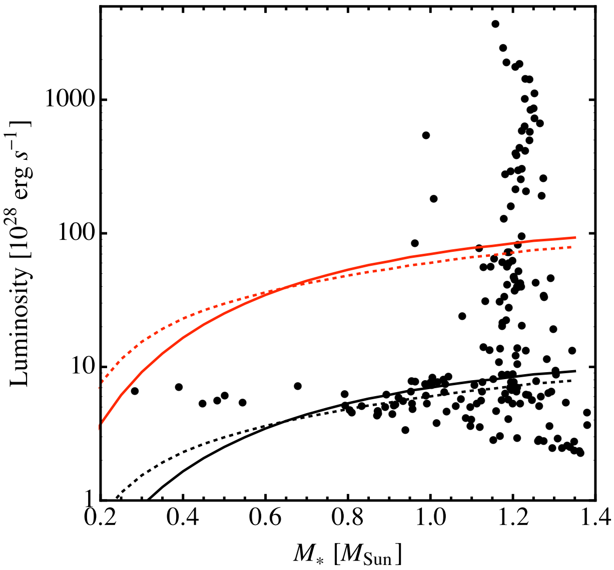

Figure 7.5: Observed WDs (black dots). Also plotted are the luminosity and temperature of WDs in the mass range $0.1 - 1.35\ M_\odot$ for the two benchmark points i1 and i2 (dashed). The upper red curves correspond to a cross-section of $\sigma_n = 10^{-41}$ cm^2 and the lower black curves to $\sigma_n = 10^{-42}$ cm^2. A DM density of $\rho_{DM,0} = 21$ M$_\odot$ pc^{-3} = 798 GeV cm^{-3} is assumed, as described in Section 7.3. For a different DM density the luminosity due DM capture is re-scaled by a factor of $\frac{\rho_{DM}}{\rho_{DM,0}}$, where ρ_{DM} is the true DM density.

As can be seen the low luminosities and temperatures of the observed WDs appear incompatible with cross sections greater than $\sigma_n \sim 10^{-42} \times \frac{\rho_{DM,0}}{\rho_{DM}}$ cm^2 for either of the benchmark points, where the factor of the assumed DM density, $\rho_{DM,0}$, over the true density, ρ_{DM}, is included to allow for the large uncertainty in this quantity. A cross-section below $10^{-42} \times \times \frac{\rho_{DM,0}}{\rho_{DM}}$ cm^2 could possibly be argued as acceptable given the uncertainties, and a cross-section as low as $10^{-43} \times \frac{\rho_{DM,0}}{\rho_{DM}}$ cm^2 would evade these bounds entirely. However any cross-section greater than $10^{-42} \times \frac{\rho_{DM,0}}{\rho_{DM}}$ cm^2 would certainly appear to contradict the existence of such cold WDs in M4 if we were to assume that M4 formed in a DM halo.

Recent analyses of iDM find a best fit cross-section of $\sim 10^{-37}$ cm^2 [7] for the benchmark point i1. As this cross-section is greater than $\sim 10^{-42} \times \frac{\rho_{DM,0}}{\rho_{DM}}$ cm^2 this scenario appears excluded by the analysis above, under the assumption that M4 formed in a DM halo, and even the lowest cross-section found for the channelled iodine region of 9×10^{-42} cm^2 [291] would be difficult to reconcile with these results. The conventional iDM scenario of quenched scattering off iodine (benchmark point i2) typically requires cross-sections greater than $\sim 3 \times 10^{-40}$ cm^2, with a best-fit point at $\sigma_n = 10^{-38}$ cm^2 [285]. This scenario also seems excluded by this analysis with the current assumption for the DM density.

These constraints can be evaded in any combination of the following scenarios:

- The DM density is less than $\sim 1\%$ of that estimated here, i.e. $\frac{\rho_{DM,0}}{\rho_{DM}} \gtrsim 10^2$. This appears plausible, however it would imply that DM makes up less than $\sim 1\%$ of the total mass of the globular cluster. If the old, metal-poor, globular clusters are born in DM halos it is hard to imagine how the ratio of DM to baryonic matter in M4 could be so far below cosmological values. If M4 did not form in a DM halo it is likely the DM density would be low enough to evade these bounds.

- The iDM couples to nuclei only through spin-dependent interactions as recently suggested in [285]. If iDM couples to neutrons then it may be possible to set limits by considering scattering off ^{13}C, however as this scenario already appears disfavoured by direct detection experiments [285] this is not investigated here. If the coupling is only to protons then limits from WDs pose little threat.

Under simple assumptions about the DM density in globular clusters (including their formation in DM halos, which is subject to much debate, and is a source of much uncertainty) and the composition of cold WDs, we find that the iDM explanation of the annual modulation observed by the DAMA and CoGeNT collaborations is incompatible with the observation of cold WDs in M4 if the DM annihilates to standard model particles. Alternatively if the inelastic DM scenario were to be confirmed and it was found to annihilate to standard-model particles then this would imply a much lower DM density in the core of M4 than would be expected if it were to have formed in a DM halo.

7.7 Summary

We now discuss some of the salient features of white dwarfs which make them a unique probe of DM.

It is interesting to note that in the case of elastic DM scattering cross-sections $\sigma_n \sim 10^{-43}$ cm^2 evade the WD bounds.[6] It is unlikely that observations of WDs much cooler than those in M4 will be made as the low luminosity cut-off has been observed, and the luminosity of WDs is limited by the age of the Universe. Therefore

[6]The difference between the conclusions presented here and those in [250] arises mostly due to the form factor suppression which has been included in this analysis.

it is unlikely that limits from WDs will ever compete with direct detection limits for weak-scale elastic DM.

However WDs constitute unique DM probes for three reasons:

- The large escape velocity enables in-falling DM particles to easily overcome inelastic splittings and leads to large energy transfers in scattering.
- The low mass of carbon gives WDs sensitivity to light DM scenarios, where most direct detection experiments lose sensitivity.
- Limits from capture in the Sun arise due to neutrino annihilation products and are therefore insensitive to DM annihilating to e^+e^-, $\mu^+\mu^-$, $\gamma\gamma$, light hadrons or gluons. It is specifically this scenario where limits from WDs are strongest.

We have only considered iDM capture in this work, however numerous possibilities exist for future study of DM capture in WDs. Examples would include DM with mass splittings of the order a few MeV or DM which scatters through a light mediator, $m_\phi \sim$ MeV, which could be enhanced in WDs through the propagator $1/(q^2 - m_\phi^2)$.

Finally we note that if DM were to be discovered in future experiments, and details of the DM-nucleon cross-section and annihilation products were to be established, then cold WDs could be used to determine an upper limit on the DM density within M4, thus giving clues as to the formation of old, metal-poor, globular clusters.

Chapter 8

Asymmetric Dark Matter via Spontaneous Co-Genesis

In this chapter we investigate, in the context of asymmetric dark matter (DM), a new mechanism of spontaneous co-genesis of linked DM and baryon asymmetries, explaining the observed relation between the baryon and DM densities, $\Omega_{DM}/\Omega_B \simeq 5$. The co-genesis mechanism requires a light scalar field, ϕ, with mass below 5 eV which couples derivatively to DM, much like a 'dark axion'. The field ϕ can itself provide a final state into which the residual symmetric DM component can annihilate away.

8.1 Introduction

As discussed in Chapter 6, it is usually assumed that the baryon and DM densities we observe in the universe today are generated by independent processes. In particular, the baryon density is entirely determined by a CP-violating asymmetry between baryon and anti-baryon densities in the early universe, while the standard assumption has been that the DM density does not depend on any corresponding asymmetry and is instead determined by thermal freeze-out [215–217] or thermal freeze-in [137]. Since the genesis mechanisms for DM and baryons are thus decoupled, the DM-to-baryon ratio, Ω_{DM}/Ω_B, could in principle lie far away from the observed close coincidence, $\Omega_{DM}/\Omega_B \simeq 5$ [25].

An alternative picture is that the DM itself possesses a particle-antiparticle asymmetry, linked in some way to the baryon asymmetry, which determines (at least the dominant component) of the DM density, thus explaining the observational fact that $\Omega_{DM}/\Omega_B \simeq 5$. This proposal goes under the name Asymmetric Dark Matter (ADM) [222, 292–330]. Recently there has been a burst of activity considering the possibility of ADM in which the baryon and DM densities are determined by such linked asymmetries, though no standard picture has yet emerged.

The aim in this chapter is to demonstrate that there exists a new mechanism of *spontaneous co-genesis* of linked baryon and DM asymmetries. We find that this mechanism for the generation of the asymmetries possesses a number of attractive features compared to previous approaches. As a prelude to our argument we start with a brief outline of the primary idea.

As is well known [40] the generation of a baryon-number asymmetry in the early Universe requires both CP violation and baryon-number violation. In addition, if the underlying theory is CPT invariant, so that particle and anti-particle masses and energy eigenvalues are equal, an asymmetry requires a departure from thermal equilibrium. However, as noted some time ago by Cohen and Kaplan [331, 332], the expansion of the universe spontaneously violates both T and CPT, allowing, in principle, the generation of a baryon asymmetry in thermal equilibrium if there are sufficiently large differences between particle and anti-particle energy eigenstates. More precisely, baryon-number violating scattering and decay processes can be in equilibrium with rates greater than the Hubble expansion rate, but, nevertheless, different thermal distributions for baryons and anti-baryons can occur if the expansion leads to a background 'potential' biasing particle versus antiparticle densities in the thermal bath. CP-violating phases leading to differences in scattering or partial decay rates between particles and anti-particles are not necessary, the spontaneous T-violation of the background being sufficient.

In the context of baryogenesis, there exist a number of detailed implementations of this mechanism, usually dubbed 'Spontaneous Baryogenesis' [331–346]. It is natural to ask whether an adaption of this mechanism can lead to a mechanism of spontaneous co-genesis of both the baryon asymmetry and a DM asymmetry.

One significant issue with previous implementations of the spontaneous genesis idea is that they require a new light degree of freedom, usually a neutral scalar field ϕ, derivatively coupled to baryon- or lepton-number carrying states, and with a time-dependent vev in the early universe. Moreover, this time-dependent vev must not be in its oscillating phase during the epoch of spontaneous genesis, or the resulting asymmetry is severely suppressed [1]. Together with laboratory and cosmological/astrophysical constraints, these requirements severely limit the utility of the spontaneous genesis mechanism. Our implementation, however, automatically solves this difficulty as the required light time-dependent field is now coupled to the DM,

[1]This suppression has been discussed by Dolgov and collaborators [336, 337], and invalidates some of the implementations of spontaneous baryogenesis studied in the literature.

generating the asymmetry in the dark sector, rather than SM states, greatly ameliorating the constraints. In addition, an unexpected and highly appealing consequence of our implementation of spontaneous co-genesis, is the fact that the new field ϕ, can naturally solve a generic problem of models of ADM, namely the efficient elimination of the symmetric part of the DM density, so that the final DM density is determined by the asymmetry alone. We view this as a very attractive added benefit of our mechanism of spontaneous co-genesis.

In Section 8.2 we introduce the basic mechanism of spontaneous genesis in the DM sector. In Section 8.3 we discuss how the resulting DM asymmetry is shared with (equivalently, partially transferred to) the visible sector via suitable 'sharing interactions' between the dark and visible sectors. We argue that along with the standard sharing paradigm where a fixed DM asymmetry is shared, there is a new regime where the DM asymmetry continues to evolve after the sharing interactions drop out of equilibrium, allowing very different DM masses and interactions compared to the usual ADM case. In Section 8.4 we discuss the cosmology of the new degree of freedom ϕ whose time-dependence drives the spontaneous co-genesis mechanism. We show, in particular, that the ϕ interactions with the DM which drive co-genesis themselves can naturally lead to sufficient elimination of the symmetric component of the DM density.

8.2 Introduction to spontaneous matter genesis

The CPT- and T-violation necessary for spontaneous co-genesis can arise dynamically, either through the Lorentz-violating vev of some vector field, or more simply through the time-dependence of a scalar field, ϕ, which, for simplicity, we here take to be a neutral scalar with derivative couplings to DM states. If, after inflation, the scalar field does not lie at the minimum of its low-temperature potential then it will evolve towards this minimum as the Universe cools. However, if the mass satisfies $m_\phi \lesssim 3H$, where H is the Hubble parameter at a given temperature, then the evolution of the field will be damped. Assuming a spatially homogeneous field, as one would expect after inflation, then as the field evolves a homogeneous Lorentz-violating vev arises; $\partial_\mu\phi = \{\dot{\phi}, \mathbf{0}\}$. Thus if ϕ is derivatively coupled to some current, which we call X-number current, as

$$\mathcal{L} \supset \frac{\partial_\mu \phi}{f} J^\mu_X \quad , \tag{8.1}$$

where f is a decay constant, the slow evolution of ϕ leads to an effective background potential for X-number density. If there are X-number violating processes occurring at a rate $\Gamma_{\not{X}} > H$, a non-zero X-number is generated in thermal equilibrium. The X-number violating processes are necessary, as although the background potential makes it energetically favorable to have a particle asymmetry this asymmetry can only develop if there are interactions which violate X-number.[2]

Although this mechanism has been previously considered in the context of baryogenesis where $X = B$, or L, it could be responsible for the generation of an asymmetry in any class of particles charged under a continuous global $U(1)_X$ symmetry, where X simply stands for an unknown symmetry.

In this work we propose a novel application of this mechanism whereby ADM is generated by the spontaneous genesis mechanism. This asymmetry can be simultaneously or subsequently shared with the visible sector, leading to a connection between the baryon asymmetry and the DM asymmetry. We posit a dark sector which exhibits a global $U(1)_X$ symmetry at low temperatures.[3] We also assume that the scalar ϕ is coupled to the X-current, as opposed to the baryon-number current, leading to an effective interaction

$$\mathcal{L} \supset \frac{\partial_\mu \phi}{f} J^\mu_X = U_X(T)(n_X - n_{\overline{X}}) \quad , \tag{8.2}$$

where $U_X(T) = \dot{\phi}(T)/f$ is the background potential for X-number. Then, if the dark sector also exhibits X-number violating interactions, which freeze-out at a temperature T_X, this leads to an X-number asymmetry given by

$$X(T, U_X) = \frac{T^2}{6} U_X g_X k\left(M_X/T, \pm 1\right) \quad , \tag{8.3}$$

where g_X is the number of degrees of freedom of X, and the function $k(x, \pm 1)$ is defined by

$$k(x, \pm 1) = \frac{6}{\pi^2} \int_x^\infty \frac{\sqrt{y^2 - x^2}}{(e^y \pm 1)^2} y e^y dy \quad , \tag{8.4}$$

for fermions and bosons respectively. For fermions in the relativistic and non-relativistic limits analytic forms for $k(x, +1)$ are

$$k\left(x, +1\right) \simeq \begin{cases} 1 & (x \ll 1) \\ 12\left(\frac{x}{2\pi}\right)^{3/2} e^{-x} & (x \gg 1) \quad . \end{cases} \tag{8.5}$$

[2]One obvious candidate for X-number violation in thermal equilibrium is through 'dark sphalerons'. Alternatively one could allow for explicit non-renormalizable X-number violating operators arising due to physics in the UV.

[3]We expect that in a theory including quantum gravitational effects all continuous global symmetries are violated, leading to the ultimate decay of baryons and/or DM. Since, however, such violation occurs through either higher-dimension operators suppressed by at least M_{GUT}, or through terms which are non-perturbatively small, the resulting lifetimes can be easily much greater than the Hubble time $1/H_0$. As discussed in Section 8.3, in this chapter we will assume that there is an exact discrete symmetry - either a $\mathcal{Z}_2$ X-parity, or in the SUSY case R-parity, which stabilizes the DM.

We will often wish to normalize the particle asymmetry given in eq.(8.3) by the entropy density at a given temperature in order to consider a dimensionless quantity which is not diluted by expansion

$$N_X(T) = \frac{X(T, U_X)}{s(T)} \quad . \tag{8.6}$$

We can translate the required properties of the background potential into those of the rolling scalar field if we make the additional assumption that the evolution of ϕ is damped throughout the generation of X-number, in other words, T_X is greater than the temperature at which $m_\phi \sim 3H$.[4] From the equation of motion, under the assumption of damping, we have

$$\dot{\phi} \simeq \frac{1}{3H}\frac{dV_T(\phi)}{d\phi} \simeq \frac{M_P m_\phi^2 \phi_0}{5 g_\star^{1/2}(T) T^2} \quad , \tag{8.7}$$

where $V_T(\phi)$ is the thermal scalar potential, M_P is the Planck mass, m_ϕ is the mass of the rolling scalar, ϕ_0 is the vacuum expectation value of the scalar and $g_\star(T)$ is the effective number of relativistic degrees of freedom. In the second equality in eq.(8.7) we have made the approximation that thermal effects are subdominant and the potential can be well described by an effective mass term.

We impose the further constraint that the scalar motion remains non-oscillatory down to the temperature, T_X, at which X-number violation freezes out, thus we require that

$$m_\phi \ < \ 1.66 g_\star^{1/2}(T_X)\frac{T_X^2}{M_P} \quad . \tag{8.8}$$

To encode this constraint we thus parameterize the scalar mass as

$$\begin{aligned} m_\phi \ &= \ \alpha \times 1.66 g_\star^{1/2}(T_X)\frac{T_X^2}{M_P} && (8.9)\\ &\simeq \ 2.1\times 10^{-3}\alpha\left(\frac{T_X}{1\ \text{TeV}}\right)^2 \ \text{eV} \quad , && (8.10)\end{aligned}$$

where, in the second line, for definiteness we have assumed a supersymmetric model with $g_\star \sim 250$.

By combining eq.(8.6) with eq.(8.10) we find that

$$\Omega_X h^2(T_{now}) = 5.9\times 10^7 \cdot \frac{g_\star^{1/2}(T_X)}{g_{\star S}(T_X)} \cdot \left[\alpha^2 \frac{\phi_0}{f}\right] \cdot \left[g_X \frac{M_X}{M_N}\frac{T_X}{M_P}\right] k\left(\frac{M_X}{T_X}, +1\right) \quad , \tag{8.11}$$

[4]For a discussion of the oscillating case see e.g. [337]. Note that in the oscillating stage the asymmetry is parametrically smaller than in the damped case. In this chapter we will only be concerned with the situation where ϕ is non-oscillating.

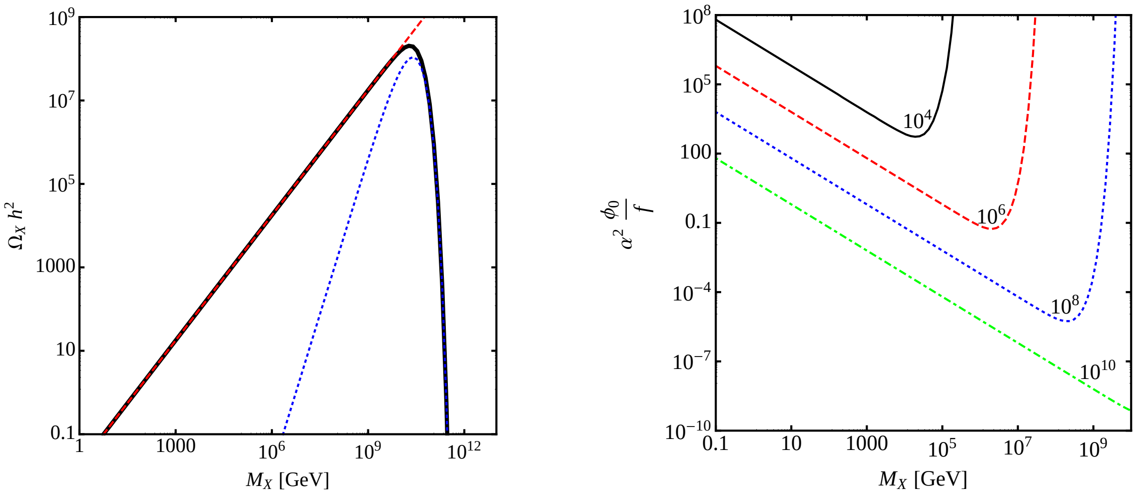

Figure 8.1: Left panel: The relic density of ADM energy density as a function of the DM mass for $\alpha^2\phi_0/f = 1$ and $T_X = 10^{10}$ GeV. The black line corresponds to the full solution calculated using eq.(8.4) and the red dashed (blue dotted) line corresponds to the relativistic (non-relativistic) approximation given in in eq.(8.5). Right panel: The required values of the scalar field parameter combination $\alpha^2\phi_0/f$ for varying DM mass at contours of fixed T_X, where the value of T_X in GeV is labelled on each line. As damped motion requires $\alpha < 1$, low values of $T_X \lesssim 10^5$ GeV require large values of ϕ_0/f.

where M_N is the mass of a nucleon and we have made the assumption that the DM particle is fermionic. We have also assumed that interactions within the dark sector allow the efficient annihilation of the symmetric component of X-density to light, or massless states, such that the final DM density is determined purely by the asymmetry. In Section 8.4 we return to this issue, and show that the interaction in eq.(8.1) automatically serves this purpose for suitable values of the scale f.

Eq.(8.11) is our master formula describing the current DM energy density. The first term in brackets depends only on the properties of the rolling scalar field, where ϕ_0/f is the ratio of the initial vev of the scalar to the decay constant in the scalar-to-current coupling. For an axion-like scalar this term will satisfy $\alpha^2\phi_0/f \lesssim 1$, however if the field corresponds to some non-compact flat direction then this factor could be $\gg 1$. The final quantities depend on the details of the dark sector; the DM mass M_X, g_X, and T_X. In Figure 8.1 we plot the relic abundance as a function of the DM mass for a given choice of $T_X = 10^{10}$ GeV. We also show contours in the $M_X - \alpha^2\phi_0/f$ plane which generate the correct relic abundance for a given value of T_X.

8.3 Relation to the baryon asymmetry

8.3.1 Sharing

In order to connect a DM asymmetry to the observed baryon asymmetry via a sharing scenario it is necessary that, at high temperatures, $U(1)_{B-L} \times U(1)_X$ is broken down to a smaller group $U(1)_{(B-L+qX)}$, for some $q \neq 0$. Specifically there must exist at least one operator, individually breaking $U(1)_{B-L}$ and $U(1)_X$, but conserving $U(1)_{B-L+qX}$, which mediates sharing processes that are in thermal equilibrium.

As this operator could, in principle, mediate DM decay to baryons and leptons one must impose a DM stabilizing symmetry. This could be a $\mathcal{Z}_2$, such as R-parity in a SUSY theory, an X-parity in a SUSY or non-SUSY theory, or a higher discrete symmetry. For definiteness, in this chapter we choose a model with an X-parity, $X \to -X$, as this allows us to consider masses $M_X \gg m_W$, as well as DM masses near, or below the weak scale. We wish to emphasize that a SUSY model where R-parity is the DM stabilizing symmetry is also consistent with our spontaneous co-genesis mechanism. This requires that the DM is the LSP.

For definiteness, we choose to focus on a supersymmetric model[5] described by the MSSM superpotential augmented by a DM Dirac mass term and a sharing operator

$$W_X = M_X \overline{X} X + \frac{1}{M_S^2} X^2 U^c D^c D^c \quad , \tag{8.12}$$

where X is the DM chiral superfield carrying X-number $+1$, U^c and D^c are the usual MSSM right-handed quark superfields, and M_S is the mass-scale of the sharing operator.

The sharing operator in eq.(8.12) can mediate X-number and baryon number violating interactions, but preserves $U(1)_{X+2(B-L)}$. We define T_S as the temperature at which sharing interactions mediated by this operator freeze out. For squark masses $m_{\tilde{q}} > 700$ GeV and a sharing scale $M_S > 1$ TeV, one finds that $T_S \gtrsim 70$ GeV.[6]

For the sharing operator of eq.(8.12) the chemical potentials for DM and right handed quarks must satisfy $2\mu_X = \mu_{u_R} + 2\mu_{d_R}$, and thus the X and B asymmetries are related at a given temperature. Other relations between chemical potentials arise

[5]It is equally possible to implement this mechanism in a non-supersymmetric framework.

[6]In W_X one can equivalently replace $U^c D^c D^c$ by LH_u if T_S is greater than the freeze-out temperature, T_{sph}, for electroweak non-perturbative processes (sphalerons). The reason for this is that while sphalerons are active the chemical potentials for SM particles satisfy $\mu_{u_L} + 2\mu_{d_L} + \mu_{\nu_L} = 0$, and the only continuous global symmetry in the MSSM is $(B - L)$. As both $U^c D^c D^c$ and LH_u have the same charge under this symmetry, these two operators lead to equivalent relative asymmetries.

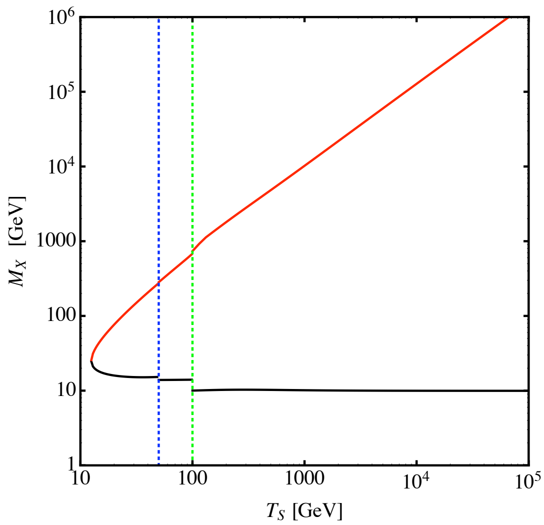

Figure 8.2: Solutions, satisfying $\Omega_X/\Omega_B = 5$, for the ADM mass, M_X, as a function of the sharing freeze-out temperature, T_S. We assume the sharing operator of eq.(8.12), and complete annihilation of the symmetric component of the DM density. We illustrate a typical electroweak phase transition temperature by the vertical green dashed line, and a representative temperature, T_{sph}, at which sphalerons have become inactive, by the vertical blue dashed line. For a given $T_S \gtrsim 20$ GeV there are two successful ADM solutions: One, plotted in black, for $M_X \simeq 10$ GeV, where the DM is relativistic at T_S, while the other, non-relativistic solution, plotted in red, has M_X increasing with T_S (as the DM density is Boltzmann suppressed in the non-relativistic regime). This is the 'sharing' paradigm.

through MSSM Yukawa couplings, gauge interactions, and the requirement of charge neutrality of the Universe. These relations are summarized in [347, 348].

Employing the relations between chemical potentials it is possible to relate X-, B- and L-number asymmetries at a given temperature, resulting in relations of the form $X(T) = \gamma(T)B(T)$, where $\gamma(T)$ is a spectrum-dependent function which we have calculated following the methods in [347, 348]. If both the DM and baryons are relativistic at a given temperature then $\gamma(T) \sim \mathcal{O}(1)$ and a DM solution exists for $M_X \sim 10$ GeV. However if the DM particles are non-relativistic, i.e. $T \ll M_X$, but some baryon number carrying state is still relativistic, then $\gamma(T)$ will be exponentially small and the correct DM density requires $M_X \sim 10T_S$. Both solutions are shown in Figure 8.2.[7] It should be noted that if, in the sharing operator in eq.(8.12), we replace X^2 with X^n then the relativistic DM solution becomes $M_X \simeq 5n$ GeV. Hence, for superpotential operators linear in X, such as $XU^cD^cD^c$ or $XQLD^c$, with the DM stabilized by R-parity, we would expect the DM mass to be closer to 5 GeV.

8.3.2 Spontaneous co-genesis

When we combine the spontaneous genesis mechanism with the asymmetry sharing paradigm there now exist two distinct regimes. If the spontaneous genesis completes before sharing has frozen out, i.e. $T_X > T_S$, then the DM mass is set by T_S. Alternatively, there exists the possibility that sharing freezes out before spontaneous genesis in the dark sector has completed, so $T_S > T_X$. In this case the DM asymmetry continues to evolve after the $B - L$ asymmetry has been set. This scenario is of interest, as it leads to alterations to the standard relationship between the DM mass and T_S.

It may appear that by adding the sharing aspect to the spontaneous genesis mechanism we have also introduced an additional free parameter, namely T_S. However this is not the case as we also have an additional constraint, given by the observed baryon asymmetry. In total there are four parameters which govern the DM relic abundance, given by T_X, T_S, M_X, and the combination of scalar parameters, $\alpha^2\phi_0/f$. However there are two constraints: $\Omega_B h^2$ and $\Omega_{DM}h^2$. Thus in total, this complete scenario only has two free parameters, which we choose to take as T_X and T_S.

In Figure 8.3 we plot contours of constant DM mass in the T_X–T_S plane which satisfy $\Omega_X/\Omega_B = 5$, and generate the observed baryon asymmetry.

[7] Complications arise if lepton-flavour violation is assumed to be out of thermal equilibrium, however as this is not central to the mechanism we are considering we assume this is not the case throughout.

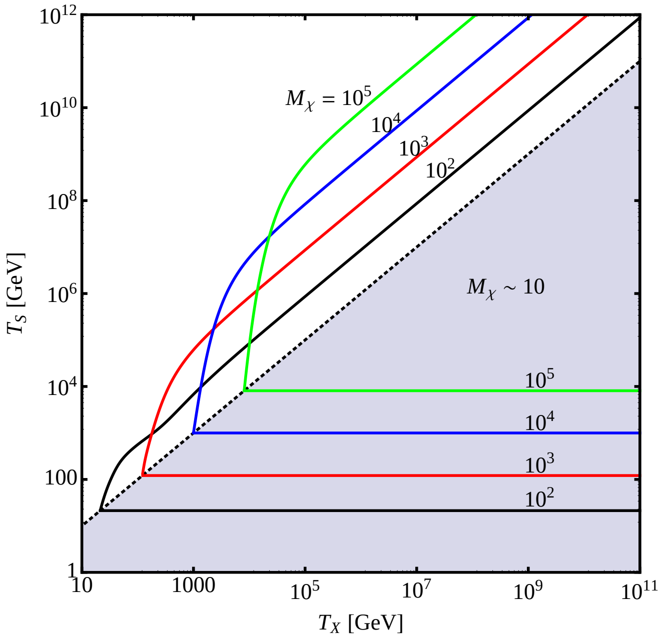

Figure 8.3: Contours of constant M_X in the T_X–T_S plane corresponding to the generation of $\Omega_X/\Omega_B = 5$, and $\Omega_B h^2 = 0.023$. For $T_S < T_X$ there are two branches of solutions corresponding to the two branches shown in Figure 8.2: The first, relativistic solution occurs when $M_X \sim 10$ GeV and fills the entire lower half plane (shaded region), while the second branch is shown by the horizontal contours in the lower half plane labelled by M_X in units of GeV. Both solutions are independent of T_X as in this case the sharing of the asymmetry is determined after the total asymmetry has been frozen in. On the other hand, for $T_X < T_S$ the DM asymmetry continues to evolve after sharing has ceased. The resulting contours of constant M_X corresponding to successful generation of Ω_X/Ω_B, and $\Omega_B h^2$ are shown in the upper half plane, and the mass, M_X, now depends on both T_X and T_S. The portions of contours where $T_S \propto T_X$ apply for the relativistic case ($M_X \ll T_X$), while the remaining portions apply to the semi- and non-relativistic cases ($M_X \gtrsim T_X$). The solution for $M_X \sim 10$ GeV lies along the line $T_S \simeq T_X$, and hence every point of this line corresponds to a solution when we continue to the $T_S < T_X$ corner, showing the continuity between solutions on either side of the line $T_X = T_S$. By allowing the DM asymmetry to evolve after sharing has ceased, a new set of solutions for a given DM mass and T_S open up in the upper left half plane, in addition to the standard solutions in the lower half plane where $T_S < T_X$.

One might wonder if it is still necessary to have X-number violation. Without X-number violation there is a conserved $U(1)_{X+2(B-L)}$ symmetry. It can be imagined that, using the operator of eq.(8.12), one could create an equal and opposite asymmetry in X and $2(B-L)$, without ever violating $U(1)_{X+2(B-L)}$. However, by considering the various chemical potentials and conserved charges, it is straightforward to show that any asymmetry in X, B, or L-number is proportional to the total asymmetry in $X+2(B-L)$.[8] Thus without violation of $U(1)_{X+2(B-L)}$ it is impossible to create an asymmetry in DM or baryons. As B or L-violating operators are more tightly constrained, we choose to have the violation of $U(1)_{X+2(B-L)}$ arising due to X-number violation in the dark sector, consistent with exact conservation of X-parity.

8.4 Cosmology of ϕ

We now consider the constraints on the scalar field parameters arising from production of the correct magnitude of baryon asymmetry, and limits on additional hot and cold DM components. We also show that there exists a range of parameter space where the ϕ interactions lead to efficient annihilation of the symmetric component of DM, leaving just the asymmetric component, as required for a complete theory of ADM.

8.4.1 Baryon asymmetry and ϕ_0/f

From eq.(8.11) we see that the generated particle asymmetry is proportional to the combination of scalar parameters $\alpha^2\phi_0/f$. In order to generate a baryon-asymmetry of $N_B = 8.7\times10^{-11}$, we find the requirement

$$\alpha^2\frac{\phi_0}{f} \simeq \frac{10^{10}\text{GeV}}{\text{Max}[T_X, T_S]} \quad , \tag{8.13}$$

where the exact relation depends on the details of the particle spectrum, but does not change by more than a factor of two when, eg, SUSY particles are included.

Sharing is efficient during the generation of the baryon asymmetry, implying $U_B(T)\propto U_X(T)$. At this temperature the majority of baryon-number carrying species are relativistic, hence, from eq.(8.11), $N_B(T)\propto T(\alpha^2\phi_0/f)$. As a result, if we wish to generate a specific baryon asymmetry for any T we require that $\alpha^2\phi_0/f\propto T^{-1}$.

[8] While sharing is active we have $2\mu_X = \mu_{u_R} + 2\mu_{d_R}$. Rearranging this equation using additional relations between chemical potentials, found in [347], it can be shown that $\mu_X \propto \mu_B$, and an asymmetry in X implies an asymmetry in B of the same sign. While sphalerons are active $\mu_{u_L} + 2\mu_{d_L} = -\mu_{\nu_L}$ and, using the previous relation, $\mu_X \propto -\mu_L$, hence an asymmetry in X implies an asymmetry in L of the opposite sign. Consequently, if we create an asymmetry in X then we must create a non-zero asymmetry in $X+2(B-L)$.

For the case $T_X > T_S$ the total asymmetry is frozen in at T_X, whereas if $T_X < T_S$ the $(B - L)$ asymmetry is frozen in at T_S, explaining the form of eq.(8.13).

Having Max$[T_X, T_S] \ll 10^{10}$ GeV requires $\phi_0 \gg f$, as $\alpha < 1$. For an axion-like scalar with a compact moduli space this is not possible, suggesting that the scalar should correspond to a non-compact flat direction such as might arise in supersymmetric models.

It should also be noted that we have assumed the simplest possible potential for ϕ, with a single, temperature-independent mass term. If this potential contained additional terms, or temperature dependence, such that at the time of spontaneous co-genesis $\frac{dV_T(\phi)}{d\phi} \gg m_\phi^2 \phi_0$ then it may be possible to achieve the required particle asymmetry, with $\phi_0 \sim f$ for $T_X \lesssim 10^{10}$ GeV. The number of possibilities for such alterations, beyond the minimal model studied here, is large.

8.4.2 Relic density of ϕ and bounds on m_ϕ and T_X

There are constraints on the ϕ field parameters arising from the requirement that neither the energy density due to coherent oscillations of ϕ nor the energy density of the thermally produced component of ϕ are too large.

Regarding the thermal component, we assume that after inflation the Universe reheats to a temperature T_I. If ϕ is in equilibrium with the dark sector and, through the sharing operator, the visible sector at early times, then the ratio of the number density to entropy density is roughly $1/g_\star(T_I)$, and the energy density at some later time is $\rho_{therm}(T) \simeq m_\phi s(T)/g_\star(T_I)$ (we assume that ϕ is in thermal equilibrium at T_I in order to set conservative constraints).

The calculation of the energy density in the coherent component is standard, and taking $g_\star(T_X) \simeq g_\star(\sqrt{\alpha}T_X) \simeq g_\star(T_I) \simeq 250$, for definiteness, then $T_{osc} \simeq \sqrt{\alpha}T_X$ and the relic energy density due to ϕ resulting from both production mechanisms is

$$\Omega h^2_{osc} \simeq 1.2 \times 10^{-7}\sqrt{\alpha}\left(\frac{T_X}{\text{TeV}}\right)\left(\frac{\phi_0}{10^{10}\text{GeV}}\right)^2 \quad (8.14)$$

$$\Omega h^2_{therm} \simeq 2.4 \times 10^{-6}\alpha\left(\frac{T_X}{\text{TeV}}\right)^2 \quad . \quad (8.15)$$

The thermal component of ϕ behaves as hot DM, and thus we require that $\Omega h^2_{therm} \lesssim 0.007$, the current WMAP7 limit on relic energy density in neutrinos [349]. Hence we require that $\sqrt{\alpha}T_X \lesssim 50$ TeV. If we maximize the scalar mass by taking $\alpha = 1$, then for $T_X \lesssim 50$ TeV (so satisfying the thermal bound), and $\phi_0 \lesssim 4 \times 10^{11}$ GeV (to satisfy the coherent bound with $\Omega h^2_{osc} < 0.01$), the scalar field constitutes a subdominant component of the DM, hot or cold, leaving the ADM as the dominant component. These inequalities then translate in to the requirement[9]

$$m_\phi|_{\rm now} \lesssim 5 \text{ eV}. \tag{8.16}$$

These bounds can be evaded if additional operators are included which enable ϕ to decay to lighter states. For minimality we do not consider these additional operators here, however, we note that such decays are, in some parameter regions, strongly constrained.

8.4.3 Annihilation of symmetric DM component by $\overline{X}X \to \phi\phi$

An appealing feature of the field ϕ is that, as well as generating a DM and baryon asymmetry, it can also enable the X-number symmetric component of DM density to annihilate away to light particles. Whenever X-number is conserved the interaction in eq.(8.1) can be rearranged into a total derivative term, and thus doesn't allow for DM annihilation while X-number is conserved. While X-number violation is efficient, and $\partial_\mu J^\mu_X \neq 0$, the interaction in eq.(8.1) may allow the symmetric component to annihilate away, however this depends on the source of X-number violation, and requires that the annihilation shuts off at the same time as the spontaneous genesis.

Alternatively, we can include additional fields and couplings to build a model which allows for efficient DM annihilation after X-number violation has ceased. As a simple example we can consider fermionic DM and add an additional real scalar field S, with mass M_S, and couplings $\mathcal{L} \supset c_S S\overline{\psi}_X\psi_X + c_\phi S(\partial\phi)^2/f$. These couplings respect the $U(1)_X$ symmetry, and preserve the shift symmetry of ϕ, keeping it light. This leads to a p-wave suppressed annihilation cross-section of

$$\langle\sigma v\rangle \approx \frac{3c_S^2c_\phi^2}{16\pi^2 f^2}\frac{M_X^4}{(4M_X^2 - M_S^2)^2 + M_S^2\Gamma_S^2}\frac{T}{M_X} \quad . \tag{8.17}$$

By comparison with the results from [325, 351] we find that for

$$f \lesssim 400\frac{c_S c_\phi M_X^2}{\sqrt{(4M_X^2 - M_S^2)^2 + M_S^2\Gamma_S^2}}\text{GeV} \quad , \tag{8.18}$$

[9]This limit is on the current value of m_ϕ, however from eq.(8.7) we see that in order to generate a background potential m_ϕ must be non-zero at T_X. Unlike the QCD axion mass, m_ϕ must be a UV-hard mass and be generated at high temperatures. Such a non-perturbatively small, UV-hard, mass could arise if the shift symmetry $\phi \to \phi + \text{const}$ is broken by UV non-perturbative effects, such as string, or gravitational, instantons, or gauge instantons in a theory with a UV Landau pole [156, 350].

the ratio X_-/X_+ is less than 10%. This feature is particularly attractive: ϕ generates the DM and baryon asymmetry, and then provides the final state into which the symmetric DM component annihilates away!

This solves a significant problem of the ADM scenarios, as the operators allowing direct annihilation of the symmetric part of the DM to light SM states are strongly constrained by direct detection and collider bounds [308, 325, 327], unless one arranges for annihilation solely to leptons.

In order for our effective field theory description to remain consistent the temperatures must satisfy $T_X, T_S \lesssim f$.

8.4.4 DM scattering and ϕ

One might also worry that the coupling $(\partial_\mu\phi)J^\mu_X/f$ for low f could lead to unacceptable DM-DM scattering. However the cross-section for such processes scales as $1/f^4$, and as $f \gtrsim 1$ GeV, the cross-section is well below current bounds [352].

We also comment that light scalars derivatively coupled to DM, such as ϕ, could lead to the novel process of enhanced stellar cooling through ϕ-sstrahlung in DM-nucleon scattering. These processes lead to bounds on f, in analogy with standard axion bounds. These are, however, significantly weaker relative to standard axion bounds as these processes involve DM-nucleon (electron) scattering, and not nucleon-nucleon (electron) scattering. Further, there is additional suppression due to the much lower density of DM compared to nucleons or electrons in a star.

8.5 Summary

We have described how, by derivatively coupling a light scalar, with a time-evolving expectation value, to the X-current, and allowing for X-number violating processes in the early Universe, it is possible to generate a DM asymmetry. By utilizing 'sharing' operators which allow for the transfer of particle asymmetries between the visible and dark sectors it is possible to simultaneously co-generate the observed baryon asymmetry and a DM particle asymmetry, providing a link between the two. All of this occurs without the need for additional CP-violating parameters in either sector. This is the spontaneous co-genesis mechanism.

The mechanism has a number of noteworthy aspects. Most notable is the prediction of a light scalar with mass $m_\phi \lesssim 5$ eV. In addition this scalar provides the attractive feature that it can automatically provide a final state for the annihilation of the symmetric DM component.

Chapter 9

Concluding Remarks

The current time is an important, and exciting time in physics. Physics beyond the SM is being investigated in a wide range of experiments. Of particular relevance to this thesis, the ATLAS and CMS experiments at the CERN LHC are accessing energy scales at which SUSY, if it is relevant to the hierarchy problem, should start to become manifest. This rich theory has been studied for over thirty years, and the time has now come where the applicability of SUSY to the hierarchy problem, and BSM physics, will be tested and known. If discovered, then it may come in the form of the MSSM, or perhaps the SOHDM described in Chapter 3, and it may even be possible to determine the nature of quantum gravity, SUSY breaking, and multiple hidden sectors, through the potentially rich spectrum of Goldstini described in Chapter 4. However, SUSY may not be discovered at the LHC, and maybe some other new physics may explain the hierarchy between the weak scale and the Planck scale, or maybe no physics beyond the SM will be discovered at all.

The boundaries of our knowledge about DM are also being pushed back by the continually improving direct and indirect detection experiments. Maybe the hints observed by the PAMELA and FERMI satellites, or by the DAMA and CoGeNT experiments, are the tip of the DM iceberg and maybe the next few years will see these hints strengthening to evidence, or perhaps they will be undermined by additional data and purely SM explanations will have to be found for these results. Undoubtedly, new hints will arise in the future, and possibly non-gravitational interactions between DM and SM particles will be unambiguously discovered. In the mean time we will have to continue to look for DM anywhere we can, even in compact stars, as described in Chapter 7. On the theoretical side, theorists should continue to pay attention to the hints we do have for the nature of DM, and construct compelling models for the dark sector, such as the model described in Chapter 8.

Whichever fate Nature has decided upon for supersymmetry, and the properties of DM, within the next few years we will have a much better picture. However this will only come once theoretical physicists have been set the enviable task of making sense of the physics and implications of numerous awaited experimental results.

Appendix A

Bounds on a light Neutralino

A.1 Collider bounds

The most stringent collider bounds come from LEP. As LEP operated at $\sqrt{s} \leq 208$ GeV, associated production of the lightest neutralino via $e^+e^- \rightarrow \widetilde{\chi}_1^0\widetilde{\chi}_2^0$ would have been kinematically forbidden for $\{\mu, M_2\} \gtrsim 208$ GeV, due to the large mass of $\widetilde{\chi}_2^0$. Thus, although such a channel would give clear signals following the decay of $\widetilde{\chi}_2^0$, it does not necessarily constrain a very light neutralino.

Radiative neutralino production via $e^+e^- \rightarrow \widetilde{\chi}_1^0\widetilde{\chi}_1^0\gamma$ provides another potential search channel. However, for a mostly bino $\widetilde{\chi}_1^0$, radiative neutrino production, $e^+e^- \rightarrow \overline{\nu}\nu\gamma$, generates a large background to this process.

A.1.1 Precision electroweak

As the decay channel $Z_0 \rightarrow \widetilde{\chi}_1^0\widetilde{\chi}_1^0$ is kinematically allowed, precision measurements of the total and invisible Z_0-width, Γ_Z and $\Gamma_{\rm inv}$, are sensitive to a very light neutralino. In the minimal version of the SOHDM the decay $Z_0 \rightarrow \widetilde{\chi}_1^0\widetilde{\chi}_1^0$ can proceed at tree-level due to the small Higgsino component of $\widetilde{\chi}_1^0$. In addition the Z_0 can decay to the large bino components of $\widetilde{\chi}_1^0$ through loops involving sfermions. Thus, by decreasing the Higgsino fraction of $\widetilde{\chi}_1^0$, and increasing the sfermion masses, these processes can be suppressed compared to decays to neutrinos.

By using the results of [353], in which the processes $Z_0 \rightarrow \widetilde{\chi}_1^0\widetilde{\chi}_1^0$ and $Z_0 \rightarrow \overline{f}f$ have been calculated at $\mathcal{O}(\alpha)$ within the MSSM, the Z_0-width was studied for a massless neutralino in [132]. In this study the bino Majorana mass M_1 was set such that the lightest neutralino is massless, and one particular choice of parameters was with sfermion masses $M_{SUSY} = 600$ GeV, $\tan\beta = 10$, and $A_\tau = A_t = A_b = M_{\tilde{g}} = M_A = 600$ GeV. Upon calculating contributions to the Z_0-width it was found that, within the MSSM, the Z-width observable Γ_Z was within 1σ of the experimental value for $|\mu| \gtrsim 200$ GeV and $M_2 \gtrsim 100$ GeV, and this small discrepancy reduced rapidly for larger values of μ.

The invisible width Γ_{inv} was within 2σ of the experimental value for $|\mu| \gtrsim 200$ GeV and $M_2 \gtrsim 100$ GeV, however there was a 1σ deviation across the entire $\mu - M_2$ plane. This should come as no surprise however, as the SM prediction for Γ_{inv} is 1.8σ greater than the experimental value [354] thus the comparative decrease in quality of fit with the addition of a light neutralino is small.

The study [132] therefore shows that Γ_Z and Γ_{inv} cannot exclude a massless neutralino within the MSSM. Although the SOHDM is in some ways quite distinct from the MSSM, the important features of this study are common to both scenarios. In particular, in both cases the light neutralino is mostly bino, with a small ($< 20\%$) Higgsino component. Thus we find it reasonable to conclude that Z_0-width measurements do not exclude the very light neutralino in the minimal version of the SOHDM.

In [132] a similar analysis of the impact of light neutralinos on M_W and $\sin^2\theta_{\text{eff}}$ within the MSSM was performed. For two selected sets of soft SUSY-breaking parameters, detailed in [132], it was shown that M_W lies within the experimental 1σ boundary, as does Γ_Z again. It is interesting that $\sin^2\theta_{\text{eff}}$ lies outside the experimental 1σ boundary, however, as detailed in [353], raising the soft scalar masses and/or the μ parameter improves this fit, and can lead to agreement at the 1σ level whenever $\tilde{m} \gtrsim 700$ GeV.

Electric dipole moments and the anomalous magnetic moment of the muon were also considered for the MSSM with a light neutralino in [132], where it was found that the SUSY contributions to EDMs go to zero for a massless $\widetilde{\chi}_1^0$. Further, the variation of $(g-2)_\mu$ stays well below the current experimental uncertainty. Thus no lower limit on the mass of the lightest neutralino in the MSSM can be set with these measurements.

A.2 Rare meson decays

In [132] decays of both pseudo-scalar and vector mesons to bino pairs are considered within the MSSM. These decays involve loops containing sfermions, and it is found that for sfermion masses of $\tilde{m} = 300$ GeV the branching ratios for the decays $\{\pi_0, \eta, \eta', B_s\} \to \widetilde{B}\widetilde{B}$, $\{\phi, J/\psi, \Upsilon(1S), \rho, \omega\} \to \widetilde{B}\widetilde{B}$, and $K^+ \to \pi^+\widetilde{B}\widetilde{B}$ all lie well below current bounds.

A.3 Astrophysical bounds

Neutrinos are produced in large abundance during a supernova explosion through electron-positron annihilation and neutrino-sstrahlung in nucleon scattering. As their mean free path is smaller than the supernova core size these neutrinos slowly diffuse out. After $\mathcal{O}(10 \text{ sec})$ the temperature-dependent mean free path exceeds the core size and they escape. During Supernova 1987a such neutrinos were observed.

A similar process can occur for very light neutralinos, whereby they are produced in a supernova through similar processes to neutrinos. If they interact more weakly than neutrinos, and have a mean free path exceeding the core size, they could escape the supernova and carry away a large amount of energy. If this occurs and the energy loss is too great the neutrino mean free path will increase more rapidly, reducing the time-scale over which neutrinos diffuse out.

In [132] it was shown that for the case of very weakly interacting neutralinos, in order that neutralino radiation energy losses do not exceed the Raffelt bound of $\leq 10^{52}$ erg, it is necessary that the production processes are sufficiently suppressed. This leads to the requirement that the selectron mass exceeds $m_{\tilde{e}} \geq 1.2$ TeV, since the process $e^+e^- \to \tilde{\chi}_1^0\tilde{\chi}_1^0$ is suppressed by four powers of the selectron mass. Similar, although much less restrictive bounds hold for the squark masses, requiring $m_{\tilde{q}} \geq 360$ GeV. Alternatively, if the neutralinos have stronger interactions with SM particles it is possible that their mean free path is less than the core size. In this case, the neutralinos will slowly diffuse out and the energy loss due to neutralino radiation will be suppressed while they are trapped within the core of the supernova. It was found in [132] that in this scenario squark and slepton masses of $m_{\tilde{e}}, m_{\tilde{q}} < 300$ GeV are compatible with observations.

It would seem from this discussion that selectron masses in the range $300 < m_{\tilde{e}} \leq 1200$ GeV are excluded, however it should be noted that to-date successful simulations of a full supernova explosion have not yet been performed, and thus the above excluded regions may be subject to change in the future.

A.4 Cosmological bounds

A very light neutralino, which is relativistic at freeze-out, will contribute to hot DM. However it is known that early universe cosmology is most compatible with cold, non-relativistic, DM.

In order that the light neutralino does not constitute too much hot DM, and does not suppress structure formation, it is necessary that the energy density of hot DM is consistent with observations, and the Cowsik-McClelland bound [355] is satisfied. One can see how this arises, as the energy density of a neutrino is proportional to its mass. Therefore if we reduce the mass of the heaviest neutrino this leaves room for energy density due to another hot DM component. Calculation of the neutralino relic density leads to the requirement that:

$$m_{\widetilde{\chi}_1^0} \lesssim 0.7 \text{ eV} \quad . \tag{A.1}$$

Thus a very light, mostly bino, neutralino is consistent with structure formation. It is intriguing that this upper limit on the lightest neutralino mass lies just above the Majorana bino mass we expect to be generated due to anomaly-mediation.

Thus we see, thanks to the study [132], that a mostly bino neutralino, with mass $m_{\widetilde{\chi}_1^0} \lesssim 0.7$ eV, is consistent with direct production collider bounds, precision electroweak observables, branching ratios in rare meson decays, supernova cooling rates, and structure formation in the early universe. Thus the prediction of a very light, mostly bino, neutralino in the minimal version of the SOHDM is phenomenologically acceptable.

Appendix B

Details of the Supergravity Calculation

B.1 Modulini masses from Supergravity

In order to calculate SUGRA effects on the ISS model we study a slightly more general case of the theory detailed in Section 4.3. We start with superfields $\boldsymbol{X}_i$ with superpotential

$$W = W_0 + f_a \boldsymbol{X}_a \tag{B.1}$$

and Kähler potential

$$K = \boldsymbol{X}_a \boldsymbol{X}^\dagger_{a^\star} + \frac{1}{|\mu|^2} A_{ab^\star cd^\star} \boldsymbol{X}_a \boldsymbol{X}^\dagger_{b^\star} \boldsymbol{X}_c \boldsymbol{X}^\dagger_{d^\star} \quad , \tag{B.2}$$

from which we may define the modified Kähler potential

$$G = \frac{K}{M_P^2} + \log \frac{W}{M_P^3} + \log \frac{W^\star}{M_P^3} \tag{B.3}$$

and field derivatives as $G_a = \partial_a G$, $G_{ab^\star} = \partial_a \partial_{b^\star} G$ with $\partial_a = M_P \frac{\partial}{\partial \boldsymbol{X}_a}$. For a modified Kähler potential of this form, then, once the goldstino direction has been rotated away, the fermion mass matrix is given as [356]

$$m_{ab} = m_{3/2} \langle \nabla_a G_b + \frac{1}{3} G_a G_b \rangle \quad , \tag{B.4}$$

where $\nabla_a G_b = \partial_a G_b - \Gamma^c_{ab} G_c$. The Christoffel connection, Γ, is of crucial importance as it encodes the effects of $A_{ab^\star cd^\star}$. Now considering the leading terms in the fermion mass matrix under the assumption that $\sqrt{f} \sim \mu \ll M_P$ one finds

$$m_{ab} = m_{3/2} \left(-\frac{2}{3} \frac{f_a f_b M_P^2}{W_0^2} - \frac{M_P^2}{W_0 |\mu|^2} \delta^{cd^\star} A_{(ad^\star bl^\star)} f_c \langle X^\dagger_{l^\star} \rangle \right) \quad , \tag{B.5}$$

where $A_{(ad^\star bl^\star)}$ has been symmetrised over pairs of holomorphic indices.[1] At this stage it is appropriate to pause and consider the validity of this result. Throughout we have assumed that as $\sqrt{f} \sim \mu \ll M_P$ then $\langle X \rangle \ll M_P$ and $W_0 \ll M_P^3$. It may seem that if one takes the limit $A \to 0$ then $m_{ab} \propto f_a f_b$ which is a rank one matrix with only one non-zero eigenvalue. However taking this limit means that the scalar fields are no longer stabilised near the origin and the derivation of this result is no longer valid. It would also appear from this result that the fermion mass matrix depends on the parameter μ; however we will see that $\langle X \rangle \sim |\mu|^2/M_P$ and this dependence drops out. Again, this independence only necessarily holds in the limit $\mu \ll M_P$.

Now considering the scalar potential $V = M_P^4 e^G(G_a G^a - 3)$ one finds that for vanishing cosmological constant

$$W_0 = M_P \sqrt{\frac{f_a f_a}{3}} = \frac{1}{\sqrt{3}} f_{eff} M_P \quad , \tag{B.6}$$

and at the minimum of the scalar potential

$$\langle X^\dagger_{l^\star} \rangle = -\frac{2|\mu|^2 W_0}{M_P^2} f_k (A_{(ab^\star kl^\star)} f_a f_{b^\star})^{-1} \quad , \tag{B.7}$$

where $(M_{kl^\star})^{-1}$ is understood as the standard matrix inverse. With these results in hand we can now write a general formula for the modulini mass matrix

$$m_{ab} = 2m_{3/2} \left(A_{(ad^\star bl^\star)} (A_{(ij^\star kl^\star)} f_i f_{j^\star})^{-1} f_{d^\star} f_k - \frac{f_a f_b}{f_{eff}^2} \right) \quad . \tag{B.8}$$

This equation is valid up to corrections of the order $\delta m \sim m_{3/2}|\mu|^2/M_P^2$. The extension of this formula to one for matrix-valued fields can be found by replacing individual indices with pairs, i.e. $\{a\} \to \{ab\}$. At first Eq.(B.8) may appear rather opaque, however one important property can be observed by inspection. As described in [356] once the goldstino direction has been rotated away one expects that $G_a m_{ab} = 0$. This is clear from Eq.(B.4) when one enforces the condition of vanishing cosmological constant and that the fields are at the minimum of the potential. At the level of Eq.(B.8) one can see that this result also holds for any form of $A_{ab^\star cd^\star}$ as $f_a m_{ab} = f_b - f_b = 0$ by inspection.

B.2 Masses to all orders in f

As described in Section 4.3.1 the effective Kähler potential only includes corrections to second order in the SUSY breaking F-terms. To include higher order corrections at

[1] By this we mean $A_{(ad^\star bl^\star)} = A_{ad^\star bl^\star} + A_{bd^\star al^\star} + A_{al^\star bd^\star} + A_{bl^\star ad^\star}$.

the level of the Kähler potential would require including higher order super-covariant derivatives. Therefore it is more straightforward to calculate the modulini masses to all orders in the F-terms by explicitly evaluating the loop diagram involving the exchange of scalar and fermionic partners of the heavy fields. In this manner the effects of SUGRA, and consequent R-symmetry breaking, are included by allowing for a non-zero vacuum expectation value for the fields which break SUSY. This vev can be calculated to all orders in the F-terms by including the tadpole term induced by SUGRA and calculating the scalar masses with the Coleman-Weinberg potential. Evaluating the one-loop contribution to the modulini masses using the masses and couplings in Eq.(4.10), one finds

$$m_{ab,cd} = 2m_{3/2}\left(\frac{1}{2}\left(\frac{H(f_a)}{H(f_b)} + \frac{H(f_b)}{H(f_a)}\right)\delta_{ad}\delta_{bc} - \frac{f_a f_c}{f_{eff}^2}\delta_{ab}\delta_{cd}\right) \quad , \tag{B.9}$$

where

$$H(f) = \sum_{i=1}^{N_f-N_c} h(f, \tilde{\mu}_{0_i}^2) \quad , \tag{B.10}$$

and

$$h(f,\mu^2) = \frac{1}{f^2}\left(2f\mu^2 + 2f\mu^2\log\left(\frac{\mu^4}{\mu^4-f^2}\right) + (\mu^4+f^2)\log\left(\frac{\mu^2-f}{\mu^2+f}\right)\right) \quad . \tag{B.11}$$

Here $\tilde{\mu}_{0_i} \geq \sqrt{f}$ is the SUSY mass of the fields which have been integrated out. One can see that all dependence on the UV cut-off has cancelled and the masses are finite. The goldstini from the diagonal components of Φ still have mass $2m_{3/2}$ and the modulini from the off-diagonal components have mass $\geq 2m_{3/2}$, limiting to $2m_{3/2}$ when the F-terms are equal, as before. Therefore the results derived using the effective Kähler potential in Section 4.3.1 are qualitatively the same as those one finds when including the F-terms to all orders.

B.3 Decay widths

Starting with Eq.(4.29) we derive the decay width to multiple goldstini under the assumption that all but one messenger scales are the same. We take the first $N-1$ messenger scales equal to $\sqrt{x}\Lambda$ and the N^{th} messenger scale as Λ. Using this, the orthogonality of V_{ia}, the fact that $V_{Ni} = f_i/f_{eff}$ and that $\sum_i f_i V_{i,a\neq N} = 0$ we can simplify the sum over squares of the couplings:

$$\begin{aligned}
\sum_{a=1}^{N-1} |C_a|^2 &= \sum_{a=1}^{N-1} \left| \sum_{i=1}^{N} \frac{f_i V_{ia}}{\Lambda_i^2} \right|^2 \\
&= \sum_{a=1}^{N-1} \frac{(x-1)^2 f_N^2}{x^2 \Lambda^4} V_{Na} V_{aN}^T \\
&= \frac{(x-1)^2 f_N^2}{x^2 \Lambda^4} \frac{f_{eff}^2 - f_N^2}{f_{eff}^2} \qquad \text{(B.12)}
\end{aligned}$$

Thus we have

$$\Gamma_{\phi^\dagger \to \zeta\psi} \simeq \frac{m_\phi}{16\pi} \left(\frac{(x-1) f_N}{x \Lambda^2} \right)^2 \frac{f_{eff}^2 - f_N^2}{f_{eff}^2} \qquad \text{(B.13)}$$

For decays to the gravitino similar steps lead to

$$|C_N|^2 = \left(\frac{f_{eff}^2 - (1-x) f_N^2}{x \Lambda^2 f_{eff}} \right)^2 \qquad \text{(B.14)}$$

and

$$\Gamma_{\phi^\dagger \to G\psi} \simeq \frac{m_\phi}{16\pi} \left(\frac{f_{eff}^2 - (1-x) f_N^2}{x \Lambda^2 f_{eff}} \right)^2 \qquad \text{(B.15)}$$

These results make no assumptions about the relative magnitudes of the various F-terms and therefore hold if there are multiple SUSY breaking sectors and all but one mediate SUSY breaking to the SSM in the same way. If all mediation sectors are the same this corresponds to the limit $x \to 1$.

Bibliography

[1] John March-Russell, Christopher McCabe, and Matthew McCullough. Inelastic Dark Matter, Non-Standard Halos and the DAMA/LIBRA Results. *JHEP*, 05:071, 2009, 0812.1931.

[2] John March-Russell, Christopher McCabe, and Matthew McCullough. Neutrino-Flavoured Sneutrino Dark Matter. *JHEP*, 03:108, 2010, 0911.4489.

[3] Matthew McCullough and Malcolm Fairbairn. Capture of Inelastic Dark Matter in White Dwarves. *Phys. Rev.*, D81:083520, 2010, 1001.2737.

[4] Nathaniel Craig, John March-Russell, and Matthew McCullough. The Goldstini Variations. *JHEP*, 10:095, 2010, 1007.1239.

[5] Matthew McCullough. Stimulated Supersymmetry Breaking. *Phys. Rev.*, D82:115016, 2010, 1010.3203.

[6] Rhys Davies, John March-Russell, and Matthew McCullough. A Supersymmetric One Higgs Doublet Model. *JHEP*, 04:108, 2011, 1103.1647.

[7] Mads T. Frandsen et al. On the DAMA and CoGeNT Modulations. 2011, 1105.3734.

[8] John March-Russell and Matthew McCullough. Asymmetric Dark Matter via Spontaneous Co-Genesis. 2011, 1106.4319.

[9] S. Tomonaga. On a relativistically invariant formulation of the quantum theory of wave fields. *Prog.Theor.Phys.*, 1:27–42, 1946.

[10] Julian S. Schwinger. On Quantum electrodynamics and the magnetic moment of the electron. *Phys.Rev.*, 73:416–417, 1948.

[11] Julian S. Schwinger. Quantum electrodynamics. I A covariant formulation. *Phys.Rev.*, 74:1439, 1948.

[12] R.P. Feynman. Space - time approach to quantum electrodynamics. *Phys.Rev.*, 76:769–789, 1949.

[13] R.P. Feynman. The Theory of positrons. *Phys.Rev.*, 76:749–759, 1949.

[14] R.P. Feynman. Mathematical formulation of the quantum theory of electromagnetic interaction. *Phys.Rev.*, 80:440–457, 1950.

[15] Chen-Ning Yang and Robert L. Mills. Conservation of Isotopic Spin and Isotopic Gauge Invariance. *Phys.Rev.*, 96:191–195, 1954.

[16] F. Englert and R. Brout. Broken Symmetry and the Mass of Gauge Vector Mesons. *Phys.Rev.Lett.*, 13:321–322, 1964.

[17] Peter W. Higgs. Broken Symmetries and the Masses of Gauge Bosons. *Phys.Rev.Lett.*, 13:508–509, 1964.

[18] G.S. Guralnik, C.R. Hagen, and T.W.B. Kibble. Global Conservation Laws and Massless Particles. *Phys.Rev.Lett.*, 13:585–587, 1964.

[19] S.L. Glashow, J. Iliopoulos, and L. Maiani. Weak Interactions with Lepton-Hadron Symmetry. *Phys.Rev.*, D2:1285–1292, 1970.

[20] Mary K. Gaillard, Benjamin W. Lee, and Jonathan L. Rosner. Search for Charm. *Rev.Mod.Phys.*, 47:277–310, 1975.

[21] Makoto Kobayashi and Toshihide Maskawa. CP Violation in the Renormalizable Theory of Weak Interaction. *Prog.Theor.Phys.*, 49:652–657, 1973.

[22] S.L. Glashow. Partial Symmetries of Weak Interactions. *Nucl.Phys.*, 22:579–588, 1961.

[23] Abdus Salam. Renormalizability of gauge theories. *Phys.Rev.*, 127:331–334, 1962.

[24] Steven Weinberg. A Model of Leptons. *Phys.Rev.Lett.*, 19:1264–1266, 1967.

[25] K. Nakamura et al. Review of particle physics. *J. Phys.*, G37:075021, 2010.

[26] M. Gellmann. A schematic model of baryons and mesons. *Physics Letters*, 8:214–215, February 1964.

[27] G. Zweig. An SU(3) model for strong interaction symmetry and its breaking. 1964.

[28] G. Zweig. AN SU(3) MODEL FOR STRONG INTERACTION SYMMETRY AND ITS BREAKING. 2. 1964. Published in 'Developments in the Quark Theory of Hadrons'. Volume 1. Edited by D. Lichtenberg and S. Rosen. Nonantum, Mass., Hadronic Press, 1980. pp. 22-101.

[29] M. Breidenbach, J. I. Friedman, H. W. Kendall, E. D. Bloom, D. H. Coward, H. Destaebler, J. Drees, L. W. Mo, and R. E. Taylor. Observed Behavior of Highly Inelastic Electron-Proton Scattering. *Physical Review Letters*, 23:935–939, October 1969.

[30] E. D. Bloom, D. H. Coward, H. Destaebler, J. Drees, G. Miller, L. W. Mo, R. E. Taylor, M. Breidenbach, J. I. Friedman, G. C. Hartmann, and H. W. Kendall. High-Energy Inelastic e-p Scattering. *Physical Review Letters*, 23:930–934, October 1969.

[31] Richard P. Feynman. Very high-energy collisions of hadrons. *Phys.Rev.Lett.*, 23:1415–1417, 1969.

[32] J.D. Bjorken and Emmanuel A. Paschos. Inelastic Electron Proton and gamma Proton Scattering, and the Structure of the Nucleon. *Phys.Rev.*, 185:1975–1982, 1969.

[33] R. Brandelik et al. Evidence for planar events in e^+e^- annihilation at high energies. *Physics Letters B*, 86:243–249, September 1979.

[34] John R. Ellis, Mary K. Gaillard, and Graham G. Ross. Search for Gluons in e+ e- Annihilation. *Nucl.Phys.*, B111:253, 1976.

[35] D.J. Gross and Frank Wilczek. Ultraviolet Behavior of Nonabelian Gauge Theories. *Phys.Rev.Lett.*, 30:1343–1346, 1973.

[36] H.David Politzer. Reliable Perturbative Results for Strong Interactions? *Phys.Rev.Lett.*, 30:1346–1349, 1973.

[37] Kenneth G. Wilson. Confinement of Quarks. *Phys.Rev.*, D10:2445–2459, 1974.

[38] Christof Gattringer and Christian B. Lang. Quantum chromodynamics on the lattice. *Lect.Notes Phys.*, 788:1–211, 2010.

[39] F.J. Hasert et al. Observation of Neutrino Like Interactions Without Muon Or Electron in the Gargamelle Neutrino Experiment. *Phys.Lett.*, B46:138–140, 1973.

[40] A.D. Sakharov. Violation of CP Invariance, c Asymmetry, and Baryon Asymmetry of the Universe. *Pisma Zh.Eksp.Teor.Fiz.*, 5:32–35, 1967. Reprinted in *Kolb, E.W. (ed.), Turner, M.S. (ed.): The early universe* 371-373, and in *Lindley, D. (ed.) et al.: Cosmology and particle physics* 106-109, and in Sov. Phys. Usp. 34 (1991) 392-393 [Usp. Fiz. Nauk 161 (1991) No. 5 61-64].

[41] Alessandro Strumia and Francesco Vissani. Neutrino masses and mixings and... 2006, hep-ph/0606054.

[42] Gianfranco Bertone, Dan Hooper, and Joseph Silk. Particle dark matter: Evidence, candidates and constraints. *Phys.Rept.*, 405:279–390, 2005, hep-ph/0404175.

[43] K.G. Begeman, A.H. Broeils, and R.H. Sanders. Extended rotation curves of spiral galaxies: Dark haloes and modified dynamics. *Mon.Not.Roy.Astron.Soc.*, 249:523, 1991.

[44] Mario Mateo, Edward W. Olszewski, Steven S. Vogt, and Michael J. Keane. The internal kinematics of the leo I dwarf spheroidal galaxy: dark matter at the fringe of the milky way. 1998, astro-ph/9807296. * Brief entry *.

[45] Mario Mateo. Dwarf Galaxies of the Local Group. *Ann. Rev. Astron. Astrophys.*, 36:435–506, 1998, astro-ph/9810070.

[46] Dennis Zaritsky, Rodney Smith, Carlos Frenk, and Simon D.M. White. More satellites of spiral galaxies. *Astrophys.J.*, 478:39–48, 1997, astro-ph/9611199.

[47] M. Azzaro, F. Prada, and C. M. Gutierrez. Motion properties of satellites around external spiral galaxies. 2003, astro-ph/0310487.

[48] F. Zwicky. Spectral displacement of extra galactic nebulae. *Helv.Phys.Acta*, 6:110–127, 1933.

[49] Neta A. Bahcall and Xiao-hui Fan. The Most massive distant clusters: Determining Omega and sigma8. *Astrophys.J.*, 504:1, 1998, astro-ph/9803277.

[50] J.Anthony Tyson, Greg P. Kochanski, and Ian P. Dell'Antonio. Detailed mass map of CL0024+1654 from strong lensing. *Astrophys.J.*, 498:L107, 1998, astro-ph/9801193.

[51] Douglas Clowe et al. A direct empirical proof of the existence of dark matter. *Astrophys. J.*, 648:L109–L113, 2006, astro-ph/0608407.

[52] D. Larson et al. Seven-Year Wilkinson Microwave Anisotropy Probe (WMAP) Observations: Power Spectra and WMAP-Derived Parameters. *Astrophys. J. Suppl.*, 192:16, 2011, 1001.4635.

[53] Wayne Hu, Naoshi Sugiyama, and Joseph Silk. The Physics of microwave background anisotropies. *Nature*, 386:37–43, 1997, astro-ph/9604166.

[54] Ya. B. Zeldovich. Gravitational instability: An Approximate theory for large density perturbations. *Astron. Astrophys.*, 5:84–89, 1970.

[55] Edward W. Kolb and Michael S. Turner. The Early universe. *Front.Phys.*, 69:1–547, 1990.

[56] J.R. Bond, G. Efstathiou, and J. Silk. Massive Neutrinos and the Large Scale Structure of the Universe. *Phys.Rev.Lett.*, 45:1980–1984, 1980.

[57] J.R. Bond and A.S. Szalay. The Collisionless Damping of Density Fluctuations in an Expanding Universe. *Astrophys.J.*, 274:443–468, 1983.

[58] Marco Cirelli, Nicolao Fornengo, and Alessandro Strumia. Minimal dark matter. *Nucl. Phys.*, B753:178–194, 2006, hep-ph/0512090.

[59] Gerard 't Hooft. Symmetry Breaking Through Bell-Jackiw Anomalies. *Phys.Rev.Lett.*, 37:8–11, 1976.

[60] Gerard 't Hooft. Computation of the Quantum Effects Due to a Four-Dimensional Pseudoparticle. *Phys.Rev.*, D14:3432–3450, 1976.

[61] R. Jackiw and C. Rebbi. Vacuum Periodicity in a Yang-Mills Quantum Theory. *Phys.Rev.Lett.*, 37:172–175, 1976.

[62] Jr. Callan, Curtis G., R.F. Dashen, and David J. Gross. The Structure of the Gauge Theory Vacuum. *Phys.Lett.*, B63:334–340, 1976.

[63] Michael Dine. TASI lectures on the strong CP problem. pages 349–369, 2000, hep-ph/0011376.

[64] R.D. Peccei and Helen R. Quinn. CP Conservation in the Presence of Instantons. *Phys.Rev.Lett.*, 38:1440–1443, 1977.

[65] R.D. Peccei and Helen R. Quinn. Constraints Imposed by CP Conservation in the Presence of Instantons. *Phys.Rev.*, D16:1791–1797, 1977.

[66] Frank Wilczek. Problem of Strong p and t Invariance in the Presence of Instantons. *Phys.Rev.Lett.*, 40:279–282, 1978.

[67] Steven Weinberg. A New Light Boson? *Phys.Rev.Lett.*, 40:223–226, 1978.

[68] D. Amati, K. Konishi, Y. Meurice, G.C. Rossi, and G. Veneziano. Nonperturbative Aspects in Supersymmetric Gauge Theories. *Phys.Rept.*, 162:169–248, 1988.

[69] Mikhail A. Shifman and A.I. Vainshtein. Solution of the Anomaly Puzzle in SUSY Gauge Theories and the Wilson Operator Expansion. *Nucl.Phys.*, B277:456, 1986.

[70] Mikhail A. Shifman and A.I. Vainshtein. On holomorphic dependence and infrared effects in supersymmetric gauge theories. *Nucl.Phys.*, B359:571–580, 1991.

[71] Marcus T. Grisaru, W. Siegel, and M. Rocek. Improved Methods for Supergraphs. *Nucl.Phys.*, B159:429, 1979.

[72] Nathan Seiberg. Naturalness Versus Supersymmetric Non-renormalization Theorems. *Phys. Lett.*, B318:469–475, 1993, hep-ph/9309335.

[73] Nathan Seiberg. The Power of holomorphy: Exact results in 4-D SUSY field theories. 1994, hep-th/9408013.

[74] Clifford Cheung, Yasunori Nomura, and Jesse Thaler. Goldstini. *JHEP*, 03:073, 2010, 1002.1967.

[75] Clifford Cheung, Jeremy Mardon, Yasunori Nomura, and Jesse Thaler. A Definitive Signal of Multiple Supersymmetry Breaking. *JHEP*, 07:035, 2010, 1004.4637.

[76] Savas Dimopoulos and Howard Georgi. Softly Broken Supersymmetry and SU(5). *Nucl.Phys.*, B193:150, 1981.

[77] Nima Arkani-Hamed and Savas Dimopoulos. Supersymmetric unification without low energy supersymmetry and signatures for fine-tuning at the LHC. *JHEP*, 0506:073, 2005, hep-th/0405159.

[78] Search for squarks and gluinos using final states with jets and missing transverse momentum with the ATLAS detector in $\sqrt{s} = 7$ TeV proton-proton collisions. Technical Report ATLAS-CONF-2011-086, CERN, Geneva, Jun 2011.

[79] S. Cassel, D. M. Ghilencea, S. Kraml, A. Lessa, and G. G. Ross. Fine-tuning implications for complementary dark matter and LHC SUSY searches. *JHEP*, 05:120, 2011, 1101.4664.

[80] Graham G. Ross and S. K. Wilkinson. MIXING ANGLES IN SUPERGRAVITY THEORIES. *Nucl. Phys.*, B282:382, 1987.

[81] K.S. Babu, Christopher F. Kolda, John March-Russell, and Frank Wilczek. CP violation, Higgs couplings, and supersymmetry. *Phys.Rev.*, D59:016004, 1999, hep-ph/9804355.

[82] Graham Ross and Mario Serna. Unification and Fermion Mass Structure. *Phys. Lett.*, B664:97–102, 2008, 0704.1248.

[83] Michael Dine, Nathan Seiberg, and Scott Thomas. Higgs physics as a window beyond the MSSM (BMSSM). *Phys.Rev.*, D76:095004, 2007, 0707.0005.

[84] S. Nandi and Zurab Tavartkiladze. A New Extensions of MSSM: FMSSM. *Phys. Lett.*, B672:240–245, 2009, 0804.1996.

[85] Peter W. Graham and Surjeet Rajendran. A Domino Theory of Flavor. *Phys. Rev.*, D81:033002, 2010, 0906.4657.

[86] Bogdan A. Dobrescu and Patrick J. Fox. Uplifted supersymmetric Higgs region. 2010, 1001.3147.

[87] Masahiro Ibe, Arvind Rajaraman, and Ze'ev Surujon. Does Supersymmetry Require Two Higgs Doublets? 2010, 1012.5099.

[88] Michael Dine and John Kehayias. Discrete R Symmetries and Low Energy Supersymmetry. *Phys. Rev.*, D82:055014, 2010, 0909.1615.

[89] Pierre Fayet. MASSIVE GLUINOS. *Phys.Lett.*, B78:417, 1978.

[90] Joseph Polchinski and Leonard Susskind. Breaking of Supersymmetry at Intermediate-Energy. *Phys.Rev.*, D26:3661, 1982.

[91] L.J. Hall and Lisa Randall. U(1)-R symmetric supersymmetry. *Nucl.Phys.*, B352:289–308, 1991.

[92] Kiichi Kurosawa, Nobuhito Maru, and T. Yanagida. Nonanomalous R-symmetry in supersymmetric unified theories of quarks and leptons. *Phys. Lett.*, B512:203–210, 2001, hep-ph/0105136.

[93] Patrick J. Fox, Ann E. Nelson, and Neal Weiner. Dirac gaugino masses and supersoft supersymmetry breaking. *JHEP*, 0208:035, 2002, hep-ph/0206096.

[94] Ignatios Antoniadis, Antonio Delgado, Karim Benakli, Mariano Quiros, and Marc Tuckmantel. Splitting extended supersymmetry. *Phys.Lett.*, B634:302–306, 2006, hep-ph/0507192.

[95] Ignatios Antoniadis, Karim Benakli, Antonio Delgado, Mariano Quiros, and Marc Tuckmantel. Split extended supersymmetry from intersecting branes. *Nucl.Phys.*, B744:156–179, 2006, hep-th/0601003.

[96] I. Antoniadis, K. Benakli, A. Delgado, and M. Quiros. A New gauge mediation theory. *Adv.Stud.Theor.Phys.*, 2:645–672, 2008, hep-ph/0610265.

[97] Santiago De Lope Amigo, Andrew E. Blechman, Patrick J. Fox, and Erich Poppitz. R-symmetric gauge mediation. *JHEP*, 0901:018, 2009, 0809.1112.

[98] Andrew E. Blechman. R-symmetric Gauge Mediation and the Minimal R-Symmetric Supersymmetric Standard Model. *Mod.Phys.Lett.*, A24:633–646, 2009, 0903.2822.

[99] K. Benakli and M.D. Goodsell. Dirac Gauginos in General Gauge Mediation. *Nucl.Phys.*, B816:185–203, 2009, 0811.4409.

[100] G. Belanger, K. Benakli, M. Goodsell, C. Moura, and A. Pukhov. Dark Matter with Dirac and Majorana Gaugino Masses. *JCAP*, 0908:027, 2009, 0905.1043.

[101] K. Benakli and M.D. Goodsell. Dirac Gauginos and Kinetic Mixing. *Nucl.Phys.*, B830:315–329, 2010, 0909.0017.

[102] Eung Jin Chun, Jong-Chul Park, and Stefano Scopel. Dirac gaugino as leptophilic dark matter. *JCAP*, 1002:015, 2010, 0911.5273.

[103] K. Benakli and M. D. Goodsell. Dirac Gauginos, Gauge Mediation and Unification. *Nucl. Phys.*, B840:1–28, 2010, 1003.4957.

[104] Linda M. Carpenter. Dirac Gauginos, Negative Supertraces and Gauge Mediation. 2010, 1007.0017.

[105] Graham D. Kribs, Takemichi Okui, and Tuhin S. Roy. Viable Gravity-Mediated Supersymmetry Breaking. *Phys.Rev.*, D82:115010, 2010, 1008.1798.

[106] Hyun Min Lee, Stuart Raby, Michael Ratz, Graham G. Ross, Roland Schieren, Kai Schmidt-Hoberg, and Patrick K.S. Vaudrevange. A unique Z_4^R symmetry for the MSSM. *Phys. Lett.*, B694:491–495, 2011, 1009.0905.

[107] Steven Abel and Mark Goodsell. Easy Dirac Gauginos. 2011, 1102.0014.

[108] Hyun Min Lee, Stuart Raby, Michael Ratz, Graham G. Ross, Roland Schieren, Kai Schmidt-Hoberg, and Patrick K.S. Vaudrevange. Discrete R symmetries for the MSSM and its singlet extensions. 2011, 1102.3595.

[109] Graham D. Kribs, Erich Poppitz, and Neal Weiner. Flavor in supersymmetry with an extended R-symmetry. *Phys.Rev.*, D78:055010, 2008, 0712.2039.

[110] Steven B. Giddings and Andrew Strominger. Axion Induced Topology Change in Quantum Gravity and String Theory. *Nucl.Phys.*, B306:890, 1988.

[111] Steven B. Giddings and Andrew Strominger. Baby Universes, Third Quantization and the Cosmological Constant. *Nucl.Phys.*, B321:481, 1989.

[112] Steven B. Giddings and Andrew Strominger. STRING WORMHOLES. *Phys.Lett.*, B230:46, 1989.

[113] Sidney R. Coleman and Ki-Myeong Lee. WORMHOLES MADE WITHOUT MASSLESS MATTER FIELDS. *Nucl.Phys.*, B329:387, 1990.

[114] L.F. Abbott and Mark B. Wise. WORMHOLES AND GLOBAL SYMMETRIES. *Nucl.Phys.*, B325:687, 1989.

[115] Stephen M. Barr and D. Seckel. Planck scale corrections to axion models. *Phys.Rev.*, D46:539–549, 1992.

[116] Marc Kamionkowski and John March-Russell. Planck scale physics and the Peccei-Quinn mechanism. *Phys.Lett.*, B282:137–141, 1992, hep-th/9202003.

[117] Richard Holman, Stephen D.H. Hsu, Thomas W. Kephart, Edward W. Kolb, Richard Watkins, et al. Solutions to the strong CP problem in a world with gravity. *Phys.Lett.*, B282:132–136, 1992, hep-ph/9203206.

[118] Renata Kallosh, Andrei D. Linde, Dmitri A. Linde, and Leonard Susskind. Gravity and global symmetries. *Phys.Rev.*, D52:912–935, 1995, hep-th/9502069.

[119] Tom Banks and Nathan Seiberg. Symmetries and Strings in Field Theory and Gravity. 2010, 1011.5120.

[120] Zohar Komargodski and Nathan Seiberg. Comments on the Fayet-Iliopoulos Term in Field Theory and Supergravity. *JHEP*, 06:007, 2009, 0904.1159.

[121] Thomas T. Dumitrescu, Zohar Komargodski, and Matthew Sudano. Global Symmetries and D-Terms in Supersymmetric Field Theories. 2010, 1007.5352.

[122] Stuart Raby and Kazuhiro Tobe. Dynamical SUSY breaking with a hybrid messenger sector. *Phys.Lett.*, B437:337–343, 1998, hep-ph/9805317.

[123] Keith R. Dienes and Brooks Thomas. Building a Nest at Tree Level: Classical Metastability and Non-Trivial Vacuum Structure in Supersymmetric Field Theories. *Phys.Rev.*, D78:106011, 2008, 0806.3364.

[124] Nathan Seiberg, Tomer Volansky, and Brian Wecht. Semi-direct Gauge Mediation. *JHEP*, 0811:004, 2008, 0809.4437.

[125] Henriette Elvang and Brian Wecht. Semi-Direct Gauge Mediation with the 4-1 Model. *JHEP*, 0906:026, 2009, 0904.4431.

[126] Luis Filipe Matos. Some examples of F and D-term SUSY breaking models. 2009, 0910.0451.

[127] Ann E. Nelson, Nuria Rius, Veronica Sanz, and Mithat Unsal. The minimal supersymmetric model without a mu term. *JHEP*, 08:039, 2002, hep-ph/0206102.

[128] G.F. Giudice and A. Masiero. A Natural Solution to the mu Problem in Supergravity Theories. *Phys.Lett.*, B206:480–484, 1988.

[129] Savas Dimopoulos, Scott D. Thomas, and James D. Wells. Sparticle spectroscopy and electroweak symmetry breaking with gauge-mediated supersymmetry breaking. *Nucl. Phys.*, B488:39–91, 1997, hep-ph/9609434.

[130] Lisa Randall and Raman Sundrum. Out of this world supersymmetry breaking. *Nucl. Phys.*, B557:79–118, 1999, hep-th/9810155.

[131] Gian F. Giudice, Markus A. Luty, Hitoshi Murayama, and Riccardo Rattazzi. Gaugino Mass without Singlets. *JHEP*, 12:027, 1998, hep-ph/9810442.

[132] Herbi K. Dreiner, Sven Heinemeyer, Olaf Kittel, Ulrich Langenfeld, Arne M. Weber, et al. Mass Bounds on a Very Light Neutralino. *Eur.Phys.J.*, C62:547–572, 2009, 0901.3485.

[133] John Preskill, Mark B. Wise, and Frank Wilczek. Cosmology of the Invisible Axion. *Phys.Lett.*, B120:127–132, 1983.

[134] L.F. Abbott and P. Sikivie. A Cosmological Bound on the Invisible Axion. *Phys.Lett.*, B120:133–136, 1983.

[135] Michael Dine and Willy Fischler. The Not So Harmless Axion. *Phys.Lett.*, B120:137–141, 1983.

[136] Frank Daniel Steffen. Dark Matter Candidates - Axions, Neutralinos, Gravitinos, and Axinos. *Eur. Phys. J.*, C59:557–588, 2009, 0811.3347.

[137] Lawrence J. Hall, Karsten Jedamzik, John March-Russell, and Stephen M. West. Freeze-In Production of FIMP Dark Matter. *JHEP*, 1003:080, 2010, 0911.1120.

[138] Clifford Cheung, Gilly Elor, Lawrence J. Hall, and Piyush Kumar. Origins of Hidden Sector Dark Matter I: Cosmology. 2010, 1010.0022.

[139] Clifford Cheung, Gilly Elor, Lawrence J. Hall, and Piyush Kumar. Origins of Hidden Sector Dark Matter II: Collider Physics. 2010, 1010.0024.

[140] Abdus Salam and J.A. Strathdee. Supersymmetry and Fermion Number Conservation. *Nucl.Phys.*, B87:85, 1975.

[141] Pierre Fayet. Supergauge Invariant Extension of the Higgs Mechanism and a Model for the electron and Its Neutrino. *Nucl.Phys.*, B90:104–124, 1975.

[142] Heinz Pagels and Joel R. Primack. Supersymmetry, Cosmology and New TeV Physics. *Phys.Rev.Lett.*, 48:223, 1982.

[143] H. Goldberg. Constraint on the Photino Mass from Cosmology. *Phys.Rev.Lett.*, 50:1419, 1983.

[144] John R. Ellis, J.S. Hagelin, Dimitri V. Nanopoulos, Keith A. Olive, and M. Srednicki. Supersymmetric Relics from the Big Bang. *Nucl.Phys.*, B238:453–476, 1984.

[145] John R. Ellis, Keith A. Olive, Subir Sarkar, and D.W. Sciama. LOW MASS PHOTINOS AND SUPERNOVA SN1987A. *Phys.Lett.*, B215:404, 1988.

[146] G. D'Ambrosio, G. F. Giudice, G. Isidori, and A. Strumia. Minimal flavour violation: An effective field theory approach. *Nucl. Phys.*, B645:155–187, 2002, hep-ph/0207036.

[147] Ricky Fok and Graham D. Kribs. mu to e in R-symmetric Supersymmetry. *Phys. Rev.*, D82:035010, 2010, 1004.0556.

[148] Steven Weinberg. Larger Higgs Exchange Terms in the Neutron Electric Dipole Moment. *Phys.Rev.Lett.*, 63:2333, 1989.

[149] K. Nakamura et al. (Particle Data Group). Review of particle physics. *J.Phys.G*, G37, 2010.

[150] Stephen P. Martin. Raising the Higgs mass with Yukawa couplings for isotriplets in vector-like extensions of minimal supersymmetry. *Phys. Rev.*, D82:055019, 2010, 1006.4186.

[151] S. Y. Choi, M. Drees, A. Freitas, and P. M. Zerwas. Testing the Majorana Nature of Gluinos and Neutralinos. *Phys. Rev.*, D78:095007, 2008, 0808.2410.

[152] S. Y. Choi, J. Kalinowski, J. M. Kim, and E. Popenda. Scalar gluons and Dirac gluinos at the LHC. *Acta Phys. Polon.*, B40:2913–2922, 2009, 0911.1951.

[153] S. Y. Choi et al. Dirac Neutralinos and Electroweak Scalar Bosons of N=1/N=2 Hybrid Supersymmetry at Colliders. *JHEP*, 08:025, 2010, 1005.0818.

[154] S. Y. Choi et al. Color-Octet Scalars of N=2 Supersymmetry at the LHC. *Phys. Lett.*, B672:246–252, 2009, 0812.3586.

[155] S. Y. Choi, D. Choudhury, A. Freitas, J. Kalinowski, and P. M. Zerwas. The Extended Higgs System in R-symmetric Supersymmetry Theories. 2010, 1012.2688.

[156] Asimina Arvanitaki, Savas Dimopoulos, Sergei Dubovsky, Nemanja Kaloper, and John March-Russell. String Axiverse. *Phys.Rev.*, D81:123530, 2010, 0905.4720.

[157] Asimina Arvanitaki, Nathaniel Craig, Savas Dimopoulos, Sergei Dubovsky, and John March-Russell. String Photini at the LHC. *Phys. Rev.*, D81:075018, 2010, 0909.5440.

[158] Kenneth A. Intriligator, Nathan Seiberg, and David Shih. Dynamical SUSY breaking in meta-stable vacua. *JHEP*, 04:021, 2006, hep-th/0602239.

[159] Steven A. Abel, Chong-Sun Chu, Joerg Jaeckel, and Valentin V. Khoze. SUSY breaking by a metastable ground state: Why the early universe preferred the non-supersymmetric vacuum. *JHEP*, 01:089, 2007, hep-th/0610334.

[160] Nathaniel J. Craig, Patrick J. Fox, and Jay G. Wacker. Reheating metastable O'Raifeartaigh models. *Phys. Rev.*, D75:085006, 2007, hep-th/0611006.

[161] Willy Fischler, Vadim Kaplunovsky, Chethan Krishnan, Lorenzo Mannelli, and Marcus A. C. Torres. Meta-Stable Supersymmetry Breaking in a Cooling Universe. *JHEP*, 03:107, 2007, hep-th/0611018.

[162] Karim Benakli and Cesar Moura. Brane-Worlds Pseudo-Goldstinos. *Nucl. Phys.*, B791:125–163, 2008, 0706.3127.

[163] Markus A. Luty and Raman Sundrum. Supersymmetry breaking and composite extra dimensions. *Phys. Rev.*, D65:066004, 2002, hep-th/0105137.

[164] Markus Luty and Raman Sundrum. Anomaly mediated supersymmetry breaking in four dimensions, naturally. *Phys. Rev.*, D67:045007, 2003, hep-th/0111231.

[165] Shamit Kachru, Liam McAllister, and Raman Sundrum. Sequestering in string theory. *JHEP*, 10:013, 2007, hep-th/0703105.

[166] Steven B. Giddings, Shamit Kachru, and Joseph Polchinski. Hierarchies from fluxes in string compactifications. *Phys. Rev.*, D66:106006, 2002, hep-th/0105097.

[167] Savas Dimopoulos, Shamit Kachru, Nemanja Kaloper, Albion E. Lawrence, and Eva Silverstein. Generating small numbers by tunneling in multi-throat compactifications. *Int. J. Mod. Phys.*, A19:2657–2704, 2004, hep-th/0106128.

[168] Arthur Hebecker and J. March-Russell. The ubiquitous throat. *Nucl. Phys.*, B781:99–111, 2007, hep-th/0607120.

[169] Edward Witten. Dynamical Breaking of Supersymmetry. *Nucl. Phys.*, B188:513, 1981.

[170] Kenneth A. Intriligator and Nathan Seiberg. Lectures on Supersymmetry Breaking. *Class. Quant. Grav.*, 24:S741–S772, 2007, hep-ph/0702069.

[171] E. Cremmer et al. Spontaneous Symmetry Breaking and Higgs Effect in Supergravity Without Cosmological Constant. *Nucl. Phys.*, B147:105, 1979.

[172] E. Cremmer, S. Ferrara, L. Girardello, and Antoine Van Proeyen. Yang-Mills Theories with Local Supersymmetry: Lagrangian, Transformation Laws and SuperHiggs Effect. *Nucl. Phys.*, B212:413, 1983.

[173] Markus A. Luty and Raman Sundrum. Hierarchy Stabilization in Warped Supersymmetry. *Phys. Rev.*, D64:065012, 2001, hep-th/0012158.

[174] Zohar Komargodski and Nathan Seiberg. From Linear SUSY to Constrained Superfields. *JHEP*, 09:066, 2009, 0907.2441.

[175] Nathan Seiberg. Exact results on the space of vacua of four-dimensional SUSY gauge theories. *Phys. Rev.*, D49:6857–6863, 1994, hep-th/9402044.

[176] N. Seiberg. Electric - magnetic duality in supersymmetric nonAbelian gauge theories. *Nucl. Phys.*, B435:129–146, 1995, hep-th/9411149.

[177] Kenneth A. Intriligator and N. Seiberg. Lectures on supersymmetric gauge theories and electric- magnetic duality. *Nucl. Phys. Proc. Suppl.*, 45BC:1–28, 1996, hep-th/9509066.

[178] Sidney R. Coleman and Erick J. Weinberg. Radiative Corrections as the Origin of Spontaneous Symmetry Breaking. *Phys. Rev.*, D7:1888–1910, 1973.

[179] Anne Christine Davis, Michael Dine, and Nathan Seiberg. The Massless Limit of Supersymmetric QCD. *Phys. Lett.*, B125:487, 1983.

[180] Ian Affleck, Michael Dine, and Nathan Seiberg. Dynamical Supersymmetry Breaking in Supersymmetric QCD. *Nucl. Phys.*, B241:493–534, 1984.

[181] Philip C. Argyres and Mohammad Edalati. Generalized Konishi anomaly, Seiberg duality and singular effective superpotentials. *JHEP*, 02:071, 2006, hep-th/0511272.

[182] Hiroyuki Abe, Tetsutaro Higaki, Tatsuo Kobayashi, and Yuji Omura. Moduli stabilization, F-term uplifting and soft supersymmetry breaking terms. *Phys. Rev.*, D75:025019, 2007, hep-th/0611024.

[183] Savas Dimopoulos, Michael Dine, Stuart Raby, and Scott D. Thomas. Experimental Signatures of Low Energy Gauge Mediated Supersymmetry Breaking. *Phys. Rev. Lett.*, 76:3494–3497, 1996, hep-ph/9601367.

[184] Yasunori Nomura, Michele Papucci, and Daniel Stolarski. Flavorful Supersymmetry. *Phys. Rev.*, D77:075006, 2008, 0712.2074.

[185] Shoji Asai, Koichi Hamaguchi, and Satoshi Shirai. Stop and Decay of Long-lived Charged Massive Particles at the LHC detectors. *Phys. Rev. Lett.*, 103:141803, 2009, 0902.3754.

[186] CMS Collaboration. Searching for Stopped Gluinos during Beam-off Periods at CMS. `http://cms-physics.web.cern.ch/cms-physics/public/EXO-09-001-pas.pdf`.

[187] Koichi Hamaguchi, Yoshitaka Kuno, Tsuyoshi Nakaya, and Mihoko M. Nojiri. A study of late decaying charged particles at future colliders. *Phys. Rev.*, D70:115007, 2004, hep-ph/0409248.

[188] Jonathan L. Feng and Bryan T. Smith. Slepton trapping at the Large Hadron and International Linear Colliders. *Phys. Rev.*, D71:015004, 2005, hep-ph/0409278.

[189] Koichi Hamaguchi, Mihoko M. Nojiri, and Albert de Roeck. Prospects to study a long-lived charged next lightest supersymmetric particle at the LHC. *JHEP*, 03:046, 2007, hep-ph/0612060.

[190] Hsin-Chia Cheng, John F. Gunion, Zhenyu Han, Guido Marandella, and Bob McElrath. Mass Determination in SUSY-like Events with Missing Energy. *JHEP*, 12:076, 2007, 0707.0030.

[191] Won Sang Cho, Kiwoon Choi, Yeong Gyun Kim, and Chan Beom Park. Gluino Stransverse Mass. *Phys. Rev. Lett.*, 100:171801, 2008, 0709.0288.

[192] Ryuichiro Kitano and Yasunori Nomura. Supersymmetry, naturalness, and signatures at the LHC. *Phys. Rev.*, D73:095004, 2006, hep-ph/0602096.

[193] Wilfried Buchmuller, Koichi Hamaguchi, Michael Ratz, and Tsutomu Yanagida. Supergravity at colliders. *Phys. Lett.*, B588:90–98, 2004, hep-ph/0402179.

[194] Clifford Cheung, A. Liam Fitzpatrick, and David Shih. (Extra)Ordinary Gauge Mediation. *JHEP*, 07:054, 2008, 0710.3585.

[195] Ryuichiro Kitano, Hirosi Ooguri, and Yutaka Ookouchi. Supersymmetry Breaking and Gauge Mediation. 2010, 1001.4535.

[196] Michael Dine, Lisa Randall, and Scott D. Thomas. Supersymmetry breaking in the early universe. *Phys. Rev. Lett.*, 75:398–401, 1995, hep-ph/9503303.

[197] Edward Witten. Constraints on Supersymmetry Breaking. *Nucl. Phys.*, B202:253, 1982.

[198] Edmund J. Copeland, Andrew R. Liddle, David H. Lyth, Ewan D. Stewart, and David Wands. False vacuum inflation with Einstein gravity. *Phys. Rev.*, D49:6410–6433, 1994, astro-ph/9401011.

[199] G. R. Dvali, Q. Shafi, and Robert K. Schaefer. Large scale structure and supersymmetric inflation without fine tuning. *Phys. Rev. Lett.*, 73:1886–1889, 1994, hep-ph/9406319.

[200] Graham G. Ross and Subir Sarkar. Successful supersymmetric inflation. *Nucl. Phys.*, B461:597–624, 1996, hep-ph/9506283.

[201] Nathaniel J. Craig. ISS-flation. *JHEP*, 02:059, 2008, 0801.2157.

[202] Michael Dine, Jonathan L. Feng, and Eva Silverstein. Retrofitting O'Raifeartaigh models with dynamical scales. *Phys. Rev.*, D74:095012, 2006, hep-th/0608159.

[203] Ofer Aharony and Nathan Seiberg. Naturalized and simplified gauge mediation. *JHEP*, 02:054, 2007, hep-ph/0612308.

[204] Ann E. Nelson and Nathan Seiberg. R symmetry breaking versus supersymmetry breaking. *Nucl. Phys.*, B416:46–62, 1994, hep-ph/9309299.

[205] Malcolm J. Duncan and Lars Gerhard Jensen. Exact tunneling solutions in scalar field theory. *Phys. Lett.*, B291:109–114, 1992.

[206] P. Binetruy and G. R. Dvali. D-term inflation. *Phys. Lett.*, B388:241–246, 1996, hep-ph/9606342.

[207] Masahiro Ibe, Yuri Shirman, and Tsutomu T. Yanagida. Cascade supersymmetry breaking and low-scale gauge mediation. 2010, 1009.2818.

[208] James M. Cline. Baryogenesis. 2006, hep-ph/0609145.

[209] Mark Trodden. Electroweak baryogenesis. *Rev. Mod. Phys.*, 71:1463–1500, 1999, hep-ph/9803479.

[210] M. Fukugita and T. Yanagida. Baryogenesis Without Grand Unification. *Phys.Lett.*, B174:45, 1986.

[211] Gianfranco Bertone and Joseph Silk. Particle dark matter. 2010.

[212] J. Merten et al. Creation of cosmic structure in the complex galaxy cluster merger Abell 2744. 2011, 1103.2772.

[213] Rupert A. C. Croft et al. Towards a Precise Measurement of Matter Clustering: Lyman- alpha Forest Data at Redshifts 2-4. *Astrophys. J.*, 581:20–52, 2002, astro-ph/0012324.

[214] James S. Bullock. Notes on the Missing Satellites Problem. 2010, 1009.4505.

[215] Ya. B. Zel'dovich. *Zh. Eksp. Teor. Fiz.*, 48:986, 1965.

[216] Ya. B. Zel'dovich, L. B. Okun, and S. B. Pikelner. *Usp. Fiz. Nauk.*, 84:113, 1965.

[217] Hong-Yee Chiu. Symmetry between particle and anti-particle populations in the universe. *Phys. Rev. Lett.*, 17:712, 1966.

[218] Benjamin W. Lee and Steven Weinberg. Cosmological Lower Bound on Heavy Neutrino Masses. *Phys.Rev.Lett.*, 39:165–168, 1977.

[219] Stephen Wolfram. Abundances of Stable Particles Produced in the Early Universe. *Phys.Lett.*, B82:65, 1979.

[220] Robert J. Scherrer and Michael S. Turner. On the Relic, Cosmic Abundance of Stable Weakly Interacting Massive Particles. *Phys.Rev.*, D33:1585, 1986.

[221] Geraldine Servant and Timothy M.P. Tait. Is the lightest Kaluza-Klein particle a viable dark matter candidate? *Nucl.Phys.*, B650:391–419, 2003, hep-ph/0206071.

[222] S. Nussinov. Technocosmology: could a technibaryon excess provide a 'natural' missing mass candidate? *Phys.Lett.*, B165:55, 1985.

[223] Mark W. Goodman and Edward Witten. Detectability of Certain Dark Matter Candidates. *Phys.Rev.*, D31:3059, 1985.

[224] A.K. Drukier, K. Freese, and D.N. Spergel. Detecting Cold Dark Matter Candidates. *Phys.Rev.*, D33:3495–3508, 1986.

[225] Katherine Freese, Joshua A. Frieman, and Andrew Gould. Signal Modulation in Cold Dark Matter Detection. *Phys.Rev.*, D37:3388, 1988.

[226] R. Bernabei, P. Belli, F. Cappella, R. Cerulli, C.J. Dai, et al. New results from DAMA/LIBRA. *Eur.Phys.J.*, C67:39–49, 2010, 1002.1028.

[227] C.E. Aalseth, P.S. Barbeau, J. Colaresi, J.I. Collar, J.Diaz Leon, et al. Search for an Annual Modulation in a P-type Point Contact Germanium Dark Matter Detector. 2011, 1106.0650.

[228] David Tucker-Smith and Neal Weiner. Inelastic dark matter. *Phys. Rev.*, D64:043502, 2001, hep-ph/0101138.

[229] David Tucker-Smith and Neal Weiner. The status of inelastic dark matter. *Phys. Rev.*, D72:063509, 2005, hep-ph/0402065.

[230] Spencer Chang, Graham D. Kribs, David Tucker-Smith, and Neal Weiner. Inelastic Dark Matter in Light of DAMA/LIBRA. 2008, 0807.2250.

[231] Jonathan L. Feng, Jason Kumar, Danny Marfatia, and David Sanford. Isospin-Violating Dark Matter. 2011, 1102.4331.

[232] Nima Arkani-Hamed, Douglas P. Finkbeiner, Tracy R. Slatyer, and Neal Weiner. A Theory of Dark Matter. *Phys. Rev.*, D79:015014, 2009, 0810.0713.

[233] S. W. Barwick et al. Measurements of the cosmic-ray positron fraction from 1-GeV to 50-GeV. *Astrophys. J.*, 482:L191–L194, 1997, astro-ph/9703192.

[234] M. Aguilar et al. Cosmic-ray positron fraction measurement from 1-GeV to 30-GeV with AMS-01. *Phys. Lett.*, B646:145–154, 2007, astro-ph/0703154.

[235] Oscar Adriani et al. An anomalous positron abundance in cosmic rays with energies 1.5-100 GeV. *Nature*, 458:607–609, 2009, 0810.4995.

[236] J. Chang, J.H. Adams, H.S. Ahn, G.L. Bashindzhagyan, M. Christl, et al. An excess of cosmic ray electrons at energies of 300-800 GeV. *Nature*, 456:362–365, 2008.

[237] S. Torii et al. High-energy electron observations by PPB-BETS flight in Antarctica. 2008, 0809.0760.

[238] Aous A. Abdo et al. Measurement of the Cosmic Ray e+ plus e- spectrum from 20 GeV to 1 TeV with the Fermi Large Area Telescope. *Phys. Rev. Lett.*, 102:181101, 2009, 0905.0025.

[239] F. Aharonian et al. Probing the ATIC peak in the cosmic-ray electron spectrum with H.E.S.S. *Astron. Astrophys.*, 508:561, 2009, 0905.0105.

[240] Philipp Mertsch and Subir Sarkar. Testing astrophysical models for the PAMELA positron excess with cosmic ray nuclei. *Phys.Rev.Lett.*, 103:081104, 2009, 0905.3152.

[241] Markus Ahlers, Philipp Mertsch, and Subir Sarkar. On cosmic ray acceleration in supernova remnants and the FERMI/PAMELA data. *Phys.Rev.*, D80:123017, 2009, 0909.4060.

[242] G. Steigman, C. L. Sarazin, H. Quintana, and J. Faulkner. Dynamical interactions and astrophysical effects of stable heavy neutrinos. *The Astrophysical Journal*, 83:1050–1061, September 1978.

[243] D. N. Spergel and W. H. Press. Effect of hypothetical, weakly interacting, massive particles on energy transport in the solar interior. *Astrophys. J.*, 294:663–673, 1985.

[244] William H. Press and David N. Spergel. Capture by the sun of a galactic population of weakly interacting, massive particles. *Astrophys. J.*, 296:679–684, 1985.

[245] Joseph Silk, Keith A. Olive, and Mark Srednicki. The photino, the sun, and high-energy neutrinos. *Phys. Rev. Lett.*, 55:257–259, 1985.

[246] Andrew Gould. WIMP DISTRIBUTION IN AND EVAPORATION FROM THE SUN. *Astrophys. J.*, 321:560, 1987.

[247] T. K. Gaisser, M. Nowakowski, and E. A. Paschos. NEUTRINO INDUCED MESON PRODUCTION IN NUCLEON DECAY DETECTORS. *Phys. Rev.*, D33:1233, 1986.

[248] T. K. Gaisser, G. Steigman, and S. Tilav. Limits on Cold Dark Matter Candidates from Deep Underground Detectors. *Phys. Rev.*, D34:2206, 1986.

[249] Mark Srednicki, Keith A. Olive, and Joseph Silk. High-Energy Neutrinos from the Sun and Cold Dark Matter. *Nucl. Phys.*, B279:804, 1987.

[250] Gianfranco Bertone and Malcolm Fairbairn. Compact Stars as Dark Matter Probes. *Phys. Rev.*, D77:043515, 2008, 0709.1485.

[251] Mads T. Frandsen and Subir Sarkar. Asymmetric dark matter and the Sun. *Phys.Rev.Lett.*, 105:011301, 2010, 1003.4505.

[252] Daniel T. Cumberbatch, Joyce.A. Guzik, Joseph Silk, L.Scott Watson, and Stephen M. West. Light WIMPs in the Sun: Constraints from Helioseismology. *Phys.Rev.*, D82:103503, 2010, 1005.5102.

[253] Marco Taoso, Fabio Iocco, Georges Meynet, Gianfranco Bertone, and Patrick Eggenberger. Effect of low mass dark matter particles on the Sun. *Phys.Rev.*, D82:083509, 2010, 1005.5711.

[254] R. Abbasi et al. Search for Dark Matter from the Galactic Halo with the IceCube Neutrino Observatory. 2011, 1101.3349.

[255] Igor V. Moskalenko and Lawrence L. Wai. Dark matter burners. *Astrophys. J.*, 659:L29–L32, 2007, astro-ph/0702654.

[256] R. Bernabei et al. Dark matter search. *Riv. Nuovo Cim.*, 26N1:1–73, 2003, astro-ph/0307403.

[257] R. Bernabei et al. First results from DAMA/LIBRA and the combined results with DAMA/NaI. *Eur. Phys. J.*, C56:333–355, 2008, 0804.2741.

[258] Shmuel Nussinov, Lian-Tao Wang, and Itay Yavin. Capture of Inelastic Dark Matter in the Sun. 2009, 0905.1333.

[259] Arjun Menon, Rob Morris, Aaron Pierce, and Neal Weiner. Capture and Indirect Detection of Inelastic Dark Matter. 2009, 0905.1847.

[260] Jing Shu, Peng-fei Yin, and Shou-hua Zhu. Neutrino Constraints on Inelastic Dark Matter after CDMS II. 2010, 1001.1076.

[261] L. R. Bedin et al. The End of the White Dwarf Cooling Sequence in M4: an efficient approach. *Astrophys. J.*, 697:965–979, 2009, 0903.2839.

[262] Luigi R. Bedin et al. Transforming observational data and theoretical isochrones into the ACS/WFC Vega-mag system. *Mon. Not. Roy. Astron. Soc.*, 357:1038–1048, 2005, astro-ph/0412328.

[263] E. E. Salpeter. Energy and Pressure of a Zero-Temperature Plasma. *The Astrophysical Journal*, 134:669–+, November 1961.

[264] P. J. E. Peebles. Dark matter and the origin of galaxies and globular star clusters. *Astrophys. J.*, 277:470–477, 1984.

[265] Georges Meylan and Carlton Pryor. Observational constraints of the internal dynamics of globular clusters. 1992. Proceedings of the Workshop on Structure and Dynamics of Globular Clusters, Berkeley, 15-17 July 1992.

[266] Sergey Mashchenko and Alison Sills. Globular Clusters with Dark Matter Halos. II. Evolution in Tidal Field. *Astrophys. J.*, 619:258, 2005, astro-ph/0409606.

[267] Ben Moore. Constraints on the Global Mass-to-Light Ratios and Extent of Dark Matter Halos in Globular Clusters and Dwarf Spheroidals. *Astrophys. J.*, 461:L13, 1996, astro-ph/9511147.

[268] Patrick Cote, Michael J. West, and R. O. Marzke. Globular Cluster Systems and the Missing Satellite Problem: Implications for Cold Dark Matter Models. 2001, astro-ph/0111388.

[269] Liang Gao, Simon D. M. White, Adrian Jenkins, Felix Stoehr, and Volker Springel. The subhalo populations of LCDM dark haloes. *Mon. Not. Roy. Astron. Soc.*, 355:819, 2004, astro-ph/0404589.

[270] Ben Moore, Juerg Diemand, Piero Madau, Marcel Zemp, and Joachim Stadel. Globular clusters, satellite galaxies and stellar haloes from early dark matter peaks. *Mon. Not. Roy. Astron. Soc.*, 368:563–570, 2006, astro-ph/0510370.

[271] Takayuki R. Saitoh, Jin Koda, Takashi Okamoto, Keiichi Wada, and Asao Habe. Tidal disruption of dark matter halos around proto- globular clusters. *Astrophys. J.*, 640:22–30, 2006, astro-ph/0511692.

[272] B. F. Griffen, M. J. Drinkwater, P. A. Thomas, J. C. Helly, and K. A. Pimbblet. Globular Cluster Formation Within The Aquarius Simulation. 2009, 0910.0310.

[273] Jean P. Brodie and Jay Strader. Extragalactic Globular Clusters and Galaxy Formation. *Ann. Rev. Astron. Astrophys.*, 44:193–267, 2006, astro-ph/0602601.

[274] Gabrijela Zaharija. Implications of the intermediate mass black hole in globular cluster G1 on dark matter detection. *Phys. Rev. D*, 78(2):027301, Jul 2008.

[275] M. Wood et al. A Search for Dark Matter Annihilation with the Whipple 10m Telescope. 2008, 0801.1708.

[276] I. King. The shape of a rotating star cluster. *The Astrophysical Journal*, 66:68–+, March 1961.

[277] I. King. The structure of star clusters. I. an empirical density law. *The Astrophysical Journal*, 67:471–+, October 1962.

[278] S. Colafrancesco, S. Profumo, and P. Ullio. Multi-frequency analysis of neutralino dark matter annihilations in the Coma cluster. *Astron.Astrophys.*, 455:21–43, August 2006, arXiv:astro-ph/0507575.

[279] Sergey Mashchenko and Alison Sills. Globular Clusters with Dark Matter Halos. I. Initial Relaxation. *Astrophys. J.*, 619:243, 2005, astro-ph/0409605.

[280] Julio F. Navarro, Carlos S. Frenk, and Simon D. M. White. A Universal Density Profile from Hierarchical Clustering. *Astrophys. J.*, 490:493–508, 1997, astro-ph/9611107.

[281] George R. Blumenthal, S. M. Faber, Ricardo Flores, and Joel R. Primack. Contraction of Dark Matter Galactic Halos Due to Baryonic Infall. *Astrophys. J.*, 301:27, 1986.

[282] Oleg Y. Gnedin, Andrey V. Kravtsov, Anatoly A. Klypin, and Daisuke Nagai. Response of dark matter halos to condensation of baryons: cosmological simulations and improved adiabatic contraction model. *Astrophys. J.*, 616:16–26, 2004, astro-ph/0406247.

[283] Michael Gustafsson, Malcolm Fairbairn, and Jesper Sommer-Larsen. Baryonic Pinching of Galactic Dark Matter Haloes. *Phys. Rev.*, D74:123522, 2006, astro-ph/0608634.

[284] David Merritt. Evolution of the Dark Matter Distribution at the Galactic Center. *Phys. Rev. Lett.*, 92:201304, 2004, astro-ph/0311594.

[285] Joachim Kopp, Thomas Schwetz, and Jure Zupan. Global interpretation of direct Dark Matter searches after CDMS-II results. 2009, 0912.4264.

[286] Gintaras Duda, Ann Kemper, and Paolo Gondolo. Model independent form factors for spin independent neutralino nucleon scattering from elastic electron scattering data. *JCAP*, 0704:012, 2007, hep-ph/0608035.

[287] Gerard Gilmore et al. The Observed properties of Dark Matter on small spatial scales. *Astrophys. J.*, 663:948–959, 2007, astro-ph/0703308.

[288] Malcolm Fairbairn and Thomas Schwetz. Spin-independent elastic WIMP scattering and the DAMA annual modulation signal. *JCAP*, 0901:037, 2009, 0808.0704.

[289] M. Kuhlen et al. Dark Matter Direct Detection with Non-Maxwellian Velocity Structure. 2009, 0912.2358.

[290] Dan Hooper, Douglas Spolyar, Alberto Vallinotto, and Nickolay Y. Gnedin. Inelastic Dark Matter As An Efficient Fuel For Compact Stars. 2010, 1002.0005.

[291] Kai Schmidt-Hoberg and Martin Wolfgang Winkler. Improved Constraints on Inelastic Dark Matter. *JCAP*, 0909:010, 2009, 0907.3940.

[292] P. Hut and Keith A. Olive. A cosmological upper limit on the mass of heavy neutrinos. *Phys. Lett.*, B87:144–146, 1979.

[293] G. B. Gelmini, Lawrence J. Hall, and M. J. Lin. What is the cosmion? *Nucl. Phys.*, B281:726, 1987.

[294] R.Sekhar Chivukula and Terry P. Walker. Technicolor cosmology. *Nucl.Phys.*, B329:445, 1990.

[295] Stephen M. Barr, R.Sekhar Chivukula, and Edward Farhi. Electroweak fermion number violation and the production of stable particles in the early universe. *Phys.Lett.*, B241:387–391, 1990.

[296] David B. Kaplan. A Single explanation for both the baryon and dark matter densities. *Phys.Rev.Lett.*, 68:741–743, 1992.

[297] Scott D. Thomas. Baryons and dark matter from the late decay of a supersymmetric condensate. *Phys.Lett.*, B356:256–263, 1995, hep-ph/9506274.

[298] Dan Hooper, John March-Russell, and Stephen M. West. Asymmetric sneutrino dark matter and the Omega(b) / Omega(DM) puzzle. *Phys.Lett.*, B605:228–236, 2005, hep-ph/0410114.

[299] Ryuichiro Kitano and Ian Low. Dark matter from baryon asymmetry. *Phys.Rev.*, D71:023510, 2005, hep-ph/0411133.

[300] Kaustubh Agashe and Geraldine Servant. Baryon number in warped GUTs: Model building and (dark matter related) phenomenology. *JCAP*, 0502:002, 2005, hep-ph/0411254.

[301] Nicolas Cosme, Laura Lopez Honorez, and Michel H.G. Tytgat. Leptogenesis and dark matter related? *Phys.Rev.*, D72:043505, 2005, hep-ph/0506320.

[302] Glennys R. Farrar and Gabrijela Zaharijas. Dark matter and the baryon asymmetry. *Phys.Rev.Lett.*, 96:041302, 2006, hep-ph/0510079.

[303] Daijiro Suematsu. Nonthermal production of baryon and dark matter. *Astropart.Phys.*, 24:511–519, 2006, hep-ph/0510251.

[304] Michel H.G. Tytgat. Relating leptogenesis and dark matter. 2006, hep-ph/0606140.

[305] T. Banks, S. Echols, and J.L. Jones. Baryogenesis, dark matter and the Pentagon. *JHEP*, 0611:046, 2006, hep-ph/0608104.

[306] Maxim Yu. Khlopov and Chris Kouvaris. Composite dark matter from a model with composite Higgs boson. *Phys. Rev.*, D78:065040, 2008, 0806.1191.

[307] Ryuichiro Kitano, Hitoshi Murayama, and Michael Ratz. Unified origin of baryons and dark matter. *Phys.Lett.*, B669:145–149, 2008, 0807.4313.

[308] David E. Kaplan, Markus A. Luty, and Kathryn M. Zurek. Asymmetric Dark Matter. *Phys.Rev.*, D79:115016, 2009, 0901.4117.

[309] Kazunori Kohri, Anupam Mazumdar, Narendra Sahu, and Philip Stephens. Probing Unified Origin of Dark Matter and Baryon Asymmetry at PAMELA/Fermi. *Phys. Rev.*, D80:061302, 2009, 0907.0622.

[310] Graham D. Kribs, Tuhin S. Roy, John Terning, and Kathryn M. Zurek. Quirky Composite Dark Matter. *Phys.Rev.*, D81:095001, 2010, 0909.2034.

[311] Timothy Cohen and Kathryn M. Zurek. Leptophilic Dark Matter from the Lepton Asymmetry. *Phys.Rev.Lett.*, 104:101301, 2010, 0909.2035.

[312] Haipeng An, Shao-Long Chen, Rabindra N. Mohapatra, and Yue Zhang. Leptogenesis as a Common Origin for Matter and Dark Matter. *JHEP*, 1003:124, 2010, 0911.4463.

[313] Maxim Yu. Khlopov, Andrey G. Mayorov, and Evgeny Yu. Soldatov. Composite Dark Matter and Puzzles of Dark Matter Searches. *Int. J. Mod. Phys.*, D19:1385–1395, 2010, 1003.1144.

[314] Timothy Cohen, Daniel J. Phalen, Aaron Pierce, and Kathryn M. Zurek. Asymmetric Dark Matter from a GeV Hidden Sector. *Phys.Rev.*, D82:056001, 2010, 1005.1655.

[315] Jessie Shelton and Kathryn M. Zurek. Darkogenesis: A baryon asymmetry from the dark matter sector. *Phys.Rev.*, D82:123512, 2010, 1008.1997.

[316] Hooman Davoudiasl, David E. Morrissey, Kris Sigurdson, and Sean Tulin. Hylogenesis: A Unified Origin for Baryonic Visible Matter and Antibaryonic Dark Matter. *Phys.Rev.Lett.*, 105:211304, 2010, 1008.2399.

[317] N. Haba and S. Matsumoto. Baryogenesis from Dark Sector. 2010, 1008.2487.

[318] Matthew R. Buckley and Lisa Randall. Xogenesis. 2010, 1009.0270.

[319] Pei-Hong Gu, Manfred Lindner, Utpal Sarkar, and Xinmin Zhang. WIMP Dark Matter and Baryogenesis. 2010, 1009.2690.

[320] Mattias Blennow, Basudeb Dasgupta, Enrique Fernandez-Martinez, and Nuria Rius. Aidnogenesis via Leptogenesis and Dark Sphalerons. *JHEP*, 1103:014, 2011, 1009.3159.

[321] Lawrence J. Hall, John March-Russell, and Stephen M. West. A Unified Theory of Matter Genesis: Asymmetric Freeze-In. 2010, 1010.0245.

[322] Bhaskar Dutta and Jason Kumar. Asymmetric Dark Matter from Hidden Sector Baryogenesis. 2010, 1012.1341.

[323] Adam Falkowski, Joshua T. Ruderman, and Tomer Volansky. Asymmetric Dark Matter from Leptogenesis. 2011, 1101.4936.

[324] Jonathan J. Heckman and Soo-Jong Rey. Baryon and Dark Matter Genesis from Strongly Coupled Strings. 2011, 1102.5346.

[325] Michael L. Graesser, Ian M. Shoemaker, and Luca Vecchi. Asymmetric WIMP dark matter. 2011, 1103.2771.

[326] Mads T. Frandsen, Subir Sarkar, and Kai Schmidt-Hoberg. Light asymmetric dark matter from new strong dynamics. 2011, 1103.4350.

[327] Matthew R. Buckley. Asymmetric Dark Matter and Effective Operators. 2011, 1104.1429.

[328] Anson Hook. Unitarity constraints on asymmetric freeze-in. 2011, 1105.3728.

[329] Clifford Cheung and Kathryn M. Zurek. Affleck-Dine Cogenesis. 2011, 1105.4612.

[330] Eugenio Del Nobile, Chris Kouvaris, and Francesco Sannino. Interfering Composite Asymmetric Dark Matter for DAMA and CoGeNT. 2011, 1105.5431.

[331] Andrew G. Cohen and David B. Kaplan. Thermodynamic generation of the baryon asymmetry. *Phys.Lett.*, B199:251, 1987.

[332] Andrew G. Cohen and David B. Kaplan. Spontaneous baryogenesis. *Nucl.Phys.*, B308:913, 1988.

[333] Andrew G. Cohen, D.B. Kaplan, and A.E. Nelson. Spontaneous baryogenesis at the weak phase transition. *Phys.Lett.*, B263:86–92, 1991.

[334] S.A. Abel, W.N. Cottingham, and I.B. Whittingham. Spontaneous baryogenesis in supersymmetric models. *Nucl.Phys.*, B410:173–187, 1993, hep-ph/9212299.

[335] Andrew G. Cohen, D.B. Kaplan, and A.E. Nelson. Diffusion enhances spontaneous electroweak baryogenesis. *Phys.Lett.*, B336:41–47, 1994, hep-ph/9406345.

[336] Alexandre Dolgov and Katherine Freese. Calculation of particle production by Nambu Goldstone bosons with application to inflation reheating and baryogenesis. *Phys.Rev.*, D51:2693–2702, 1995, hep-ph/9410346.

[337] Alexandre Dolgov, Katherine Freese, Raghavan Rangarajan, and Mark Srednicki. Baryogenesis during reheating in natural inflation and comments on spontaneous baryogenesis. *Phys.Rev.*, D56:6155–6165, 1997, hep-ph/9610405.

[338] O. Bertolami, Don Colladay, V.Alan Kostelecky, and R. Potting. CPT violation and baryogenesis. *Phys.Lett.*, B395:178–183, 1997, hep-ph/9612437.

[339] Ming-zhe Li, Xiu-lian Wang, Bo Feng, and Xin-min Zhang. Quintessence and spontaneous leptogenesis. *Phys.Rev.*, D65:103511, 2002, hep-ph/0112069.

[340] Masahide Yamaguchi. Generation of cosmological large lepton asymmetry from a rolling scalar field. *Phys.Rev.*, D68:063507, 2003, hep-ph/0211163.

[341] Robert H. Brandenberger and Masahide Yamaguchi. Spontaneous baryogenesis in warm inflation. *Phys.Rev.*, D68:023505, 2003, hep-ph/0301270.

[342] Fuminobu Takahashi and Masahide Yamaguchi. Spontaneous baryogenesis in flat directions. *Phys.Rev.*, D69:083506, 2004, hep-ph/0308173.

[343] G.L. Alberghi, R. Casadio, and A. Tronconi. Radion induced spontaneous baryogenesis. *Mod.Phys.Lett.*, A22:339–346, 2007, hep-ph/0310052.

[344] Jose Manuel Carmona, Jose Luis Cortes, Ashok K. Das, Jorge Gamboa, and Fernando Mendez. Matter-antimatter asymmetry without departure from thermal equilibrium. *Mod.Phys.Lett.*, A21:883–892, 2006, hep-th/0410143.

[345] Sean M. Carroll and Jing Shu. Models of baryogenesis via spontaneous Lorentz violation. *Phys.Rev.*, D73:103515, 2006, hep-ph/0510081.

[346] Gabriela Barenboim and Joseph D. Lykken. Quintessence, inflation and baryogenesis from a single pseudo-Nambu-Goldstone boson. *JHEP*, 0710:032, 2007, 0707.3999.

[347] Jeffrey A. Harvey and Michael S. Turner. Cosmological baryon and lepton number in the presence of electroweak fermion number violation. *Phys.Rev.*, D42:3344–3349, 1990.

[348] Daniel J. H. Chung, Bjorn Garbrecht, and Sean Tulin. The Effect of the Sparticle Mass Spectrum on the Conversion of B-L to B. *JCAP*, 0903:008, 2009, 0807.2283.

[349] E. Komatsu et al. Seven-Year Wilkinson Microwave Anisotropy Probe (WMAP) Observations: Cosmological Interpretation. *Astrophys. J. Suppl.*, 192:18, 2011, 1001.4538.

[350] Peter Svrcek and Edward Witten. Axions In String Theory. *JHEP*, 0606:051, 2006, hep-th/0605206.

[351] Alexander Belyaev, Mads T. Frandsen, Subir Sarkar, and Francesco Sannino. Mixed dark matter from technicolor. *Phys.Rev.*, D83:015007, 2011, 1007.4839.

[352] Matthew R. Buckley and Patrick J. Fox. Dark Matter Self-Interactions and Light Force Carriers. *Phys.Rev.*, D81:083522, 2010, 0911.3898.

[353] S. Heinemeyer, W. Hollik, A. M. Weber, and G. Weiglein. Z Pole Observables in the MSSM. *JHEP*, 04:039, 2008, 0710.2972.

[354] Precision electroweak measurements on the Z resonance. *Phys. Rept.*, 427:257–454, 2006, hep-ex/0509008.

[355] R. Cowsik and J. McClelland. An Upper Limit on the Neutrino Rest Mass. *Phys. Rev. Lett.*, 29:669–670, 1972.

[356] Jonathan Bagger and Julius Wess. Supersymmetry and Supergravity. Princeton University Press; 2nd Revised edition (Princeton, 1992).